Automated collection of intertidal beach bathymetries from Argus video images

Automated collection of intertidal beach bathymetries from Argus video images

Laura Uunk

MSc Thesis

Supervisors

Prof. dr. S.J.M.H. Hulscher
Dr. K.M. Wijnberg
Ir. R. Morelissen

WL | delft hydraulics

Title:	Automated collection of intertidal beach bathymetries from Argus video images

Abstract:

Knowledge of the beach behaviour is required for both coastal management and coastal research. The little information that is currently available on smaller spatiotemporal scales limits our understanding of the beach behaviour. An easy and relatively cheap way of collecting bathymetric data of, amongst others, the intertidal beach, is offered by the use of Argus images. The intertidal bathymetry can be derived from Argus images by detecting the shoreline on the image and combining its location with its calculated elevation. Shorelines detected throughout the tidal cycle provide elevation contours of the intertidal beach. Currently, the quality control on the detected shoreline points is still performed manually. As this is very time-consuming, only monthly bathymetries have been derived so far. The performance of a completely automated shoreline detection and quality control algorithm (Auto Shoreline Mapper - ASM) was not satisfactory on the Dutch beach. After mapping only a few bathymetries the ASM generally quitted because, in time, it ran out of shoreline data. In this research improvements to the ASM are made that prevent it from collapsing. The quality control in the ASM is performed by comparing all detected shoreline points to a bench-mark bathymetry, which is obtained from shoreline points detected on previous images. A maximum vertical difference between the newly detected shoreline points and the bench-mark bathymetry determines which points are accepted. Tests were carried out with three different acceptance criteria to study the impact on the performance of the ASM and on the quality of the obtained bathymetries by means of coastal state indicators (CSIs). The conclusion is that the acceptance criterion does not significantly affect the automatically obtained bathymetries, as long as those were obtained from shoreline points within a time window in the order of 6 days and with smoothing scales in the order of 25 m cross shore and 100 m alongshore. The bathymetries obtained with the ASM show a good agreement with manually obtained bathymetries. The daily ASM bathymetries show a direct response of the beach to storm events. This direct response was not visible from the monthly IBM data. The human effort that is saved by automatically mapping shorelines is tremendous. Previously, it took 2 to 4 man-hours to detect shorelines of one day for 5 cameras. The ASM needs approximately 7 hours for this, but human support is not required. The way to obtaining daily bathymetries is opened by the improved ASM.

References:

Ver	Author		Date	Remarks	Review		Approved by	
	Laura Uunk	RL	31-3-2008		Morelissen	RrC	Schilperoort	

Project number:	
Keywords:	Argus, intertidal beach bathymetry, monitoring
Number of pages:	79
Classification:	None
Status:	Final, MSc Thesis

Preface

This report describes the research I have performed to complete my Master's education in Civil Engineering and Management at Twente University.

The study concerns the automated extraction of intertidal beach bathymetries from Argus video images and the use of these bathymetries in studies on beach behaviour on the short time scale. The research was carried out at WL|Delft Hydraulics, nowadays part of Deltares, as a part of the Beach Wizard project under the framework of the VOP (Voortschrijdend Onderzoeks Programma) reseach program for the Dutch Ministry of Public Works (Rijkswaterstaat).

I would like to thank my supervisors ir. R Morelissen (WL|Delft Hydraulics), dr. K.M. Wijnberg (Twente University) and prof. dr. S.J.M.H. Hulscher (Twente University) for their support, critical notes and enthusiasm.

Furthermore, I would like to say that I enjoyed my time at WL|Delft Hydraulics. I had a great time with the other graduate students. The pancakes on Friday won't be forgotten soon.

Finally, I would like thank my friends and family for their support and the interest they have shown in my studies in Twente and Delft.

Laura Uunk

April 2008

Summary

Knowledge of the beach behaviour is required from both a coastal management as well as a scientific point of view. The little information that is currently available on the smaller spatiotemporal scales limits our understanding of the beach behaviour. An easy and relatively cheap way of collecting bathymetric data is offered by the use of Argus video images. From these images information on the beach can be derived, such as the position of subtidal bars or the bathymetry of the intertidal beach. The latter is subject of this research.

The bathymetry of the intertidal beach can be derived from Argus video images by detecting the shoreline on the image and combining its location with its calculated elevation, based on tide, wave set-up and swash. In this way shorelines detected throughout the tidal cycle provide elevation contours of the intertidal beach. Currently, detection of the shoreline and calculation of the elevation are automated, but determining where on the image to search for the shoreline (region of interest) and acceptance of the correct shoreline points (i.e. quality control) are actions that still require human control. The tool that is used for this is the Intertidal Beach Mapper (IBM). As manual quality control is very time-consuming, only monthly bathymetries have been derived from Argus images so far. The advantage that the (half-)hourly collected Argus images could provide is thus not yet used to its fullest extent.

A completely automated shoreline detection and quality control algorithm was developed by Plant (Madsen and Plant, 2001): the Auto Shoreline Mapper (ASM). Cerezo and Harley improved this tool later on for the Dutch beach. The ASM automatically determines the region of interest and automatically performs a quality control on the detected shoreline points. For both these steps a bench-mark bathymetry is used. This bathymetry is interpolated from shoreline points detected on previous images within a certain time window. The region of interest is then determined as an area around the expected shoreline location. For the quality control all detected shoreline points are compared to the bench-mark bathymetry. A user-defined, spatially non-varying maximum vertical difference between the shoreline point and the bench-mark bathymetry determines whether a shoreline point is accepted or rejected. This bench-mark bathymetry, in combination with the vertical difference criterion, has taken over manual quality control.

The performance of the ASM, however, was not satisfactory on the Dutch beach, because after mapping only a few bathymetries the ASM generally quitted because, in time, it ran out of shoreline data. It appeared that this was mainly due to problems with the determination of the region of interest and with the quality control. These problems were in turn caused by gaps in the bench-mark bathymetry. Improvements to the way the region of interest was determined and the way quality control was performed solved most of the problems. The ASM has now detected shorelines continuously on images covering a period of 4 months without human intervention.

Two problems were encountered with the fixed vertical acceptance criterion: a) sometimes wrongly detected shoreline points are accepted; b) sometimes correctly detected shoreline points are rejected. If the vertical acceptance criterion is set very loose, many points, including the wrongly detected ones, will be accepted on low-sloping beaches like the Dutch ones. In case of a very strict criterion, elevation changes that could naturally occur within one tidal cycle are not accounted for, leading to the rejection of many good points. The

setting of the criterion is therefore a trade-off between accepting wrong shoreline points in case of a larger value and rejecting good points in case of a smaller value.

Several tests have been carried out with different values for the acceptance criterion to study the impact on the performance of the ASM and also to study the influence of the trade-off on the quality of the obtained intertidal bathymetries. The intertidal bathymetries are composed of detected shoreline points within a time window that is larger than one tidal cycle. The interpolation method that is used is the loess interpolation. This is a linear smoother that is a suitable method to obtain bathymetries. The obtained bathymetries are compared to IBM bathymetries by means of coastal state indicators (momentary intertidal coastline and elevation contours). The comparison has shown that the value of the vertical acceptance criterion has no influence on the obtained coastal state indicators, as long as a time window of 3 to 6 days and smoothing scales of 25 m cross-shore and 100 m alongshore are used in the loess interpolation.

Comparison of daily ASM derived CSIs with monthly IBM obtained CSI shows that the ASM CSIs give better insight into the immediate response of the beach to high wave-energy events (such as storms). Monthly IBM data did not provide this insight. Figure 1 shows that bathymetries obtained with ASM can be useful for data analysis on time scales as small as days to weeks.

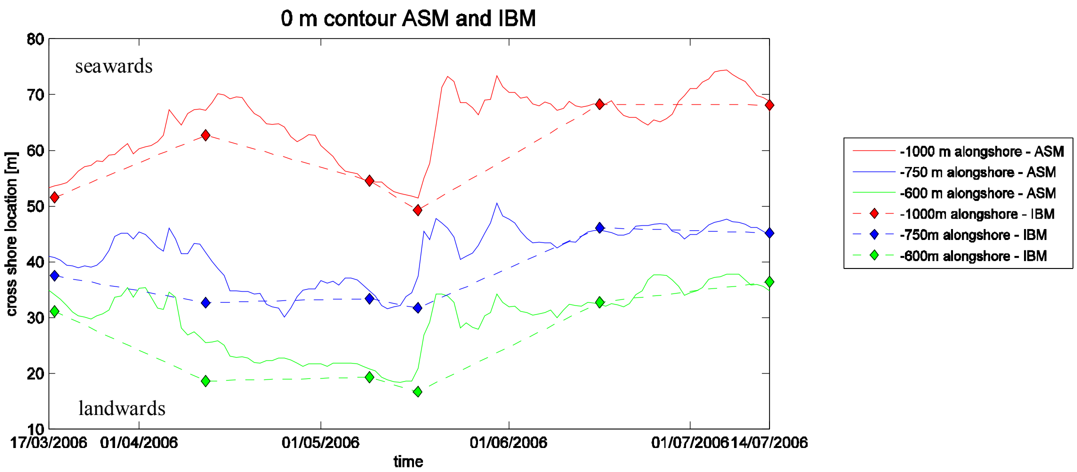

Figure 1: cross shore movement of the 0 m contour in time at three alongshore locations derived from IBM and ASM bathymetries. The ASM data clearly show a good agreement with the IBM data. The ASM data provides a much higher resolution in time.

The smoothing scales that are used in the loess interpolation limit the size of the morphologic features that can be studied with the ASM obtained bathymetries. The smallest morphological features that are visible in bathymetries obtianed with smoothing scales in the order of 25 m cross-shore and 100 m alongshore have length scales of 50 m cross-shore and 200 m alongshore (Plant et al., 2002). Examples of such features are salients and embayments that were recognized by Aagaard et al. (2005) and Cohen and Brière (2007).

The human effort that was needed to obtain bathymetries has been reduced to a great extent. The ASM provides a way to easily obtain daily bathymetry data of large stretches of the beach for very long periods at acceptable costs. The man-hours that would have been

required to manually obtain the daily bathymetry data in Figure 1 would probably be 60 to 120 hours.

Examples of studies that could benefit from the increased availability of bathymetry data are studies on storm impact and beach recovery and studies on the influence of nearshore and beach nourishments. Furthermore, the performance of prediction models may benefit from frequently updated intertidal bathymetries. It is recommended to also test the use of the ASM in support of management decisions. Compared to the yearly Jarkus measurements the ASM provides data on much higher spatial and temporal resolutions.

Contents

Appendices

1 Introduction

1.1 Background

The bathymetry of the beach and the nearshore zone is a subject that is studied extensively all over the world to monitor coastal safety, erosional and accretional processes, movement of nearshore and intertidal bars and to provide good initial bathymetries for numerical models to forecast coastal behaviour. In the Netherlands, management decisions concerning for example beach and nearshore nourishments, are supported by measurements and studies of the coastal morphology.

There are several ways to obtain bathymetry data of the beach and nearshore zone. In the Netherlands most beach data are currently obtained by DGPS (Differential Global Positioning System) and LIDAR (Light Detection and Ranging) measurements. Extensive traditional field campaigns have been held at the Egmond beach and the whole of the Holland coast for various sorts of research and management purposes. The high expenses involved are a drawback of the traditional methods. Additionally, DGPS measurements are very time-consuming. Because of these reasons, measurements using traditional techniques are performed sparsely in time and often only cover a small span of the beach. Whenever a large spatial area is covered the sampling interval is often large, like with the JARKUS measurements. These are performed yearly as transects along the entire Dutch coast with an alongshore spacing of 250 m.

The sparse availability of data in time and space is a limiting factor to both coastal research and coastal management. Especially research on the short time scale (e.g. storm impact and beach recovery) suffers from this lack of data, because detailed day-to-day bathymetry data are demanded for well-funded statements on short time scale beach behavior. Several studies on storm impact on Egmond beach are based on relatively limited data. Their results are described in Appendix A. Although their results are still valuable to both scientists and managers there are two conditions that limit the general applicability of the statements in these studies: a) all studies only compare very few storms and b) different morphological conditions are not always taken into account, both because of the lack of data.

A promising development in obtaining daily bathymetries is the rise of remote sensing techniques. These techniques are generally cheaper, while easily covering a larger span of the beach with a higher resolution in time and space. In 1992 a shore-based remote video technology was developed at Oregon State University: the Argus system. The Argus system consists of unmanned, automated video stations that collect digital video data at spatiotemporal scales of decimeters to kilometers and hours to years. A video station typically consists of four to five cameras that together span a 180º view covering approximately 4 km of beach. The images of the Argus cameras are used to monitor coastal processes and to support coastal management and engineering. Information that can be derived from these images include amongst others the sub- and intertidal beach bathymetry (Aarninkhof et al., 2003; Holland and Holman, 1997; Plant and Holman, 1997; Quartel et al., 2007).

In the Netherlands, Argus cameras are placed at three locations along the Holland coast. Two Argus stations are located at the town of Egmond. One is placed on top of the Jan van Speijk lighthouse and the other on a high tower south of the town. A third Argus station is located at Noordwijk and is placed on the roof of the 'Huis ter Duin' hotel. Figure 1.1 shows the Argus station on top of the Huis ter Duin hotel in Noordwijk.

Figure 1.1: Argus station at Noordwijk on top of the Huis ter Duin hotel (RIKZ, 2001)

1.2 Benefits of Argus

Kroon et al. (2007) concluded that coastal evolution could be monitored with a much higher resolution in time and space using Argus images than is feasible with traditional monitoring techniques. They state that the advantages of video derived information over infrequent traditional derived information are that the former can better 'quantify the magnitude, accurate location, precise timing and rates of change associated with individual extreme events and seasonal variability in the wave climate'.

Wijnberg et al. (2004) showed that video-derived data provide a more detailed insight in coastal development than traditional monitoring surveys can. They showed that longshore variability was not well sampled with the 250 m longshore spacing of the JARKUS measurements, but that it could be derived from Argus observations. Hence, video-derived data reduce the risk of missing localized threats. Furthermore, Wijnberg et al. (2004) concluded that a higher sampling resolution in time may indicate other than linear trends in coastal evolution.

Smit et al. (2007) explored the added value of high resolution data sets for prediction purposes. They concluded that data-driven predictions of the nearshore flow and sediment transport field benefit from the inclusion of intertidal bathymetry data derived from Argus images. The use of video-derived information was found to improve confidence levels and allow the use of more sophisticated data extrapolation methods. Process based prediction models benefited from the availability of frequent high-resolution video observations through frequent updating of the intertidal bed level and better opportunities for model calibration and validation.

The opportunities that video imagery provides to obtain daily bathymetry data thus enables the study of processes that take place on time and spatial scales that are not well sampled by the traditional measuring campaigns.

1.3 Mapping the intertidal beach

Only processes and features on the beach and within nearshore zone that leave a visible and detectable trace on the Argus images can be used to gain data on the beach and nearshore morphology. This section briefly explains how the bathymetry of the intertidal beach can be derived from Argus images. This subject is described in more detail in Chapter 2.

The bathymetry of the intertidal beach can be derived from ten minute time exposure (timex) images (see Figure 1.2 for examples) by mapping the location of the shoreline[1] and combining its location to the shoreline elevation calculated from hydraulic conditions. Several shoreline detection and elevation models have been developed over time (Plant and Holman, 1997; Aarninkhof, 2003; Plant et al., 2007). By mapping the shoreline thoughout the tidal cycle, a set of elevation contours is obtained. This set functions as a contour map of the intertidal beach. This approach assumes that a bathymetry of the intertidal beach can be obtained from shoreline points that were detected on different hours of the day, because it assumes that morphological changes at tens to hundreds of meters are small over the period of data collection (typically one half to one tidal cycle) (Aarninkhof, 2003).

Currently, mapping the shoreline is a semi-manual process. For this purpose the Intertidal Beach Mapper (IBM) was developed (Aarninkhof, 2003). This is a Matlab based tool to detect shorelines and assign elevations to them. Human quality control on the detected shorelines is still required. Although this assures the quality of the detected shoreline points it is very time-consuming, which limits the use of the tool and hence limits the availability of vast amounts of daily bathymetry data to support research and management.

To speed up shoreline detection and to allow greater availability of intertidal beach bathymetries in time, Plant (Madsen and Plant, 2001) developed a routine to automatically derive waterlines from the timex images: the Auto Shoreline Mapper (ASM). Later, Harley and Cerezo (Appendix B) further improved the tool for the Dutch beach. Although the Auto Shoreline Mapper (ASM) showed to be a promissing addition to the IBM on several beaches around the world (e.g. Duck, NC USA and Narrabeen, Australia), its performance is still not satisfactory on the Dutch beach. The Dutch beach is characterized by a complicated morphology of sand bars and troughs (Appendix A). Furthermore, the distinction between sea and beach is not always clear, as both sea and beach can look brown-grayish depending on the weather conditions. See Figure 1.2 for examples of these problems.

The main problem of the ASM on the Dutch beach is that it stops running within a few days because it runs out of bathymetry data. In short, the ASM requires a certain amount of (self detected) shoreline points for setting the region to detect shoreline points in and for quality control. Unfortunately, it appeares that in the initial version of the ASM the number of detected shoreline points deminishes in time, causing the ASM to finally collapse.

---

1. In this research the waterline is also indicated as the shoreline

A

B

Figure 1.2: Difficulties when mapping shorelines on the Dutch beach. Images from camera 1 of the Egmond Coast 3D site. A: Complicated morphology on March 17th 2006. The sand bar in front of the image is half visible. Should it be mapped? B: Fog blurring the image on March 25th 2006.

Another problem of the ASM was that was not easily usable at all Argus locations. This problem is caused, in the first place, by the inflexibility of the tool. Application of the ASM on beaches, different from the Dutch ones, may demand a different shoreline detection or elevation model. The initial set-up of the ASM did not allow the implemented models to be replaced easily. Also, the structure of the ASM was very complicated as it was still research code. This limits the user friendliness of the tool. Because of the inflexibility and the low user friendliness the ASM was not generally usable.

The difficulties encountered when deriving bathymetry data automatically from video images hamper the large-scale collection of data on high spatiotemporal resolutions. The possibilities offered by the (half) hourly collected Argus images are thus not yet used to their fullest extent. Improvement of the automatic routine is necessary to let research and management benefit from the opportunities that (half) hourly collected video images provide.

1.4 Goal, objectives and research questions

As research has shown, data on small spatiotemporal scales provide better insight into the coastal evolution. Traditional measuring techniques however cannot provide this data at acceptable costs. Argus video cameras collect hourly (or half-hourly) images of the beach, but the manual efforts needed to derive information from these images are too time-consuming to let research and management really benefit from this remote sensing technique. Attempts were made to automatically extract information on the intertidal beach from the Argus images and to make human quality control superfluous. In principle, this would allow for the unlimited daily collection of intertidal bathymetries. However, the automated tool is still in a developmental stage and it has thus far not performed well on the Dutch beach. Another drawback is that the quality of the automatically detected shoreline points may not always be as good as the manually checked points. This raises questions on the use and limitations of automatically detected intertidal bathymetries in data analysis. Therefore, the following research goal is set.

Goal

To automatically derive the intertidal beach bathymetry from Argus images by improving the routine of the Auto Shoreline Mapper and to assess the quality and use of the ASM derived intertidal bathymetries in order to provide recommendations on the application of the ASM in research and management.

The first objective to reach this goal is to improve the ASM tool, both the performance and general usability.

The research questions associated with this objective are:
1) Why does the ASM run out of bathymetry data and collapse in time?
2) What improvements to the ASM are necessary to improve its performance?
3) How can the usability of the ASM be improved?

The second objective is to assess the quality of the ASM derived data and to study the use and possible limitations of ASM derived bathymetries in research and management.

The research questions that belong to this objective are:
4) What is the quality of the ASM bathymetries compared to IBM bathymetries and compared to DGPS data?
5) What are the smallest spatiotemporal scales that can be studied adequately with the ASM bathymetries?
6) What are the possible applications of the ASM obtained intertidal bathymetries in research and management?

1.5 Research approach and outline

To reach the research goal and to obtain answers to the research questions the below approach is followed.

First the usability of the ASM is improved. To achieve this, a new set-up for the ASM is made that allows easy exchange of, for example, different detection models and that is more transparent. Next the performance of the ASM is improved by analyzing what problems cause the ASM to run out of bathymetry data. These problems were solved by creating safety nets to avoid the ASM from running out of data and collapsing. The problems of the current version of the ASM are described in Chapter 2. The new set-up and solutions to the problems are presented in Chapter 3.

Next, the performance of the ASM is tested by comparing ASM obtained intertidal bathymetries to DGPS measurements. This comparison is made based on summary statistics and provides insight into the quality of the ASM data. Thereafter ASM obtained bathymetries are compared to IBM obtained bathymetries by means of coastal state indicators (CSIs). The results of these two comparisons are presented in Chapter 4.

The application of the ASM in studies on the beach behaviour is investigated in Chapter 5. Chapter 6 presents the discussion and finally Chapter 7 presents the conclusions and the recommendations of this research.

2 Shoreline mapping: developments & problems

This Chapter presents the developments of mapping shorelines so far. Particular attention is paid to the Auto Shoreline Mapper. First, the basics of shoreline mapping are given in Section 2.1. Section 2.2 deals with the Intertidal Beach Mapper and serves as background information. Section 2.3 introduces the Auto Shoreline Mapper and Section 2.4 gives an analysis of the problems that need to be solved. The improvements to the ASM and the settings used in this research will be presented in Chapter 3.

2.1 Shoreline mapping in general

The general idea behind shoreline mapping is to link the shoreline location to the shoreline elevation. The shoreline location is detected on images taken by the Argus cameras, the elevation is calculated from offshore measured hydraulic conditions at the time of image collection. The shorelines, detected throughout the tidal cycle, function as elevation contours from which the bathymetry of the intertidal beach can be composed.

2.1.1 Images

An Argus station typically collects three types of images. The snap shot images (see Figure 2.1) function as simple documentation of the conditions, but offer little quantitative information. Time exposure (timex) images are the average of images taken at 2 Hz over a period of 10 minutes. They average out separate waves and all other moving objects, like the people in the front of the snap shot image near the waterline. Variance images help identify regions which are changing in time (like the instantanious waterline) and regions that are not changing (e.g. the dry beach) .

Figure 2.1 A, B and C are oblique images. Using standard photogrammatic theory, oblique images can be rectified to plan images (Holland et al., 1997). An example of a plan view timex image is given in Figure 2.1D. Oblique images provide a poor representation of the far field pixel intensities, owing to decreasing pixel resolutions. In plan images the number of pixels per unit area is constant. This means that all pixels represent an equal area in the real world.

For mapping shorelines two approaches are possible. The first approach starts with detecting the shoreline on an oblique image. Then the elevation of the mapped shoreline (z_s) is calculated[2]. By means of the geometry solution, derived from photogrammatic theory, the image coordinates of the shoreline are transformed to world coordinates. These steps are given in equation (2.1).

$$U_s, V_s + z_s + geom \rightarrow x_s, y_s, z_s \tag{2.1}$$

2. For the Dutch coast z_s is related to the Dutch ordinance level (NAP).

where U_s and V_s are the image pixel coordinates of the shoreline and z_s is the shoreline elevation. x_s and y_s are the world coordinates of the shoreline.

For the second procedure, first the shoreline elevation (z_s) is calculated. Then the oblique image is rectified to a plan image, projected on a plane at elevation z_s, by means of the geometry solution (Equation (2.2)). The shoreline is detected on the plan image. This approach is currently used in ASM.

$$z_s + U, V + geom \rightarrow x, y, z_s \rightarrow x_s, y_s, z_s \qquad (2.2)$$

Where z_s is the shoreline elevation, U and V the image coordinates, and x and y the world coordinates in the plan image. x_s and y_s are the world coordinates of the shoreline.

A: Oblique snap shot B: Oblique time exposure C: Oblique variance

D: Plan view time exposure of the area marked by the red line in B

Figure 2.1: Images taken by camera 1 of the Coast 3D Argus site on May 7th at 10.30 hours.

2.1.2 Detection and elevation models

Several models have been developed to detect the shoreline on timex images. The first models that were developed (e.g. Plant and Holman, 1997) used the distribution of gray-scale pixel intensities, as Argus images were only available in gray-scale. The performance of these models is negatively affected when a clear gray-scale contrast between wet and dry pixels is absent. The introduction of color images led to the development of several new detection models, all using the color contrast between wet and dry pixels to detect the shoreline (Aarninkhof, 2003). Some models allow the detection of only one shoreline feature per transect, which leads to problems in case of emerging sand bars. One of the models that was developed to overcome this problem, uses pixel colors in the HSV (Hue-Saturation-Value) color space to find those pixels that can be identified as the shoreline (Aarninkhof, 2003). Appendix C.1 explains the detection model of Aarninkhof (pixel intensity clustering (PIC)), which is used in this research, in more detail. Other detection models are mentioned Appendix C.2. An overview of the differences and similarities of the models is given in Appendix C.3.

As the detection model identifies the shoreline on time exposure images, the calculated elevation that is assigned to the detected shoreline points, has to take into account all physical processes that affect the location of the waterline during the ten minutes of time exposure (Aarninkhof, 2003). These processes are: the offshore tidal level, offshore wind-induced or surge set-up, breaking-induced wave set-up and swash oscillations. The model to calculate the shoreline elevation is explained in Appendix D.

Error in data points

With shoreline mapping the idea is to find the shoreline location that corresponds to a certain calculated shoreline elevation, or the other way around, to calculate the shoreline elevation that corresponds to a certain detected shoreline location. An erroneous data point can thus be the result of a wrongly detected shoreline, an incorrect elevation, or a combination of both errors. An example of the first two can be seen in Figure 2.2, where the blue dot is the shoreline point that is found. Compared to the true bathymetry, this point is not correct. This could either be the result of a error in the shoreline detection model (x_s is located too much landwards) or the result of an error in the elevation model (z_s is too low).

A combination of the two errors sources might lead to smaller absolute errors, compared to the true bathymetry, than caused by either the detection or elevation model alone. For the case of Figure 2.2, the error compard to the true bathymetry would have been smaller if the shoreline would have been detected more seawards and the elevation would have been calculated a bit higher. The combined result of the two errors (the red dot) results in a better representation of the true bathymetry. However, the combination of the two error sources may also lead to a larger absolute error.

Aarninkhof found that the vertical absolute error between PIC detected shoreline points and DGPS surveyed shorelines is less than 15 cm along 85% of the 2-km-long area of interest. In case of a beach slope of 1:40 this corresponds to a 6 m horizontal offset. On average the vertical offset was -8.5 cm, which reflects a landward offset of the shoreline indicated by the PIC detection model, from the location that corresponds to the calculated elevation (see Figure 2.2).

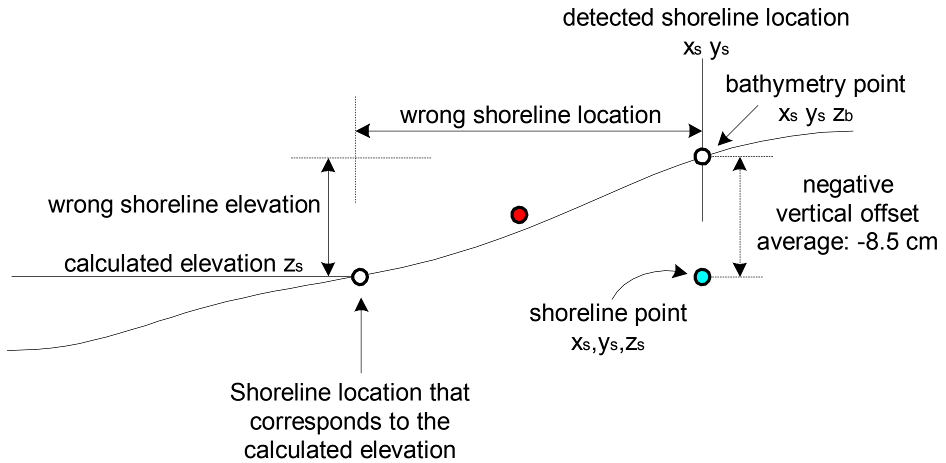

Figure 2.2: Error sources in shoreline detection

2.1.3 Argus database

Both the IBM and ASM are part of the Argus Runtime Environment (ARE). This is a Matlab-based software environment that combines Argus related functionalities. The ARE uses images from the Argus image archive. In the underlying Argus database, meta-information on the images is stored. This information includes, for example, the characteristics of the local site, video station, image processor, camera characteristics and the geometry solutions. Field data such as wave information and tidal levels can also be accessed easily from the ARE. More information is found in the ARE Guidelines (Aarninkhof et al., 2007).

2.2 Intertidal Beach Mapper

Currently, the shorelines are mapped semi-manually using the Intertidal Beach Mapper (IBM) tool. Several researches described in Appendix A used data of the intertidal beach derived with the IBM tool. The IBM is a Matlab-based tool that automatically detects a shoreline within a user-defined region of interest using the PIC detection model. After detection the user needs to accept or reject (parts of) the shoreline. In the latter case the user can manually pick (parts of) the shoreline pixel by pixel. This is a rather time-consuming way to detect the shoreline: it can take up to 4 hours of work for one person to obtain a one-day bathymetry (daylight hours) from five cameras in case of halfhourly images. On the Dutch coast five cameras cover approximately 3 to 4 kms of the beach. The long time needed to detect shorelines with the IBM severely hampers the collection of bathymetry data on a day to day basis. The user interface of the IBM is shown in Figure 2.3.

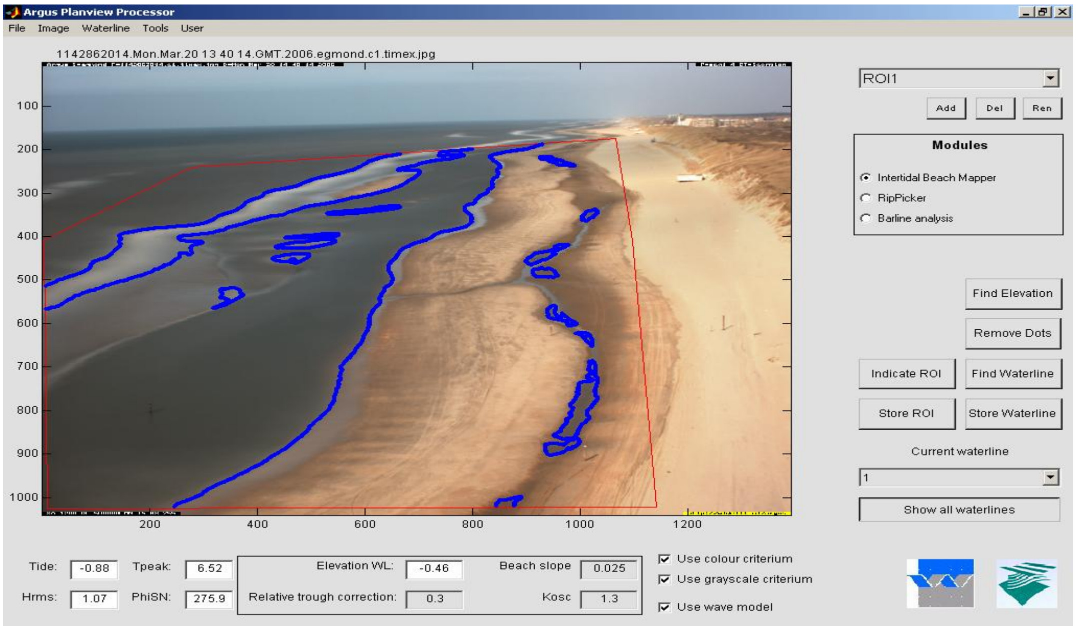

Figure 2.3: User interface of the Intertidal Beach Mapper tool. The user can define the area (region of interest – ROI, the area enclosed by the red line) in which the tool searches for the waterline (blue). The user can manually select the wrong shoreline points and edit these.

2.3 Auto Shoreline Mapper

Because the use of the IBM is still labour-intensive way of deriving bathymetry data, an automated version of the IBM was developed by Plant (Madsen and Plant, 2001): the Auto Shoreline Mapper (ASM). Later on, Cerezo and Harley (Appendix B) made improvements to the ASM to allow its use on the Dutch beach. The ASM is also a Matlab-based tool that uses the same principles as the IBM to detect shorelines. The main differences between the IBM and the ASM are that the ASM automatically determines where to search for the shoreline (region of interest – ROI) and which of the detected shoreline points correctly represent the shoreline.

The next section provides an overview of the developments the ASM has undergone so far. The problems that are encountered are treated in Section 2.4. The solutions proposed to these problems are presented in Chapter 3.

2.3.1 Previous versions of the ASM

Plant's version

Plant's first version of the ASM was based on the SLIM detection model (Appendix C.2). The plan image was projected such that it always filled the bathymetry grid domain, which functioned as a Region of Interest. All points, detected as the shoreline, that were within an area around the expected shoreline location were accepted: so called Area of Acceptance. The location of this area was determined starting with a guess of the bathymetry and an understanding of the variation of the shoreline with changes in tide. The width of this area is determined by the expected variation of the expected shoreline location. In time the Area of Acceptance moves up and down the beach with the tide and is as wide as the variance (Madsen & Plant, 2001; Plant, 2008).

This approach worked rather well on reflective beaches in combination with the SLIM detection model, as this model can detect only one shoreline location per transect. On dissipative beaches however, where emerging sand bars also need to be detected, the former approach did not suffice. Plant then changed from a line based approach to a raster based approach to obtain the Area of Acceptance. Again starting with a guess of the bathymetry the expected location of the shoreline was found. Then, using an estimate of the topographic error, introduced by the interpolation of the bathymetry, the Area of Acceptance was found to be those locations around the expected shoreline were the elevation difference with the calculated water level was less than a certain factor times the topographic error. The rational behind this approach is that if the estimate of the bathymetry is poor, the topographical error will be large and the Area of Acceptance will be wide. Many of the detected shoreline points will then be accepted. The hope is that the detected points are indeed correct. As the bathymetry estimate benefits from more observations, the topographical error becomes smaller in subsequent time steps, leading to a smaller Area of Acceptance (Plant, 2008).

Improvements by Cerezo and Harley

Cerezo and Harley (Appendix B) adapted Plant's version of the ASM and checked its performance against DGPS measurements. They introduced:
1) a rejection criterion based on maximum vertical difference instead of horizontal location;
2) additional rejection criteria
3) two options for a shifting Region of Interest
4) the ability to deal with post-storm conditions.

Ad 1) Instead of accepting those detected shoreline points that are located within the Area of Acceptance, Cerezo and Harley (Appendix B) compare all detected points with a calculated bathymetry: the bench-mark bathymetry. This bathymetry is interpolated from previously detected shoreline points within a certain time window. All points that have a difference with the bench-mark bathymetry that is smaller than a certain value (Z_{dif}) are accepted. The rational behind this type of criterion is that from day to day no large changes occur in the beach bathymetry. This type of criterion does not directly take into account the topographical error introduced by the interpolation.

Points within the bench-mark bathymetry that exceed a certain interpolation induced error can be deleted, leaving gaps in the bathymetry. At these locations detected shoreline points will not be accepted. The rationale here is that there is a maximum error in the bathymetry against which the detected shoreline points are checked.

Under fair weather conditions Cerezo and Harley (Appendix B) found an initial value of 0.50 m for Z_{dif} to be appropriate for the Jan van Speijk Argus site. Later, after a calibration of 18 days of images, Cerezo (Appendix B) found a value of 0.20 m to 0.30 m to be more appropriate.

Ad 2) The additional rejection criteria contain a check on the number of accepted shoreline points. If too many or too little of the detected shoreline points are accepted by the vertical criterion Z_{dif} all points are rejected. A minimum and maximum acceptable number of points is determined as a percentage of the length of the region of interest. The second additional check is on the ratio good points to total points detected. If the ratio is less than one third, the shoreline is rejected entirely.

These checks were probably introduced as a check on the detection itself. An example is the detection of two shorelines, one representing the real shoreline, the other following for example the visible difference between wet and dry sand. Because of the flatness of the Dutch beach both lines might pass the quality check of Z_{dif}. In this case one of the lines should not have been accepted. Cerezo and Harley solved this by rejecting all detected points.

Cerezo concludes that the additional checks are not as accurate as they should be. He suggests calibration for each site and camera.

Ad 3) The shifting region of interest can be achieved in two ways. The first option is that the region of interest is defined as an area around the elevation contour of the calculated shoreline elevation on the bench-mark bathymetry. The second option is that the region of interest has a pre-defined shape that moves in cross-shore direction according to the elevation and the beach slope. The first option is more dynamic than the second one and is used in this research. An example can be seen in Figure 3.5.

Ad 4) Because major morphological changes can be induced by a storm, the post-storm bathymetry is unlikely to be similar to the pre-storm bathymetry. The pre-set acceptable difference (Z_{dif}) between detected shoreline points and a bench-mark bathymetry is therefore loosened (from Z_{norm} to Z_{storm}) for a period of two days after a storm. A storm is defined as an event with H_{rms} wave heights above a certain level ($H_{rms,storm}$). Under storm conditions a value of 0.80 m for Z_{dif} was found to give good results for the site of Narrabeen, Australia. The value for $H_{rms,storm}$ was set at 1.50 m. No values for Z_{storm} and $H_{rms,storm}$ are determined for the Dutch beach yet.

Set-up of Cerezo and Harleys version

A schematic representation of the algorithm of the ASM, with the adaptations of Cerezo and Harley, is given in Figure 2.4 and explained below. This version of the ASM is the starting point of this research.

After initiation, where the settings are loaded, the routine checks whether a storm duration criterion is specified. This is the period in time, set at two days by Cerezo and Harley, that the program looks back to see if any wave higher than $H_{rms,storm}$ occurred within the previous two days. This determines what value for Z_{dif} is used, Z_{storm} or Z_{norm} (step 1). Then the elevation of the shoreline is calculated. The elevation model of Appendix D is used for this. All separate steps are visible in step 2 of the algorithm.

In the third step the image is loaded from the database and rectified to a plan image using the elevation calculated in the previous step and the geometry solution corresponding to the camera (Equation (2.2)).

From data points within a certain time window, that were already stored in the database, the bench-mark bathymetry is interpolated (step 4). For the first few time step the ASM needs human detected shoreline points to obtain a bench-mark bathymetry. This bathymetry is used to determine the region of interest and to check the detected shoreline points against. The region of interest is defined in step 5 as the area around the elevation contour on the bench-mark bathymetry (see also Figure 3.5). Within the region of interest the shoreline is detected (step 6) using the PIC detection model of Aarninkhof (2003).

At last the detected shoreline points are compared to the bench-mark bathymetry in step 7 using the acceptance criterion Z_{dif}. After this comparison the additional checks on the number of data points and the ratio good points to total number of points are performed. If all criteria are met, the accepted shoreline points are stored in the database (step 8) and the routine continues with the next image in time.

Compared to the IBM, the bench-mark bathymetry, in combination with the vertical acceptance criterion has taken over the human control factor in detecting waterlines.

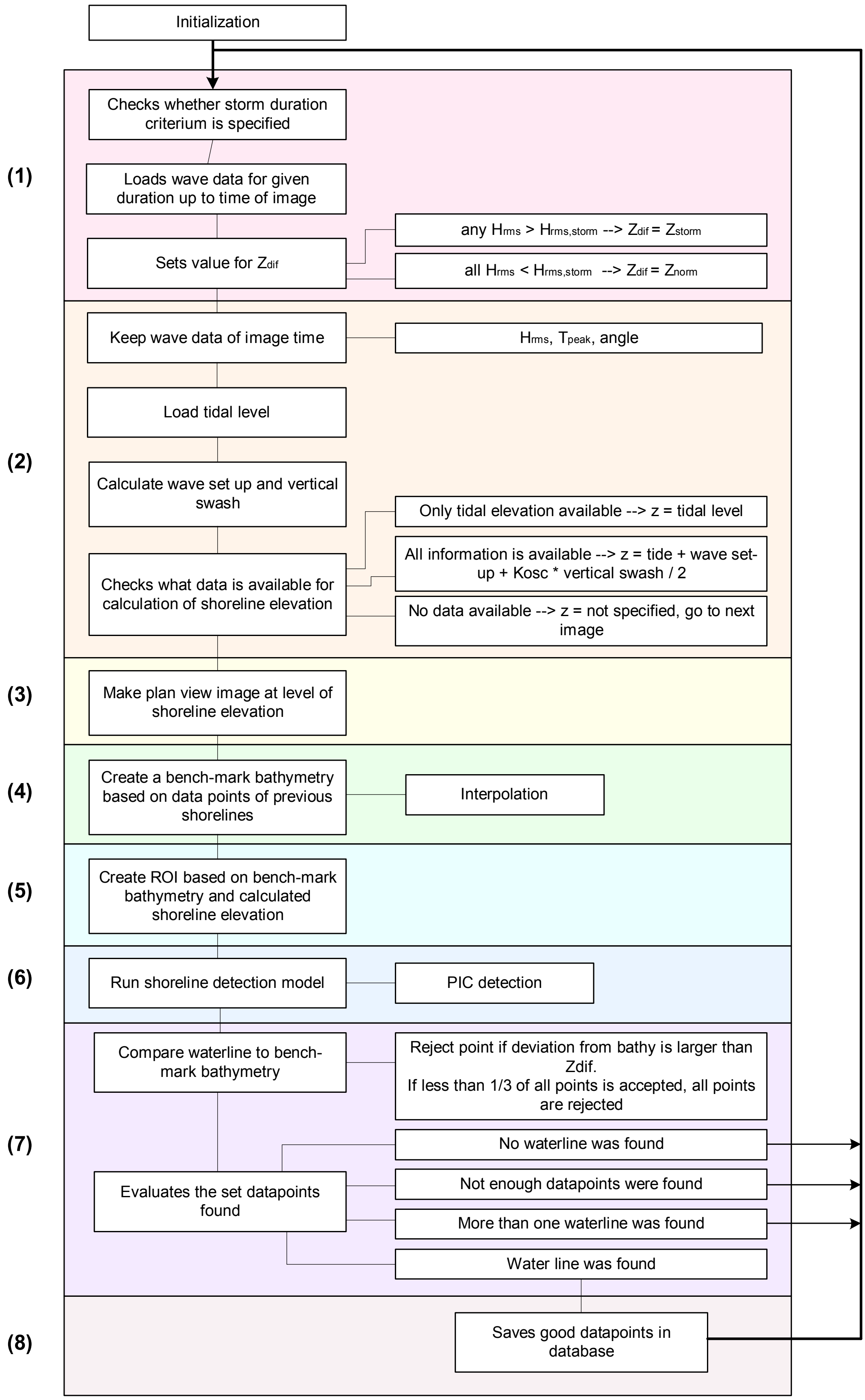

Figure 2.4: Set-up of the ASM version of Cerezo and Harley. Some parts are vary chaotic. The ASM was not flexible nor user-friendly.

Tests by Cerezo and Harley

Cerezo and Harley (Appendix B) ran their version of the ASM on Narrabeen camera 1 for one month from August to September 2005. The output of September 19th was compared to an in situ survey using RTK-GPS. The maximum errors of the Argus derived bathymetry were ±0.3 m.

Cerezo (Appendix B) also ran the ASM at the Jan van Speijk site for September 15th 2000. The maximum errors that were found between a surveyed bathymetry and an ASM derived bathymetry were in the order of ±0.2 m cm. These offsets were not much larger that the offsets that were found between the surveyed bathymetry and an IBM derived bathymetry. Cerezo concluded that the ASM is valid for finding shorelines and also in making accurate bathymetries compared to DGPS data.

2.4 Problems encountered in the ASM

The problems that are encountered with the ASM are twofold. The first problem is that the ASM lacks general usabilty. The second problem is that the performance of the ASM is not satisfactory on the Dutch beach. This section provides an overview of the problems encountered when using the ASM.

2.4.1 Usability

The usability of the ASM is a combination of user friendliness and the ability of flexible application of the tool. Both aspects are not offered by the ASM. The tool is not user friendly as it is intransparant and complicated. This is mainly due to the fact that the ASM is still research code. The tool is not flexible as, for example, the detection and elevation models could not be changed easily to use the ASM on other beaches than the Dutch ones. Furthermore, the code did not allow extensions to be implemented easily. In Chapter 3 therefore a new set-up is presented that provides a more flexible application and that is more user friendly.

2.4.2 Performance on the Dutch beach – a downward spiral

As was already stated in the introduction, the main problem of the ASM is that it stops running within a few days because it runs out of bathymetry data. This data is needed to obtain a bench-mark bathymetry which plays an important role in the determination of the region of interest and which is also used to check the quality of the detected shoreline points (see Figure 2.5). The quality of the bench-mark bathymetry therefore severely affects the performance of the ASM.

The quality of the bench-mark bathymetry itself is in turn affected by the interpolation method and the number and quality of the data points used in the interpolation. If several succeeding time steps result in incomplete bathymetric data, the number of shoreline points used for the interpolation of the bench-mark bathymetries reduces over time. This severely reduces the quality of the bench-mark bathymetry. The result may be that the region of interest no longer covers the entire shoreline (e.g. sand bars are no longer included in the region of interest or that parts of the shoreline are excluded from it). Another result may be that the bathymetry contains many gaps, due to which not all detected shoreline points can be checked. Those points on which no quality control can be performed will be rejected. These problems may start a downward spiral, where, in time, a decreasing number of shoreline points is detected. This means that in time, the quality of the obtained bench-mark bathymetry decreases, which affects the region of interest and the quality control. This finally leads to the collapse of the ASM. The loop of the ASM, with indications for the downward spiral, is presented in Figure 2.5.

The steps that play the most important roles in the initiation of the downward spiral are:

- composing the bench-mark bathymetry;
- determining the region of interest;
- the quality control of the detected shoreline points.

The problems of these steps are treated in more detail in Sections 3.2, 3.3 and 3.4 that also introduce the solutions.

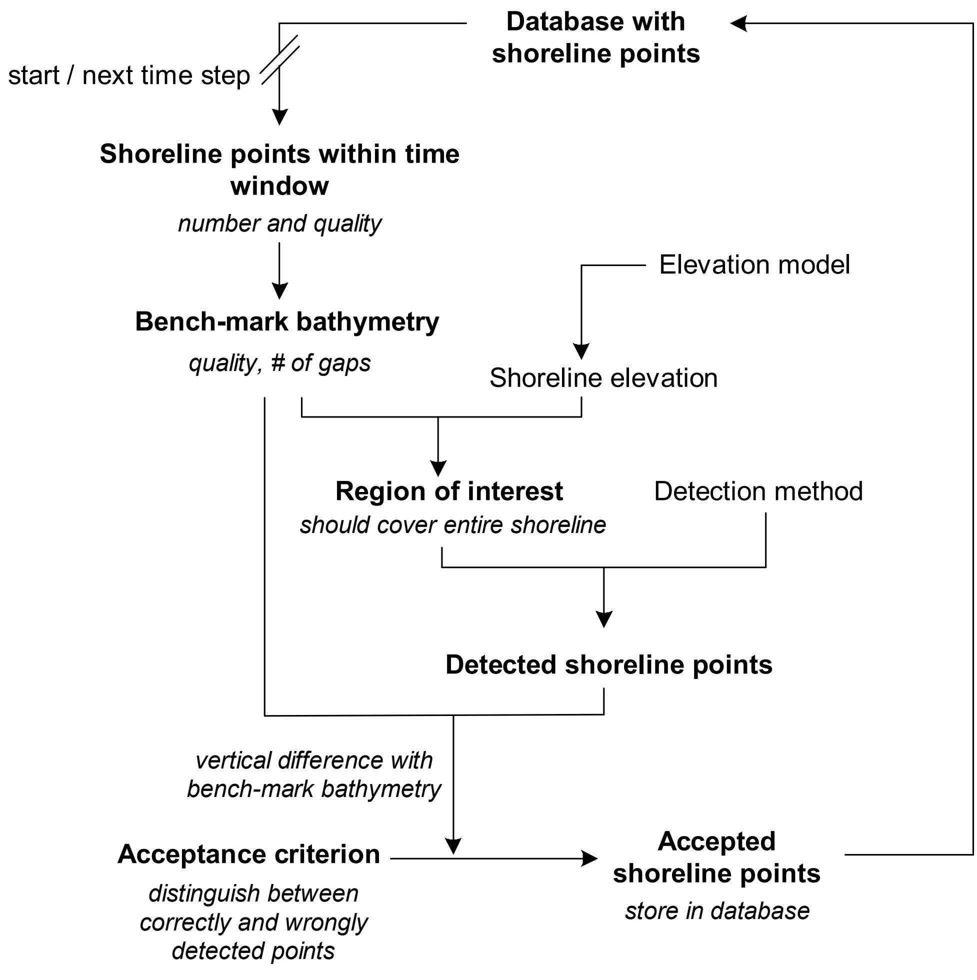

Figure 2.5: Routine of the ASM. When several succeeding time steps do not result in sufficient accepted shoreline points, a downward spiral may be initiated. The bench-mark bathymetry, that is obtained from previously detected shoreline points, cannot be well defined if not enough shoreline points are available within the time window. This affects the region of interest and the quality control.

2.4.3 Shoreline detection

Although the performance of the detection model itself is not investigated in this research it should be mentioned that, using the PIC detection model, it depends on the region of interest which points are detected as the shoreline. This is because the color criterion used to discriminate between wet and dry pixels is a function of the pixel colors within the region of interest. Another region of interest results in another criterion which in turn results in the detection of other points as being the shoreline. Figure 2.6 shows this effect.

2.4.4 Image quality

In the detection of the shoreline points the quality of the images plays an important role. Cerezo (Appendix B) entitles bad image quality as one of the biggest problems at the Jan van Speijk site. The bad image quality is either caused by weather conditions or image characteristics as brightness or contrast. Depending on the conditions, good shorelines can be picked on 30% to 60% of the images. According to Cerezo this still suffices to make a good bathymetry.

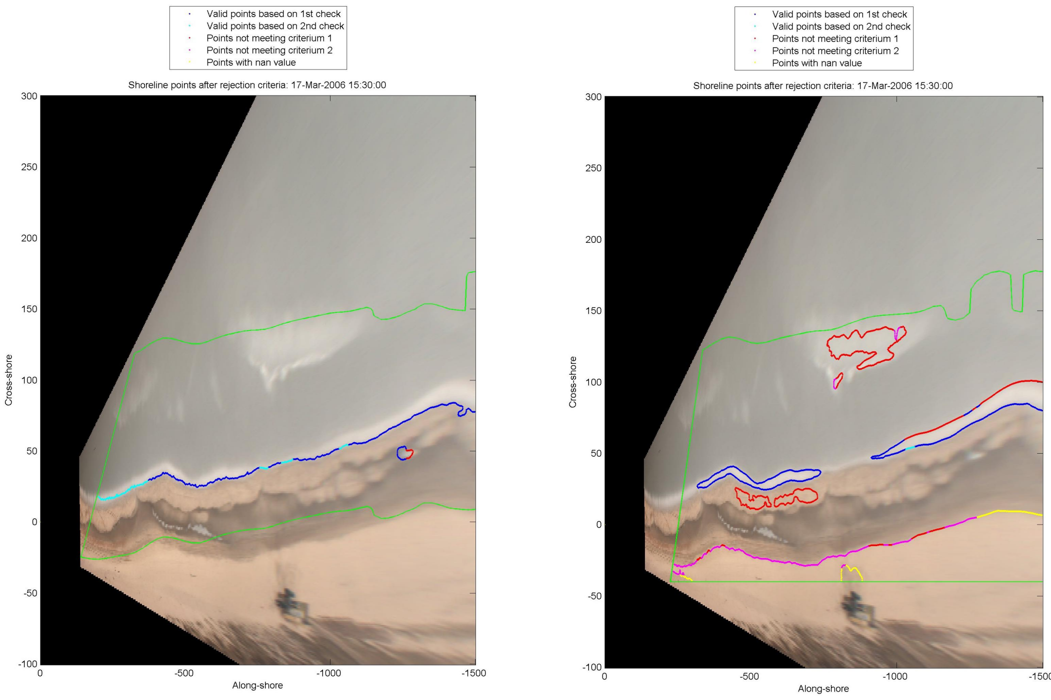

Figure 2.6: Effect of the region of interest on the detected shoreline points. Another shape of the region of interest leads to a different detected shoreline, because the pixel colors within the region of interest are used to determine the color criterion of the PIC detection model. A. Detected shoreline points with a small landward shift of the expected shoreline location. B. Detected shoreline points with a large landward shift of the expected shoreline location. Landward side of the region of interest is cut off at x = -40 m.

3 Improvements to the Auto Shoreline Mapper

The version of the ASM described in the previous chapter is the starting point of this research. The problems listed in Section 2.4, especially those where the bench-mark bathymetry plays a role, cause the ASM to collapse after only a few days of shoreline mapping. Therefore the first research objective was to improve the performance of the ASM and to increase its usability. This section presents the improvements made to the ASM.

Before any improvements on the performance of the Auto Shoreline Mapper are made, the set-up of the tool is reorganized into a flexible environment that easily allows for improvements and extensions and that simplifies the use. The new set-up is addressed in Section 3.1. Section 3.2 gives some details on the bench-mark bathymetry as it plays an important role in both the determination of the region of interest and the quality control on the detected points. Section 3.3 presents the improvements made to the determination of the region of interest. The improvements made to the quality control of the detected shoreline points are treated in more detail in Section 3.4. Other smaller improvements made to the ASM are included in Appendix E.3. Section 3.5 discusses the improved performance of the ASM and the remaining problems. Suggestions for further improvements are made in Section 3.6.

3.1 Usablity improved by new set-up

As can be seen in Figure 2.4 the old set-up of the ASM was very complex in some parts, since the ASM was still research code. The old set-up was very inflexible as it did not easily allow extensions or use on beaches that are not similar to the Dutch ones[3]. Examples of the inflexibility are the detection and elevation models and the quality control that are included in the program in a fixed manner (hard coded). These steps can only be changed by altering the code itself, which makes the tool rather user unfriendly.

Therefore, a new set-up was developed that can be easily understood and that provides flexibility for use and possibilities for improvement and extension. The basic idea is that, for every image, one main routine calls different second-level routines one by one to perform the various steps needed for shoreline detection. This set-up allows one second-level routine to be replaced easily by another routine that provides the same kind of output (e.g. replace the PIC detection model by another detection model). The new set-up and the second level routines that are called in this research are visualized in Figure 3.1. The colors of the second-level routines correspond to the steps of the ASM in Figure 2.4.

Output from one second-level routine is stored in a structure[4] that is passed on to the next second-level routine by the main routine. The settings that are used by the various second-level routines are also stored in the structure. They are loaded in the first step of the main routine. The second-level routines that are called by the main routine are also listed in the

3. Other detection and elevation models might be needed on beaches not similar to the Dutch ones.
4. A structure is a variable with various fields (that can contain fields itself)

settings. So, for every time step, the main routine first reads from the structure which second-level routine to call, then the second-level routine reads the settings it needs from the structure and finally the output of the second-level routine is stored in the structure. Then the next second-level routine is called. Second-level routines can be deleted or added by simply not calling for them or extending the number of second-level routines called respectively. More technical details on the new set-up are given in Appendix E.

This new set-up provides an environment that allows the use of different second-level routines that better fit the conditions on beaches other than the Dutch ones. It even allows the use of the ASM in laboratory conditions[5].

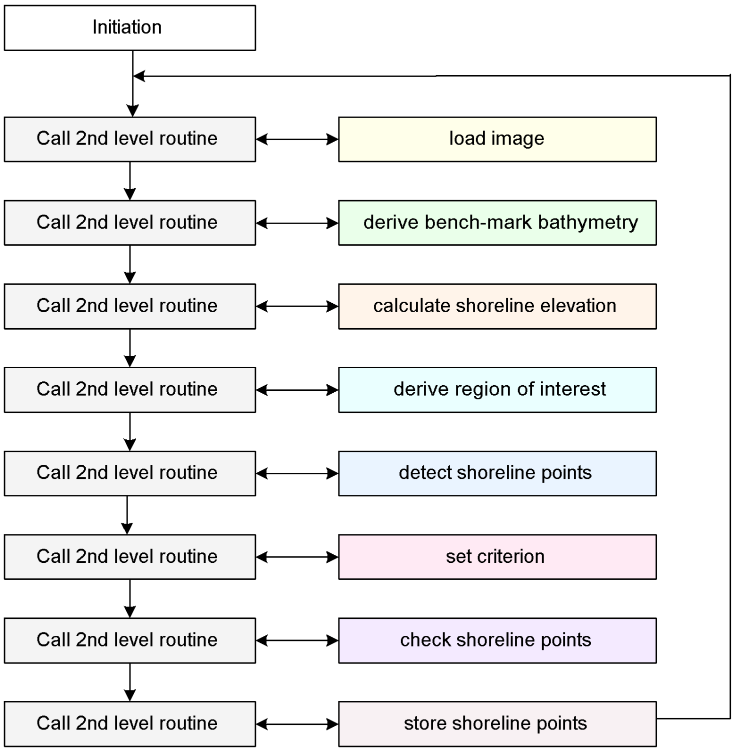

Figure 3.1: The main routine calls for secondary routines to perform the various steps needed to map the intertidal bathymetry. Output of one secondary routine is passed on to the next by the main routine.

3.2 The bench-mark bathymetry

Cerezo and Harley (Appendix B) introduced a moving region of interest and a quality control that both depended on the bench-mark bathymetry. In this research these two steps will be performed the same way as in the ASM version of Cerezo and Harley. Therefore the derivation of the bench-mark bathymetry is looked at in more detail in this section.

The bench-mark bathymetry is composed from previously detected shoreline points within a certain time window. Two things that affect the bench-mark bathymetry are the type of

5. Research currently performed at Deltares

interpolation that is used and the number of shoreline points within the timeframe. In this study the loess interpolation method is used to derive bathymetries, as this is an suitable interpolation method to obtain bathymetries (Plant et al., 2002). The loess interpolation method is a linear smoother. Different smoothing scales can be applied, which affect the quality of the bench-mark bathymetry. This section shows the effect of a) using different smoothing scales and b) the time window. But first the loess interpolation method is explained shortly.

3.2.1 Loess interpolation

The loess interpolation method is a linear smoother that interpolates the randomly spaced observations (shoreline points) to a regularly spaced grid. The interpolated point is calculated using Equation (3.1) (Storlie and Helton, 2008; Nipius, 2002).

$$z_i = \hat{\alpha} + \hat{\beta}\vec{z}_j \tag{3.1}$$

Where z_i is the calculated value in the interpolated point and $\vec{z}_j$ the set of observations that is used to calculate z_i. The values for $\hat{\alpha}$ and $\hat{\beta}$ are determined as those values for α and β that minimize the sum in Equation (3.2).

$$\sum_{i=1}^{N} (\alpha + \beta z_i - z_j)^2 \cdot W_{ij} \tag{3.2}$$

where W_{ij} is the weight assigned to the location of z_j. W_{ij} is given by Equation (3.3)

$$W_{ij} = \left[1 - (w_{ij})^3\right]^3 \text{ if } w_{ij}<1, \text{ otherwise } W_{ij} = 0 \tag{3.3}$$

where w_{ij} is given by Equation (3.4)

$$w_{ij} = (\vec{x}_j - \vec{x}_i)^2 \left[L\right]^{-1} \tag{3.4}$$

where $\vec{x}_j$ and $\vec{x}_i$ are the locations of the observation and the interpolation point respectively. L is the 2-by-2 (2 is the number of dimensions in $\vec{x}$) diagonal matrix. L is given by Equation (3.5).

$$L = \begin{bmatrix} (L_x)^2 & 0 \\ 0 & (L_y)^2 \end{bmatrix} \tag{3.5}$$

Its smoothing properties are thus controlled by two scaling parameters: L_x ([m] cross-shore) and L_y ([m] alongshore).

An advantage of the loess interpolation is that it removes variability from the data producing a more reliable and smoother estimate of the bathymetry. Other interpolation methods that do not remove variability in the data (e.g. nearest neighbor interpolation) might show short scale variability that is not necessarily accurate.

3.2.2 Interpolation errors

Every interpolation introduces errors. For all linear interpolation methods the interpolation reliability can be described using three measures of error.

The first is the normalized mean square error. This describes the fraction of the measurement error that passes unchecked through the interpolation method. This error can be computed independent from the actual data; it depends only on the choice of the interpolation method and the distribution of the observations. It is given by equation (3.6).

$$\hat{\varepsilon}_i^2 = \sum_j \hat{a}_{ij}^2 \tag{3.6}$$

where $\hat{a}_{ij}$ is a set of weights assigned to the observations

If, for example, the average value of $\hat{\varepsilon}$ is 0.50 and the expected measurement error of the observations is 0.15 m then interpolation method is expected to yield bathymetry estimates with an rms error of 0.075 m due to this contribution.

The second measure is the weighted mean square residual. This describes the spatially varying misfit between the smooth, interpolated surface and the observations. This measure may be used to reflect the damage done by the interpolation to the resolved scales of the true bathymetry. It is given by equation (3.7).

$$\hat{q}_i^2 = \frac{1}{\hat{\varepsilon}_i^2} \sum_j (\hat{z}_i - z_j)^2 \hat{a}_{ij}^2 \tag{3.7}$$

where $\hat{z}_i$ is the calculated elevation at point i and z_j is the observation in point j.

If the residuals are due to measurement errors alone, the estimate of the mean square interpolation error is given by equation (3.8).

$$\hat{s}_i^2 = \frac{\varepsilon_i^2}{1-\varepsilon_i^2} (\hat{q}_i)^2 \tag{3.8}$$

This error estimate is the expected variance of the difference between the true bathymetry and the interpolated bathymetry (Plant et al., 2002).

3.2.3 Effect of smoothing scales and timeframe

The interpolated surface thus contains errors introduced by the interpolation itself. $\hat{\varepsilon}$ can be used to restrict analysis of the interpolated bathymetry to those parts where the errors are tolerably low (Plant et al., 2002). In this research a value of 0.50 is used. At those locations where $\hat{\varepsilon}$ is larger than 0.50 the elevation data are removed leaving gaps in the bathymetry.

This leads to problems in determining the region of interest and checking shoreline points, as no contour can be determined and no points can be checked at the locations of the gaps.

One way to reduce the number of points that are removed is to use larger smoothing scales (L_x and L_y). Another way is to use more shoreline points in the interpolation by enlarging the time window. Figure 3.2 shows the effect of both measures.

As can be seen when comparing Figure 3.2 A and C, increasing the smoothing scales reduces the gaps. A drawback of the larger smoothing scales is that the detail in the obtained bathymetry reduces. This can be seen at the alongshore location of -700 m, where a bulge in the +0.50 m NAP contour is visible in bathymetry A. This bulge is absent in bathymetry C. Also the sand bar is less pronounced in the C bathymetry than it is in the A bathymetry. Reducing the number of gaps by using larger smoothing scales thus comes at the cost of loosing detail in the obtained bathymetry.

Increasing the time frame seems to reduce the gaps somewhat, as can be seen when comparing Figure 3.2 A and B or C and D. Increasing the time window is especially important if very little shorelines are detected on one day, because in that case even the large smoothing scales lead to a bathymetry with many gaps. Enlarging the time window in such a case could result in less gaps the batymetry, which makes it better usable for data analysis.

3.3 Region of interest

In this research the region of interest is determined as the area around the expected shoreline location. This location is found by determining the contour of the shoreline elevation on the bench-mark bathymetry. An example of the expected shoreline location can be seen in Figure 3.5, the blue line. The red line in Figure 3.5 encloses the region of interests. The extent of the region of interest seawards and landwards of the expected shoreline location is user-defined.

3.3.1 Extension of the region of interest

The quality of the bench-mark bathymetry has great influence when defining the region of interest. On a bathymetry with many gaps there may not be an expected shoreline location at every alongshore location (see Figure 3.3). The blue lines in Figure 3.3 are the expected shoreline locations. These locations are shifted seaward and landward to form the region of interest (green line). From Figure 3.3 it becomes clear that this expected waterline does not result in a suitable region of interest as it does not cover the entire alongshore direction. As only within the region of interest shoreline points can be detected, a problem like this might initiate the downward spiral described in Section 2.4.2.

To overcome the problem of a ‘short’ region of interest, the region of interest is extrapolated to the edge of the image. A drawback of this solution is that the extrapolated region of interest does not follow the curves of the beach. Especially on non-straight coasts this can lead to problems. Therefore the cause of the problem, the gaps in the bench-mark

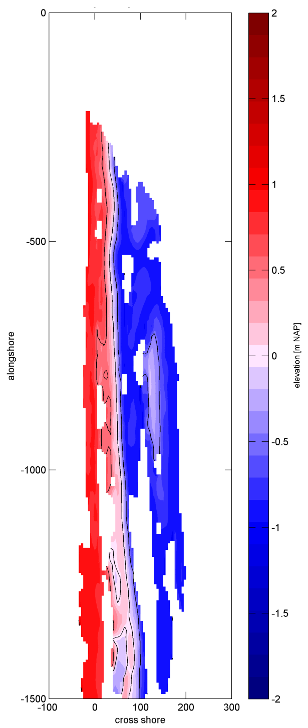

A: L_x = 10 m; L_y = 25 m;
time window = 1 day

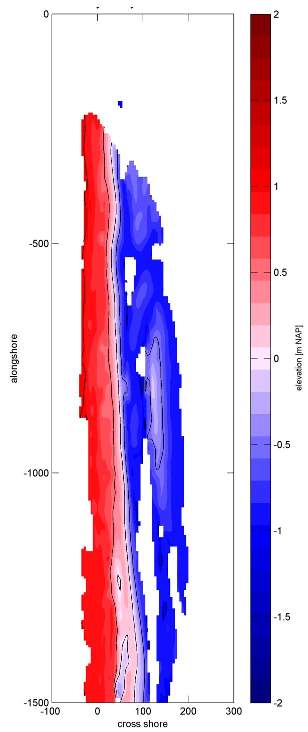

B: L_x = 10 m; L_y = 25 m;
time window = 3 days

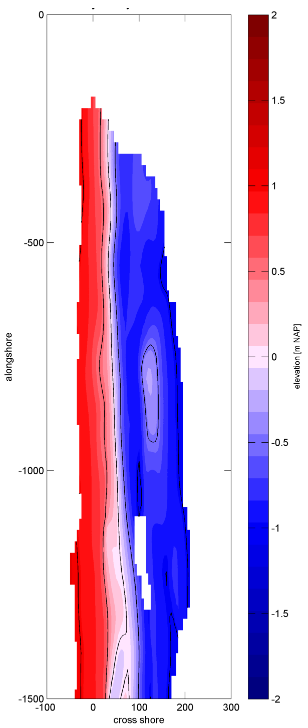

C: L_x = 25 m; L_y = 100 m;
time window = 1 day

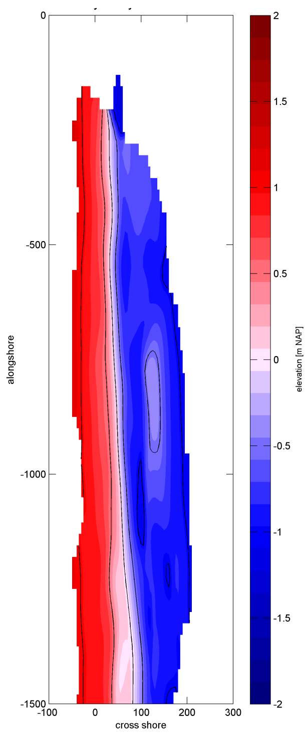

D: L_x = 25 m; L_y = 100 m;
time window = 3 days

Figure 3.2: Influence of smoothing scales and time window on the number and size of gaps in the interpolated bathymetry of March 18th 2006. The bathymetries derived with a time window of three days are composed of shoreline points of March 17th to 19th.

bathymetry, was treated by using a bench-mark bathymetry with a large time window and large smoothing scales. In this research the region of interest is determined on a bench-mark bathymetry with smoothing scales Lx = 25 and L_y = 100 and a time window of two or five days. As even on these bathymetries nan-values can occur, extension of the region of interest remains necessary.

3.3.2 Zigzagging region of interest

Another problem encountered when defining the region of interest are the double or triple expected shoreline locations at a certain alongshore location. This problem arises in images with emerging sand bars. As all expected shoreline locations are transposed landward and seaward this leads to zigzagging of the region of interest. This can be clearly seen in Figure 3.4. Zigzagging of the region of interest might result in exclusion of sand bars or parts of the shoreline from the region of interest. The latter is the case in Figure 3.4. This makes detection impossible and thus bathymetry information at the time step of that image is incomplete. This can initiate the downward spiral described in Section 2.4.2.

To overcome the problem of the zigzagging region of interest, only the outer points of the zigzagging part are used to define the region of interest. This leads to inclusion of both the sand bar as well as the entire shoreline (see Figure 3.5), which allows for correct detection.

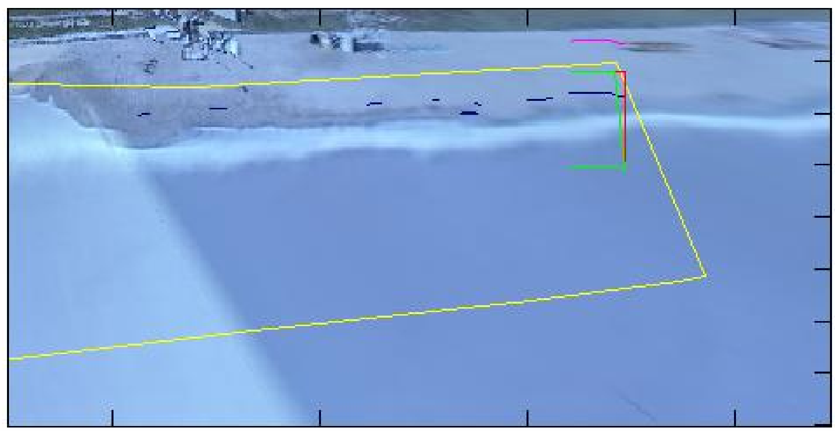

Figure 3.3: Bad definition of the region of interest on a rectified and merged timex image. The yellow line is the old region of interest that is too big; the blue line is the expected location of the waterline; the purple line is the landward extension of the blue line; the green line is the eventual region of interest, of which the lower line is the seaward extension of the blue line and the upper line is a cut off value to exclude buildings close to the dunes. The red line is an intermediate step in defining the green line.

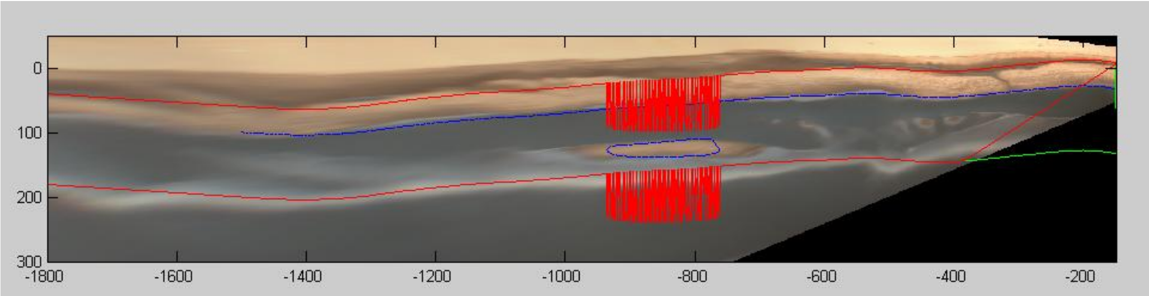

Figure 3.4: Zigzagging region of interest (red) blocks part of the shoreline; this part of the shoreline will not be detected. The blue line is the expected shoreline location. The red line is extended towards the end of the image at the left. At the right the region of interest is cut of, to exclude the black pixels. The green line is an intermediate region of interest in which the black pixels were not yet eliminated.

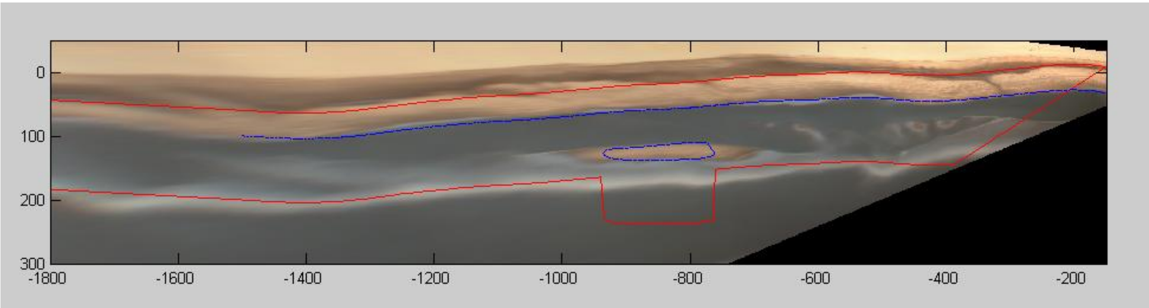

Figure 3.5: Region of interest including the entire shoreline, both the continuous shoreline and the emerging sand bar.

3.3.3 Seaward and landward shift

The seaward and landward shifts of the expected shoreline location determine the width of the region of interest. How far the expected shoreline location should be shifted landward and seaward is different for every beach site and depends on the dominant morphology.

Dissipative beaches as the Dutch ones often show emerging sand bars. These also need to be included in the region of interest. This however is not always the case. The reason for this is that sometimes the sand bars in the bench-mark bathymetry do not have the calculated shoreline elevation or are not present at all. This is either because they are smoothed by the loess interpolator or because the bench-mark bathymetry is based on shoreline data where the sand bar has not been identified. Because of these reasons the sand bars may not be included in the region of interest if the seaward shift is set too small. This is visualized in Figure 3.6. A solution is to increase the seaward shift. However, if it is set too large, water pixels may be overrepresented in the region of interest, which can lead to detection problems when using the PIC detection model. In this research a shift of 100 m showed to give good results for Egmond. The seaward shift that should be applied is site dependent. On beaches flatter than the Dutch ones, a larger seaward shift might be necessary, while on steeper beaches the problem described above may not even occur as emerging sand bars are mostly not present on such beaches.

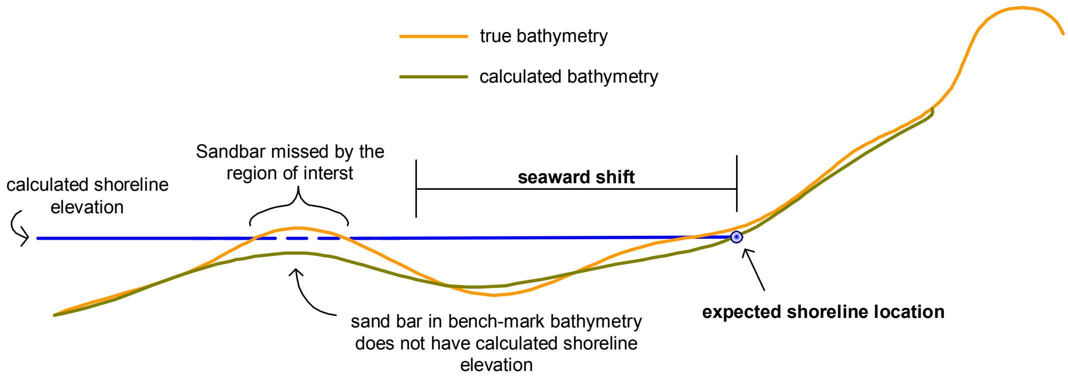

Figure 3.6: Sand bar excluded from the region of interest because it is not recognized as an expected shoreline location.

Also the landward shift on dissipative beaches is unfortunately not straightforward. Ideally, the landward shift should be small enough to exclude pools on the beach from the region of interest and large enough to include enough sand pixels to support colour-based detection models. This combination is however hardly possible. Another problem with the landward shift results, as with the seaward shift, from the loess interpolation and the absence of elevation data a certain points. If bathymetry data are missing from the area in between the sand bar and the beach, the bench-mark bathymetry may be too high. In that case only the most seaward location of the shoreline is identified as the expected shoreline location. A too small landward shift then excludes parts of the landward shoreline. This is visualized in Figure 3.7. Figure 3.8A shows the problem in reality. Many parts of the landward shoreline are excluded from the region of interest. Figure 3.8B shows how the problem is solved by using a large landward shift; at x= -40 the region of interest is cut off, to exclude buildings from the region of interest. A drawback of the large landward shift is that pools on the beach are included in the region of interest and can mistakenly be identified as the shoreline. In Chapter 4 the bathymetries derived with a small and with a large landward shift are compared. In the rest of this research however, a large landward shift is used, as the advantage of including the entire shoreline is considered to be more important to gain good results than it is to exclude pools.

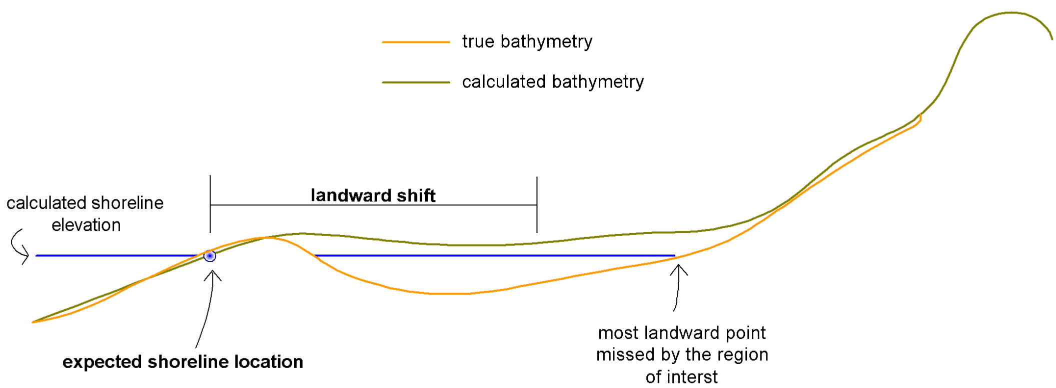

Figure 3.7: Landward shoreline excluded due to a too high bench-mark bathymetry

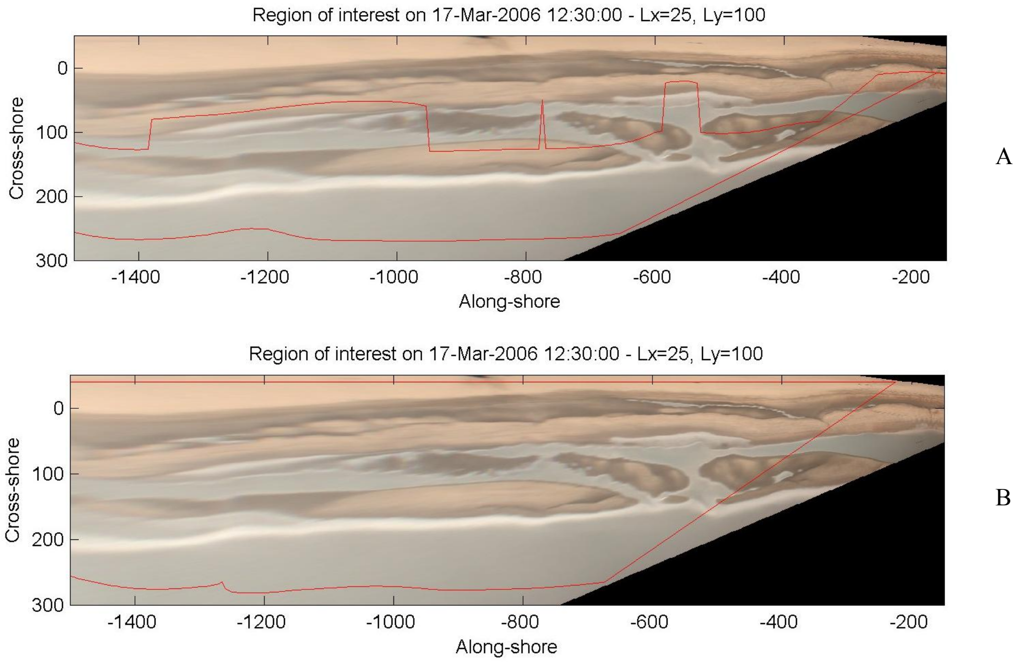

Figure 3.8: Landward shift. A: small landward shift (40 m). Parts of the shoreline are excluded from the region of interest. B: large landward shift (300m). The complete shoreline is included in the region of interest

3.4 Quality control

In the updated version of the ASM the basics of checking the detected shoreline points are similar to the version of Cerezo and Harley. The detected shoreline points are still compared to a bench-mark bathymetry. All points that differ too much from the bench-mark bathymetry are not accepted. This step is thus greatly influenced by the quality of the bench-mark bathymetry. The acceptable verticale difference is defined by the user.

3.4.1 Bench-mark bathymetry in quality control

Problems in comparing the detected shoreline points against a bench-mark bathymetry occur when a detected shoreline point is compared to a gap in the interpolated bathymetry. As no comparison can be made in that case, the detected point is rejected, although it may have perfectly detected the shoreline. This problem of rejection against gaps is clarified by Figure 3.9.

As mentioned before, the gaps in the bench-mark bathymetry result from a lack of data points and small smoothing scales. Increasing the smoothing scales would result in less gaps, but also affects the detail of the interpolated bathymetry (compare Figure 3.2A and C). Too much smoothing is therefore not advisable. Another option is to include more shorelines points in the interpolation by increasing the time window. A combination of both solves most problems with nan-values.

To combine the advantage of high detail resulting from small smoothing scales with the advantage of few nan-values in case of large smoothing scales, two bench-mark bathymetries are used in this research. The first bathymetry is based on shoreline points within a time window of one day with smoothing scales of L_x =10 m and L_y =25 m. The second is based on shoreline points within a time window of two days[6] with smoothing scales of L_x = 25 m and L_y = 100 m. The time window of the second bathymetry is set at two days to ensure the derivation of a bench-mark bathymetry when no or hardly any shorelines were detected at one day due to, for example, fog.

When checking the quality of the detected shoreline points, all points are first compared with the first bathymetry. Those points that were rejected because they are located at a gap location are then checked against the second bathymetry. This leads to a much higher number of accepted shoreline points (see Figure 3.10).

It has not been investigated what the advantage of the large detail, provided by the first bathymetry, is for the performance of the ASM. If the same large smoothing scales were used for both bathymetries, the advantage of the second bathymetry would still be the larger time window that can be used. The second bathymetry can function as a safety net after a few days of poor detection or in case of a storm. The shorelines that have been detected just after a storm can then be used to compose the first bathymetry, so that newly detected shorelines are compared to the post-storm bathymetry in the first place. It is expected that this is the biggest advantage of the two-step check.

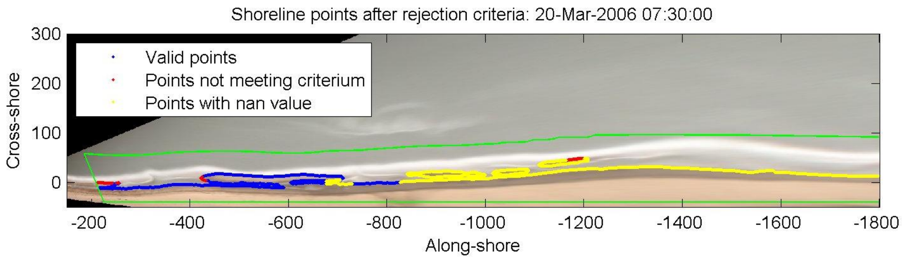

Figure 3.9: Detected shoreline points. Many points are rejected because the bathymetry against which the points are checked contains gaps at the location of the points.

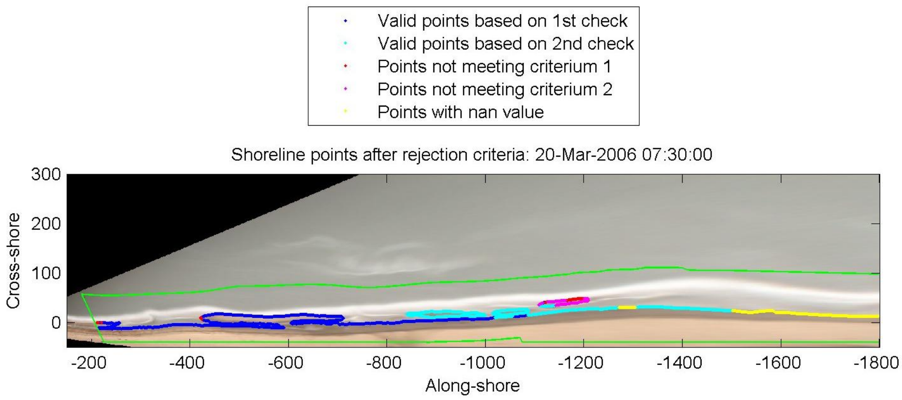

Figure 3.10: Detected shoreline points checked against two bathymetries. Fewer points are rejected against gaps in the bathymetry.

6. In some runs five days has also been used as a time window

3.4.2 Acceptance criteria

One of the most important parameters in automatically accepting or rejecting the detected shoreline points is the rejection criterion Z_{dif} that was introduced by Cerezo and Harley (Appendix B). If the vertical difference between the detected point and the bench-mark bathymetry is smaller than a user-defined value the shoreline point is accepted. If the value for Z_{dif} is set too large, wrong shoreline points might be accepted. If the value is too small hardly any shoreline point might be accepted. The choice for the value of Z_{dif} is a trade-off between possibly accepting wrongly detected shoreline points or possibly rejecting good shoreline points. In addition, Z_{dif} has to be sufficiently large to accommodate any changes of the bathymetry at daily time scales. The influence of the acceptance criterion on shoreline detection and the influence on the derived bathymetries of Egmond beach will be looked at in more detail in Chapter 4.

One major flaw of this type of acceptance criterion is that it does not take into account the uncertainty of the bench-mark bathymetry. The errors introduced by the interpolation (Section 3.2) vary spatially with the number and variation of the shoreline points that are used in the calculation of each interpolation point. If the error band of a certain point in the bench-mark bathymetry is larger than the used acceptance criterion, this leads to the odd situation where the detected points is rejected, while it may better represent the true bathymetry than the bench-mark bathymetry itself. The next section presents a suggestion to adopt the vertical acceptance criterion to include interpolation errors.

The additional checks that were introduced by Cerezo and Harley showed to be unnecessary in the improved version of the ASM. As Cerezo had already concluded that these tests were not as accurate as they should be, they were removed as acceptance criteria.

3.5 ASM performance and remaining problems

To examine how the improvements have affected the performance of the ASM, the tool was run from March 17th 2006 till July 14th 2006 when it was terminated. The settings that were used for this run are listed in Appendix E.4. The only human controlled information that the ASM could use were the manually mapped shorelines of March 15th and 16th 2006. These shorelines were used by the ASM to construct the first bench-mark bathymetries. Although manually mapped shorelines are available for subsequent days, these were made temporarily unavailable for the ASM to see how well the ASM would perform on its own account and to see for how long it would run without human intervention.

The next sections present the conclusions on the improved performance of the ASM, the man-hours that are saved and on the remaining problems. Also suggestions for even further improvements are given.

3.5.1 Improved performance

The most significant improvement to the performance of the ASM is that it continues running for a very long time, 4 months, without the need of human support. The ASM did not collapse on two days of fog, when very little shorelines were accepted, nor on a minor storm. The second bench-mark bathymetry functioned well as a safety net on both occasions, both in finding the expected shoreline location and in the quality check. The combination of a well defind region of interest and the double quality check were the most important improvements. A visual inspection of the detected shoreline points suggests that on 70% of the images the shoreline was mapped more or less correct, but grave errors are also still made on some images.

The problems of the version of Cerezo and Harley with the short region of interest and the persisting exclusion of sand bars or parts of the shoreline from the region of interest are completely solved by the improvements. For all images of the test period the region of interest was well defined, no parts of the shoreline were excluded which allowed, in principal, the detection of the entire shoreline.

3.5.2 Man-hours saved

The automatic detection of shorelines saves many man-hours. Manually mapping daily bathymetries for one camera for a period of 4 months would have taken at least 60 hours, in case of half-hourly images. The ASM needed approximately 180 hours, but no human control was required. This time can probably be reduced by further improving the ASM and running it on a faster computer. In practice the ASM could be run each night detecting shorelines on images of the day before.

The ASM allows for the collection of shoreline data on those images that were already collected and those that will be collected in the future. A huge amount of daily bathymetries would then become available. Manually mapping shorelines on such a large scale is not feasible because of the enormous effort it would require. Both research and management are expected to benefit from the large amount of daily bathymetries that can become available by use of the ASM.

Although the chance that the ASM collapses has been greatly reduced, it is still possible. In that case shorelines should be mapped manually for two or three days from which the ASM can be restarted. Quality control on the obtained bathymetries should be performed once in a while. It is advised to use all available DGPS data for this quality control and to compare the ASM obtained bathymetries to the yearly Jarkus measurements. Comparison to manually mapped shorelines may also remain necessary.

3.5.3 Remaining problems

For some images, no or hardly any shoreline was found. This was either due to the weather conditions (fog) or because the PIC detection algorithm did not find a good color distinction (general detection problem). These problems are not always straightforward, as sometimes shoreline points were detected on fog-images and sometimes hardly any shoreline points were detected on a fair-weather-images. Detection problems such as these are not a part of the scope of this research. Figure 2.6 showed that the detected shoreline was also influenced by the region of interest. This is inherent to the use of the PIC detection model and it is also not further investigated in this research.

One problem that still remains with these settings is that of the 'disappearance' of the sand bars. When the water elevation is higher for a few days, the sand bar does not emerge at low tide and is thus not detected. If the water level, after a few days of high elevations, becomes low enough for the sand bar to emerge again it can be detected because it is included in the ROI due to the improvements on that part. However, the sand bar points may not be accepted as the sand bar may no longer be present in either of the bench-mark bathymetries. The same problem can occur when the sand bar is not detected for two days due to fog or bad detection in general. A solution to avoid disappearance of sand bar would be to increase the time window of the second bathymetry such that sand bar bathymetry data are included. A study of the shoreline elevation changes over time for the period of the test might give some clues on the needed time window.

The test showed that even with the small time windows of one and two days the sand bar was 'rediscovered' after some time. This was caused by the large smoothing scales of the second bench-mark bathymetry. These not only smooth the bench-mark bathymetry, but also stretch it slightly seawards and landwards beyond the most seaward and landward located shoreline points within the time window. How far the bench-mark bathymetry is stretched depends on the smoothing scales. Detected shoreline points can then be compared to the stretched parts of the bench-mark bathymetry. The accepted points are stored in the database, and are included in the time window of the next bench-mark bathymetry. In this way the bench-mark bathymetry can build outwards in time, which can eventually lead to the rediscovery of the sand bar. The build out can be seen in Figure 3.11.

A point of discussion is the value of Z_{dif}. Sometimes good shoreline points are rejected while at the same time, for the same criterium, wrong shoreline points are accepted. This was already indicated by Cerezo and Harley (Appendix B), and it is confirmed by this test. The value of Z_{dif} is a trade-off between accepting wrong points and rejecting good points. As the bench-mark bathymetries are constructed from self-detected shoreline points this trade-off probably affects the performance of the ASM as the bench-mark bathymetry play an important role in both the determination of the region of interest as well as in the quality control. To gain some insight into the effect of the value for Z_{dif} on the obtained data two case studies are performed. These are presented in Chapter 4.

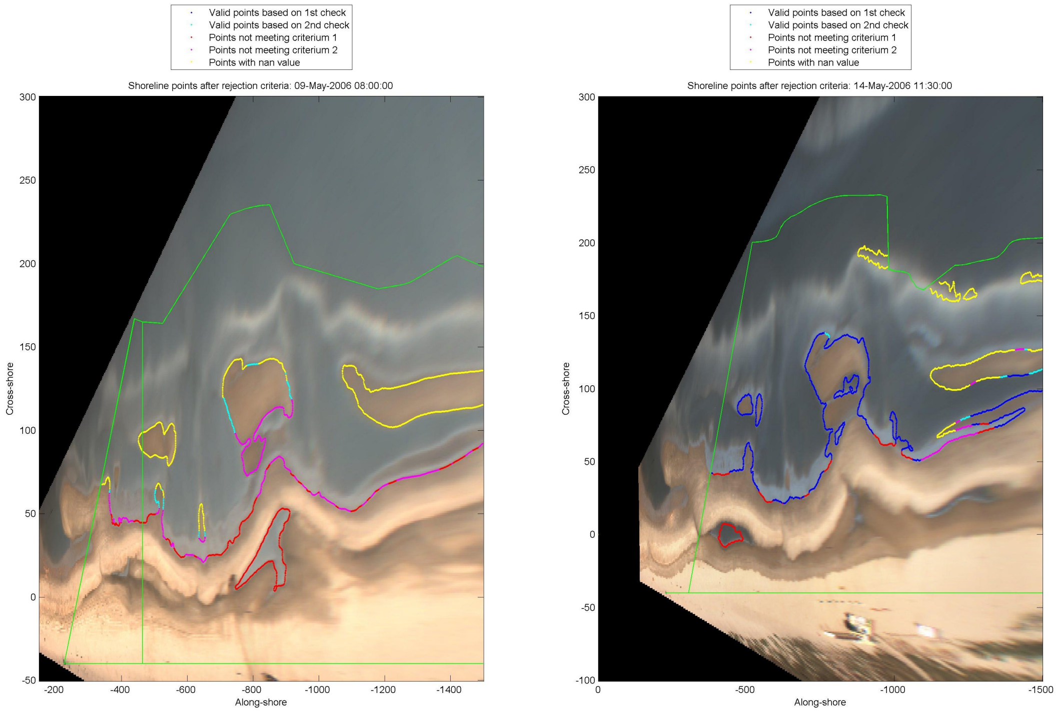

A B

Figure 3.11: Rediscovery of the sand bar. A: Parts of sand bar are rejected based because they are compared to gaps in the bench mark bathymetry. B: The sandbar is completely accepted completely again, the gaps in the bench mark bathymetry have disappeared.

3.6 Suggestions for further improvement

Although the performance and usability of the ASM have been improved tremendously there are still some points on which the algorithm could be improved even further. These points are indicated in this section.

3.6.1 Bench-mark bathymetry

Elevation dependent region of interest width

The landward and seaward shifts of the expected shoreline location are fixed distances at the moment. As discussed in Section 3.3 large values for these parameters solve problems that occur at low water levels when sand bars are emerged. At higher water levels, when the problems described in Section 3.3 do not occur, the large values for the landward and seaward shift are not needed. At higher water level large shifts only cause problems such as the inclusion of the white band that is associated with wave dissipation and pools on the beach, although the latter are not always present with higher water levels. The white band and the pools might mistakenly be detected as the shoreline. A site-specific shoreline elevation could be used, above which the landward and seaward shifts are set narrower. This elevation would have to be at least higher than the possible occurring sand bar elevation, which is site dependant.

Not allowing sudden large shifts of the region of interest

The problem of parts of the shoreline being missed by the region of interest due to a too small landward shift seems to occur from one image to another. At the first image the region of interest is well defined, for the next image the landward boundary of the region of interest shows a sudden seaward shifts on some locations (see Figure 3.12). This shift is caused by the absence of a landward expected shoreline location due to overly smoothing or a lack of data. These problems were already described in Section 3.3. By keeping track of the former position of the landward boundary, limits could be set on the maximum allowable seaward shift of the landward boundary from on image to another.

Larger time window bench-mark bathymetries

The problem of loosing sand bars can be solved by increasing the time window. Increasing the time window to construct a bench-mark bathymetry from shoreline points of several days assumes that morphological changes over some days are minor. This may indeed be the case under fair whether conditions, but it may not be the case under storm conditions. Storm conditions may need longer time windows for other reasons than loosing sand-bars. For a storm of a few days the time window has to be increased to have a bench-mark bathymetry at all. During fair weather conditions the time window of the second bathymetry could be made dependant on the calculated shoreline elevations within the time window. The time window would be that number of days that include a minimum number of daylight hours time steps with a maximum water elevation or the number of days that cover a minimum vertical range of waterlines. A minimum and maximum length could be assigned to this time window.

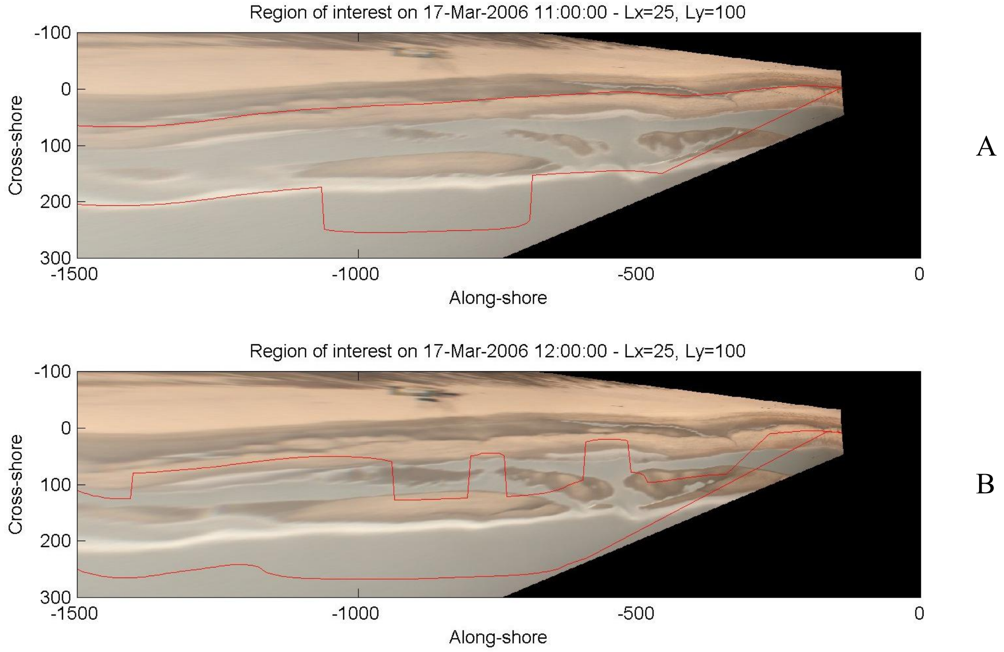

Figure 3.12: Sudden seaward shift in time of some parts of the landward side of the region of interest. In A the ROI is well defined, in B it misses parts of the shoreline due to sudden shifts of the landward boundary of the region of interest.

3.6.2 Topographical error included in the acceptance criterion

As was already mentioned in Section 3.4.2, a major flaw in the fixed acceptance criterion is that it does not take into account the uncertainty of the bench-mark bathymetry. This section proposes a new type of acceptance criterion that does take into account the uncertainty. Like the fixed criterion the newly introduced criterion will be used to vertically check the detected shoreline point against the bench-mark bathymetry. The three types of error measurements, introduced in Section 3.2, will be used to construct the new criterion. Unlike the fixed criterion, the new criterion varies spatially as the errors measures that are used do too.

The mean square error (mse, equation (3.8)) is a measure of the expected variance of the difference between the true bathymetry and the interpolated bathymetry. It shows how well the true bathymetry is approached by the interpolated bathymetry. Using mse $Z_{dif,i}$ can be set at:

$$Z_{dif,i} = P * \sqrt{mse} \tag{3.9}$$

For P = 1 the true elevation at that location is within a range of $\pm Z_{dif}$ around the bathymetry point with 68% probability, for P = 2 and P = 3 this chance is 95% and 99% respectively. However, if very little data are available mse approaches 0 and no shoreline points will be accepted, whereas the bench-mark bathymetry may actually benefit from extra shoreline points at that location as this will reduce uncertainty in subsequent time-steps. Therefore another term, based on the normalized mean square error (nmse, equation (3.6)) is introduced in the calculation of Z_{dif}. This error measure goes to 1 if little data are available. As this error measure describes the fraction of measurement error that passes though the interpolation method, its term should be combined with the typical error of the data.

$$Z_{dif,i} = P * \sqrt{(mse + typical\_error * nmse)} \tag{3.10}$$

Last, the mean square residual (msr, equation (3.7)) error measurement is included in the calculation of Z_{dif}. Msr is a measure of the misfit between the observations (shoreline points in the time window) and the calculated bathymetry. Msr deals with the problem of not knowing whether the observations or calculated bathymetry is wrong. Z_{dif} is now:

$$Z_{dif,i} = P * \sqrt{(mse + typical\_error * nmse + msr)} \tag{3.11}$$

This criterion does not yet take into account the possible morphological change that can occur within on tidal cycle. Therefore a last term is added to the calculation of Z_{dif}.

$$Z_{dif,i} = P * \sqrt{(mse + typical\_error * nmse + msr + beach\_change^2)} \tag{3.12}$$

With this criterion the value of the $Z_{dif,i}$ is now better substantiated, or at least partly, as the values of beach_change and P are still a source of discussion. Also, the criterion is now better connected to the smoothing scales used to calculate the bench-mark bathymetry. As this new criterion is not yet used in practice it is unsure whether it will perform better than the fixed criterion and whether it is still necessary to remove all parts of the bench-mark bathymetry that have a nmse larger that 0.5. If it turns out that many wrong points are accepted at locations that would otherwise have been set to nan-values, this might need some consideration. A problem that still exists with this new criterion is that wrong shoreline points can still be accepted and good points can still be rejected. It is unsure whether this acceptance criterion will lead to an improvement on that part.

3.6.3 Measure of trust

The quality control on the detected shoreline points is currently performed rather rigidly: a shoreline point is either rejected or accepted. Once a shoreline point is accepted it is treated, in later time steps and in data analysis, as being absolutely true. All points that are stored in the database are treated equally, for example in obtaining the bench-mark bathymetry of the next time step. A measure on how much a detected shoreline point is trusted as representing the true bathymetry should be ‘attached’ to each accepted shoreline point. In the interpolation of the bench-mark bathymetry or in data-analysis a lower weight could then be assigned to those points that we trust less. The PIC detection method currently has not yet a measure on how much a detected shoreline point is actually believed to be a true shoreline point. As the bench-mark bathymetry to which the detected shoreline points are compared also contains errors (Section 3.2.1), the uncertainty of the bench-mark bathymetry should also be taken into account when attaching a measure of probability to the detected shoreline points.

3.6.4 Storm values

No storm values are yet determined for the Dutch beach. Based on Quartel et al. (2007) the value of $H_{rms,storm}$ is currently set at 2 m. Other demands on e.g. storm duration or surge levels could also be included to check if a certain period can be qualified as a storm. Quartel et al. (2007) found that abrupt morphological changes occurred during storm events of at least 30 hours with an offshore surge level at least 0.50 m. In this research the value for Z_{dif} was set at 80 cm, similar to the value that Cerezo and Harley (Appendix B) found for Narrabeen, Australia. A good value for $Z_{dif,storm}$ has still to be found for the Dutch beach. The ASM proved to be able to pass two periods with H_{rms} wave heigths above 2 m.

3.6.5 Running ASM more than once

The initial idea of Plant was to run the ASM more than once, so that it can use its self-detected shoreline points in the next run to construct a bench-mark bathymetry. The time window of the bench-mark bathymetry could look forward in time as well. This allows future information to be used in the interpolation of the bench-mark bathymetry. Running the ASM for several times might enable the it to better overcome gaps in time and space. It is thought that the ASM should not be run too many times over a certain period. Because the ASM compares newly detected shoreline points to bathymetries obtained from previously self detected points, errors might continue into following runs.

3.6.6 Image quality and collection

Image quality has not been considered in this research. On fog images it is understandable that no good shoreline can be detected. However, on fair weather images it is expected that the PIC detection model is able to detect the correct shoreline. It seems that this is not always the case. Enhancing the image quality might help in this respect. Another way to circumvent the problems with image quality might be to collect more timex images at every time step. A suggestion is to collect 3 timex images in stead of 1. The three timex images could then together cover 20 minutes, where the first and second timex overlap and also the second and third. Shorelines could then be detected on each of the three timex images. This approach would increase the chances on a detectable timex. Also, it would lead to a larger number of detected shoreline points at that location.

4 Calibration and validation of the ASM

As explained in Section 3.5, the performance of the ASM depends on the settings used. This chapter shows the effect of different ASM settings on the obtained bathymetries. Especially the influence of the acceptance criterion is investigated. Next to the settings, the quality of the obtained bathymetries also depends on the post-processing interpolation method[7]. For this interpolation also the loess interpolation is used; the smoothing scales and the time window are varied to see what interpolation settings can be used best with video data.

In this chapter two case studies are performed. The ASM bathymetries, obtained with different ASM settings and different interpolation settings, are compared to a DGPS survey and to IBM bathymetries. This comparison provides insight into:

- the best settings to obtain shoreline points from video images;
- the best post-processing smoothing scales and time window;

The comparison is performed in two ways:

- The ASM bathymetries of different runs (different settings) and IBM bathymetries are compared to DGPS measurements using summary statistics. This comparison is only performed for the first case study and provides some insight into the quality of the obtained bathymetries.
- Coastal state indicators (CSIs) are derived from ASM and IBM bathymetries. These are then compared to investigate if ASM data provide useful bathymetries for data analysis based on CSIs.

Section 4.1 first introduces the summary statistics and CSIs by which the ASM bathymetries are compared to the DGPS data and to IBM bathymetries. Then Section 4.2 introduces the two case studies. Finally, Section 4.3 and Section 4.4 present the comparison of different ASM bathymetries to DGPS measurements and to IBM bathymetries. Section 4.5 lists the conclusion on the use of the ASM and its data. Section 4.6 finally gives an overview of the best settings for the Egmond Coast 3D site based on the application of the obtained data.

4.1 Methods for comparison

4.1.1 Summary statistics

Summary statistics provide some insight into the errors of the ASM and IBM bathymetries with DGPS measurements. As the DGPS data are not densely spaced interpolation of the DGPS data to the grid of the ASM and IBM bathymetries would introduce too large errors. Therefore, the comparison of the video bathymetries with the DGPS measurements can only

7. The bathymetry that is referred to here is the bathymetry that is obtained for data analysis, not the bench-mark bathymetry that is used when detecting shorelines. The loess scaling parameters of the bench-mark bathymetry are not varied in this research.

take place at the DGPS measurement locations. IBM and ASM bathymetries are interpolated from their grid to the locations of the DGPS measurements. The video data is first interpolated to a 5 m x 5 m grid, and from that it is interpolated to the locations of the DGPS data. It is assumed that the error that is introduced by this two step interpolation is negligible. As the Dutch beach is rather flat, linear interpolation is used for the second step.

The summary statistics that are used in this comparison are:

Mean difference:

$$\overline{diff} = \frac{\sum_{i=1}^{N}(Z_{i,video} - Z_{i,DGPS})}{N} \tag{4.1}$$

where $Z_{i,video}$ is the elevation of the video derived bathymetry in the DGPS measurement location i, $Z_{i,DGPS}$ is the elevation of the DGPS measurement at location i and N is the total number of points.

Standard deviation of the difference:

$$s = \left(\frac{\sum_{i=1}^{N}(diff_i - \overline{diff})^2}{N-1} \right)^{\frac{1}{2}} \tag{4.2}$$

Where $diff_i$ is the difference between the video derived bathymetry and the DGPS points at point i. The standard deviation provides a measure for the spread of the errors.

If Z_{video} is both larger and smaller than Z_{DGPS} at different locations the mean difference could be close to zero. This might give a distorted view of the error. The root mean square error avoids this problem. If the mean difference is close to zero and if N is large, the root mean square error and the standard deviation are almost similar.

Root mean square difference:

$$rms = \left(\frac{\sum_{i=1}^{N}(diff_i^2)}{N} \right)^{\frac{1}{2}} \tag{4.3}$$

To complete the overview of the quality of the video bathymetries the maximum over- and underestimation are given. The summary statistics provide insight into the accuracy of the manually and automatically obtained bathymetries. The overview provides insight into which ASM settings and post-processing interpolation scales give the most accurate results.

4.1.2 Coastal state indicators

The study of the coastal evolution can be quite complicated if only a narrative description of the beach state is given. Therefore a more standardized, quantitative method is used: a set of coastal state indicators (CSIs). CSIs have been used by various researchers to distinguish different types of beach (e.g. Wright and Short, 1984) and to study beach behaviour (e.g. Kroon et al., 2007; Aagaard et al., 2005). Davidson et al. (2007) describe CSIs as "a reduced set of issue-related parameters that can simply, adequately and quantitatively describe the dynamic-state and evolutionary trends of coastal systems". According to Kroon et al. (2007) a CSI is "a simple parameter which assists the monitoring and management of the coast and directly initiates management intervention when predefined threshold values are exceeded".

CSIs enable the user to gain an easily understandable overview of the beach evolution processes of interest. CSIs can be applied in various situations and allow comparison of separate events. They also enable the comparison of different researches that used the same CSIs. Furthermore, CSIs can be used to facilitate the decision making on beach and foreshore nourishments. Several CSIs have been used by various authors to describe the beach state. Some examples of CSIs are: beach volume (Aarninkhof, 2003; Kroon et al., 2007); momentary intertidal coastline (MICL) (Wijnberg et al., 2004); elevation contour (Kroon et al., 2007); beach width (Van Rijn et al., 2002; Davidson et al., 2007); high water exceedence curves (Van Koningsveld et al., 2007; Davidson et al., 2007).

In this research three CSIs are extracted from IBM and ASM bathymetries. These CSIs are listed in Table 4.1. Appendix F explains how they are extracted from the bathymetries. Comparison of CSIs obtained from IBM and ASM provides insight into the best ASM settings and the best post-processing smoothing scales and time window to use with video data.

Table 4.1: Coastal state indicators used in this research

CSI	What it indicates
1) Elevation contours	Indicates location of the intertidal beach and sand bars
2) Slope intertidal beach	Indicates width of the intertidal beach
3) MICL	Indicates volume of the intertidal beach

4.2 Case studies

The influence of the ASM settings on the obtained bathymetries and the post-processing interpolation methods are studied in two case studies. Two periods are selected as case studies based on a) the availability of DGPS data within the range of the Argus cameras (only first case study) and b) the quality of the collected images (no rain or otherwise disturbed images). This section provides information on the case studies and introduces the various ASM runs (with different settings) that were done for each of the case studies.

4.2.1 First case study

The first case study covers the period from March 15th to March 19th. Manual bathymetry data are obtained for the entire period by means of the IBM. The first two days of the IBM data are used as start up bench-mark bathymetries for the ASM runs. ASM data are thus available for March 17th to March 19th. DGPS data are available for March 17th. This is listed in Table 4.2.

In the various ASM runs the value of the acceptance criterion and the definition of the region of interest are varied. For the acceptance criterion three values are used to study the trade-off between accepting wrong shoreline points and rejecting good points. The three values used are: 0.10 m, 0.25 m and 0.50 m. For the region of interest the landward shift of the contour was varied: 40 and 300 m. The overview of ASM runs for the first case study and the names by which they are refered to subsequentely can be seen in Table 4.3. The small landward shift was only run in combination with the 0.25 m criterion.

Table 4.2: Overview of the bathymetry data available for the first case study

DGPS measurements	March 17th
IBM shoreline points	March 15th to 19th
ASM shoreline points	March 17th to 19th for various runs

Table 4.3: ASM runs for the first case study

Z_{dif}	**0.10 m**	**0.25 m**	**0.50 m**
40 m landward shift		1_smallRoi_25	
300 m landward shift	1_largeRoi_10	1_largeRoi_25	1_largeRoi_50

4.2.2 Second case study

The second case study covers the period from May 5th to May 12th. Manual bathymetry data are obtained for the entire period by means of the IBM. For this case study the start day of the ASM runs was varied. Three runs are started anew from the manually detected shorelines of May 5th and 6th, one run is continued from a run of the first case study (run 1_largeRoi_25). This run has detected shorelines on every day in between the two case studies. No DGPS data are available for this case study. An overview is listed in Table 4.4.

Like in the first case study the acceptance criterion is varied. This is only done for the newly started runs. The applied acceptance criteria are the same as for the first case study. The various ASM runs for this case study are listed in Table 4.5.

Table 4.4: Overview of the bathymetry data available for the second case study

DGPS measurements	not available
IBM shoreline points	May 5th to 12th
ASM shoreline points	May 7th to 12th newly started runs, May 5th to 12th for the continued run

Table 4.5: ASM runs for the second case study

Z_{dif}	0.10 m	0.25 m	0.50 m
continued run		2_continued_25	
new start up	2_newStartUp_10	2_newStartUp_25	2_newStartUp_50

4.3 Comparison to DGPS data

In this part ASM and IBM data of the first case study are interpolated with various smoothing scales and time windows. The obtained bathymetries are compared to DGPS data by means of summary statistics.

For each data set (per run) two time windows and three smoothing scales are used. The time window is either one day (only data of March 17th) or three days (data of March 17th to 19th)

The smooting scales that are used for the interpolation are:

- L_x = 10 m, L_y = 25 m
- L_x = 10 m L_y = 100 m
- L_x = 25 m, L_y = 100 m

The rms errors for the various runs are listed in Table 4.6. The number of DGPS points against which the bathymetry is checked is included in brackets. The values of the other summary statistics are listed in Appendix G. The overview of Table 4.6 shows that for most runs the rms errors are smallest for the smallest smoothing scales. Larger smoothing scales generally lead to higher rms errors. The overview also shows that for all ASM runs the rms error increases slightly if the time window is increased from one to three days, this was not the case for the IBM bathymetries. Generally, for a time window of one day, the rms errors are between 0.25 m and 0.39 m. For a time window of three days, the rms errors have values between 0.25 m and 0.55 m. The large rms errors of 1_largeRoi_25 and 1_smallRoi_25 for a time window of three days and large smooting scales seem to be the result of some extreme errors as can be seen in histograms of figure Figure 4.1 (1_largeRoi_25 only) .

The overview in Table 4.6 shows that for a time window of one day the rms errors increase for larger values of Z_{dif}. Run 1_smallRoi_25 is an exeption to this rule for the two smallest smoothing scales. This is probably because the points detected by this run are not good, due to the bad definition of the region of interest. The smallest smoothing scales are apparently not able to resolve these detection problems. For a time window of three days an increase of the rms error is observed when Z_{dif} is increased from 0.10 m to 0.25 m. A small decrease of the rms error is observed when Z_{dif} is increased to 0.50 m.

Overall the IBM bathymetries show the smallest rms errors. This was as expected, as human quality control is supposed to lead to the best results. Only one bathymetry (1_largeRoi_10 with a time window of 1 day and small smoothing scales) has a smaller rms error. A reason for this may be that this rms error is based on far less points than the other rms calculations. This is because this bathymetry of 1_largeRoi_10 misses elevation data on many locations. With the use of a large time window or larger smoothing scales, the error of the 1_largeRoi_10 run increases.

For the mean error and the standard deviation no connection with the value for Z_{dif} or the smoothing scales was found. However, a large time window seems to lead to a reduction of the mean error and to an increase of the standard deviation. For the maximum over- and underestimation, there is no clear correspondance with the value of Z_{dif} or the time window. Larger smoothing scales generally lead to larger maximum over- and underestimations.

Table 4.6: Rms errors (m) for different ASM and IBM bathymetries compared to DGPS data. The number of DGPS points against which the ASM / IBM bathymetry is checked is included in brackets.

run	**time window**	**10 25**	**10 100**	**25 100**
IBM	1 day	0.25 (169)	0.27 (181)	0.32 (215)
	3 days	0.25 (184)	0.27 (196)	0.31 (232)
1_largeRoi_10	1 day	0.24 (78)	0.30 (108)	0.32 (168)
	3 days	0.31 (138)	0.30 (159)	0.34 (186)
1_largeRoi_25	1 day	0.29 (165)	0.31 (182)	0.37 (222)
	3 days	0.35 (191)	0.37 (205)	0.53 (246)
1_largeRoi_50	1 day	0.29 (155)	0.32 (176)	0.39 (221)
	3 days	0.34 (180)	0.36 (191)	0.42 (228)
1_smallRoi_25	1 day	0.33 (129)	0.36 (158)	0.38 (199)
	3 days	0.38 (175)	0.41 (200)	0.55 (249)

4.4 Comparison of CSIs derived from ASM and IBM obtained bathymetries

In this section, CSIs derived from the various ASM and IBM bathymetries are compared for both case studies. As Section 4.3 shows, the smallest smoothing scales and the smallest value for Z_{dif} (0.10 m) provide the smallest rms error with the DGPS data for the first case study. This section investigates whether these also result in a bathymetry that is useful for data analysis based on CSIs. First a general overview is given of the effects the smooting scales and the time window of the interpolation have on the CSIs extracted from the various

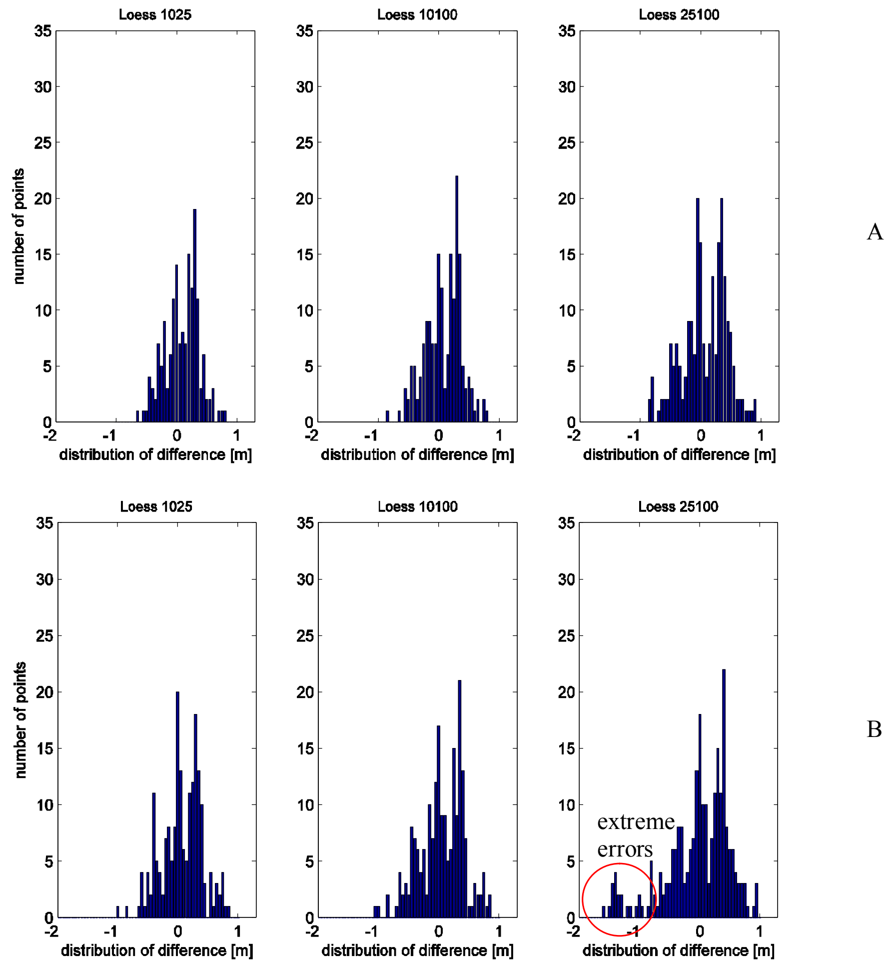

Figure 4.1: Histograms of difference between DGPS data and the bathymetry of 1_largeRoi_25 per smoothing scales for time windows of one and three days. A: Time ndow of one day. B: Time window of three days.

ASM bathymetries. Next the comparison is made between the CSIs derived from the ASM and IBM bathymetries. The IBM bathymetries are considered the best that can be derived from Argus images, but they also contain errors as Section 4.3 showed. For the first case study IBM bathymetries with a time window of three days have rms errors in the range of 0.26 to 0.31 m for different smoothing scales.

4.4.1 CSIs, smoothing scales and time windows

In section 4.1.2 the MICL, the elevation contours and the intertidal beach slope were proposed as CSIs to be used in this study. This section provides an overview of the best interpolation settings to obtain bathymetries to derive these CSIs.

MICL

Analysis showed that extraction of the MICL from bathymetries obtained with a one day time window does not always give good results. This is the direct effect of bad shoreline detection on some days. Figure 4.2A shows the MICL per day as detected for run 2_newStartUp_50 with a one day time window and the largest smoothing scales (L_x = 25 m, L_y = 100 m). This figure shows that a one day time window does not give good results for some days, but the general alongshore variation of the MICL position can still be seen. For smaller smoothing scales the derived MICL is less well defined on a one day base, because those bathymetries are less complete, which affects the calculation of the MICL.

MICLs derived from bathymetries with a time window of a few days show to be more consitent (Figure 4.2B). Even for the smallest smoothing scales they provide generally good MICL estimates, as more data are available within the larger time window, which also makes the data more dense. In this research a comparison is made between ASM and IBM MICL positions derived from bathymetries with a time window of several days.

Elevation Contours

Three elevations were considered to find contours at: -0.50 m, 0 m and +0.50 m NAP. Analysis showed that on bathymetries with a time window of one day not all contours can be derived on some days. This is especially the case for small smoothing scales.

On bathymetries with larger time windows most contours seems to be well defined for most ASM runs, especially the larger smoothing scales give good results. From bathymetries obtained from run 1_largeRoi_10 no good contours could be extracted at all. The contour positions of this run do not even show the same alongshore variation as those of other runs (see Figure 4.3). This is probably due to a lack of data. As for a value of 0.10 m for Z_{dif} many points are rejected, a time window of three days may not be long enough to include enough data points to interpolate a proper bathymetry.

In the next section the elevation contours derived from ASM bathyemetries with a time window of several days will be compared to those derived from IBM bathymetries. For this analysis the largest smoothing scale will be used, as the contours can be best derived from these bathymetries.

Slope

The slope is determined using the distance between the 0.50 m and -0.50 m NAP contours. If these contours cannot be well defined, the slope can neither and will be excluded from the comparison. It was already concluded that these elevation contours can be best derived from a bathymetry obtained with a time window of several days and large smoothing scales.

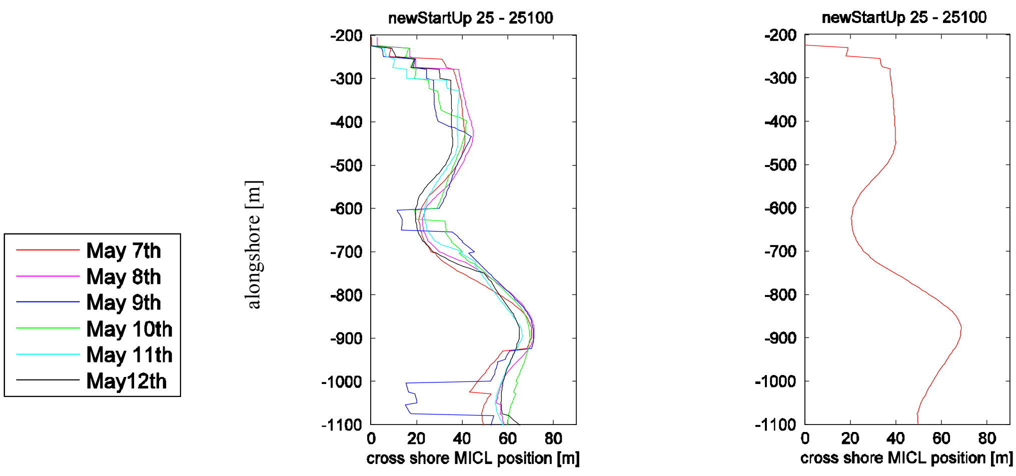

A B

Figure 4.2: MICL positions for run 2_newStartUp_25 based on A) a one day time window and B) a six day time window. Both smoothings scales $L_x = 25$ and $L_y = 100$. The x-axis is positive in seaward direction, the y-axis is positive in southward direction.

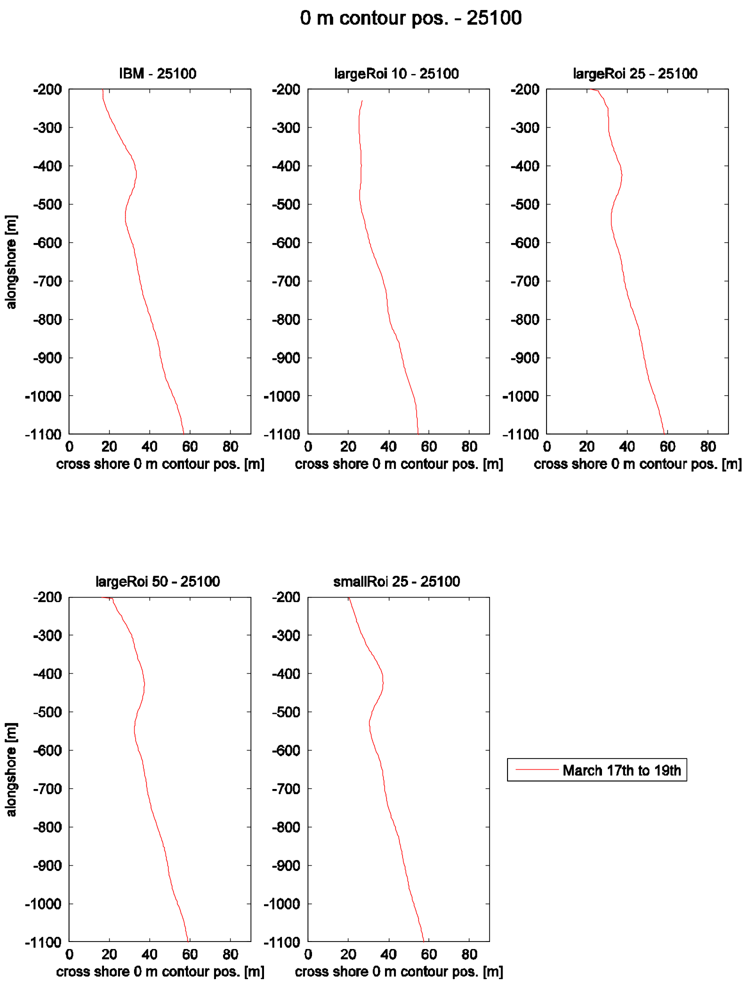

Figure 4.3: 0 m contour from IBM and ASM bathymetries for the largest smoothing scales. Run 1_largeRoi_10 does not show the same alongshore variation in the contour position as the other runs. This is probably due to a lack of data

4.4.2 ASM and IBM CSIs compared

In this section CSIs derived from the ASM bathymetries are compared to CSIs derived from IBM bathymetries. The previous section showed that CSIs are best derived from bathymetries with a time window of several days and smoothing scales in the order of 25 m cross-shore and 100 m alongshore. Therefore only these are compared.

MICL

Figure 4.4 shows the results of the comparison of the ASM MICL position to the IBM MICL position for the second case study for the largest smoothing scales. For all runs the seaward shift is in the order of 2 to 3 m, with maxima up to 5 m, at most alongshore locations. Similar results are found for the runs of the first case study.

All runs in Figure 4.4 show a sudden increas in the relative seaward MICL position at -350 m alongshore. It is thought that this is the result of the large landward shift in the determiniation of the region of interest. This large landward shift causes the exclusion of parts of the shoreline close to the camera from the region of interest, as can be seen in Figure 2.6B. This affects the obtained bathymetry and thus the derived CSI. This problem might be avoided somewhat by using a smaller landward shift.

Comparison of the long run (2_continued_25) with the newly started run (2_newStartUp_25) (see Figure 4.4) shows that the ASM still performs well and that good data can be derived from it even after almost two months of detecting shorelines.

Overall it can be concluded that for the derivation of the MICL the value of Z_{dif} does not so much affect the outcome.

Contours and slope

For both case studies it seems as if the ASM 0.50 m contours are positioned on or just slightly seawards or landwards of the IBM 0.50 m contour. The differences with the IBM contour are mostly within a range of 1 to 2 m landwards or seawards, depending on the settings.

The 0 m ASM countours are positioned consistently seawards of the IBM contour for both case studies. The average seaward shift is around 2 to 3 m. For the first case study, the seaward shift seems to be larger in the south, close to the camera, than in the north. For the second case study the seaward shift seems to be more alike along the entire alongshore direction (see Figure 4.5).

The -0.50 m ASM contours also show a seaward shift compared to the IBM contour. The aveage shift, over the two case studies, is in the range of 4 to 5 m, a little larger than the shift of the 0 m contour.

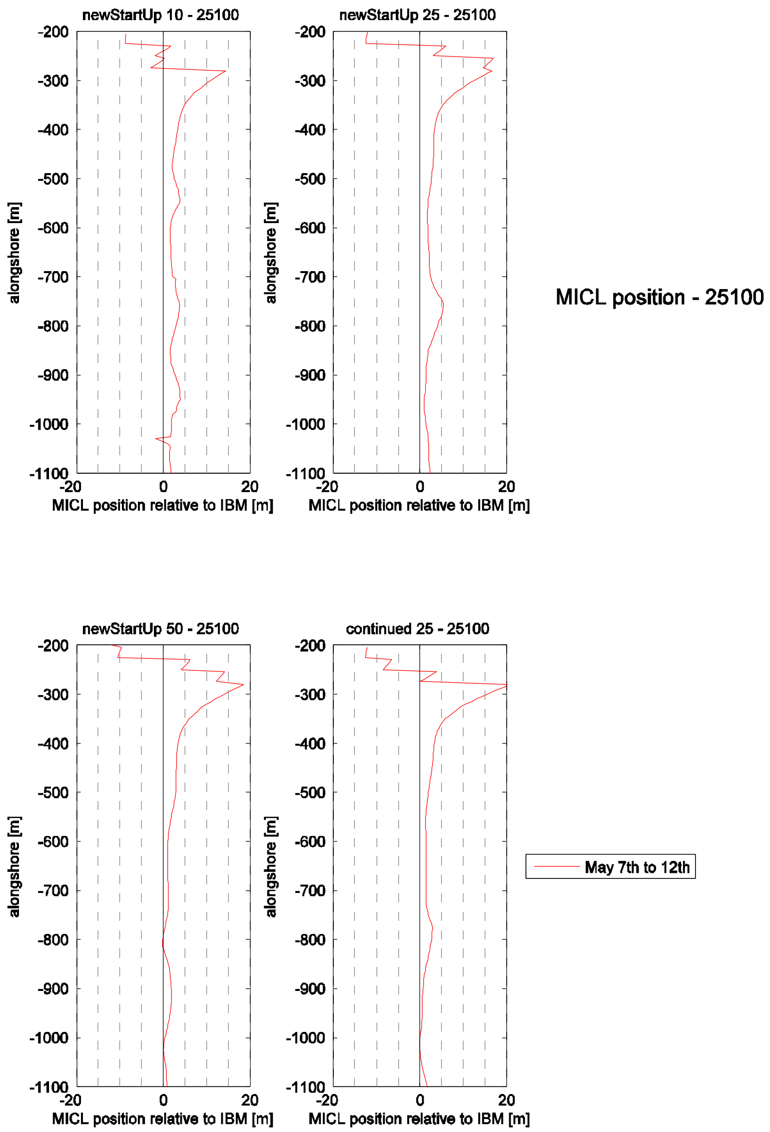

Figure 4.4: ASM MICL positions relatieve to the IBM MICL position for the runs of the second case study. Positive values indicate a seaward ASM MICL position compared to the IBM MICL position.

When an intertidal beach slope of 1:40 is assumed, a horizontal shift of 1 m corresponds to a vertical shift of 2.5 cm. For a value for Z_{dif} of 25 cm a horizontal difference of 10 m is implicitely accepted. This would suggest that the horizontal differences smaller than 10 m are not necessarily a real difference, but merely the result of detection errors. However, the results of landward and seaward shifts are consistent for both case studies which strengthens the conclusion that the obtained shifts are indeed a difference between IBM and ASM contours.

For two runs of the two case studies with the same settings (1_largeRoi_25 and 2_newStartUp_25) Figure 4.6 and Figure 4.7 show the differences with the IBM contours. The increasing seaward shift for the lower contours suggests that the ASM obtained bathyemtries have a gentler slope that the IBM bathymetries. This was confirmed for both case studies by the comparison of the IBM slope with the ASM slopes. An explanation could be the detection and acceptance of 'shoreline' points that are located seawards of the true shoreline. These points 'pull' the bathymetry seawards in the interpolation. Apparently, this type of detection problem occurs more during low water.

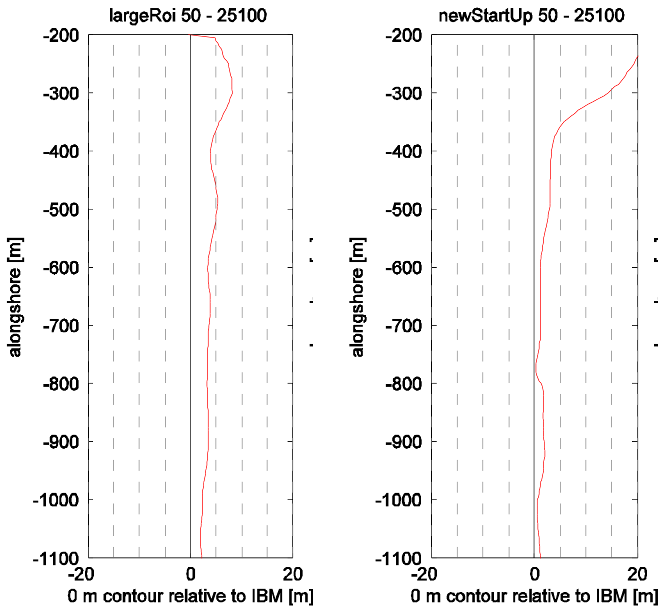

A B

Figure 4.5: Difference in seaward shift of the 0 m contour between the two case studies with a Z_{dif} of 50 cm. Positive values on the x-axis indicate a seaward shift of the ASM compared to the IBM contour position. A: The first case study shows a varying alongshore seaward difference with the IBM contour. B: The second case study shows a constant alongshore seaward difference with the IBM contour

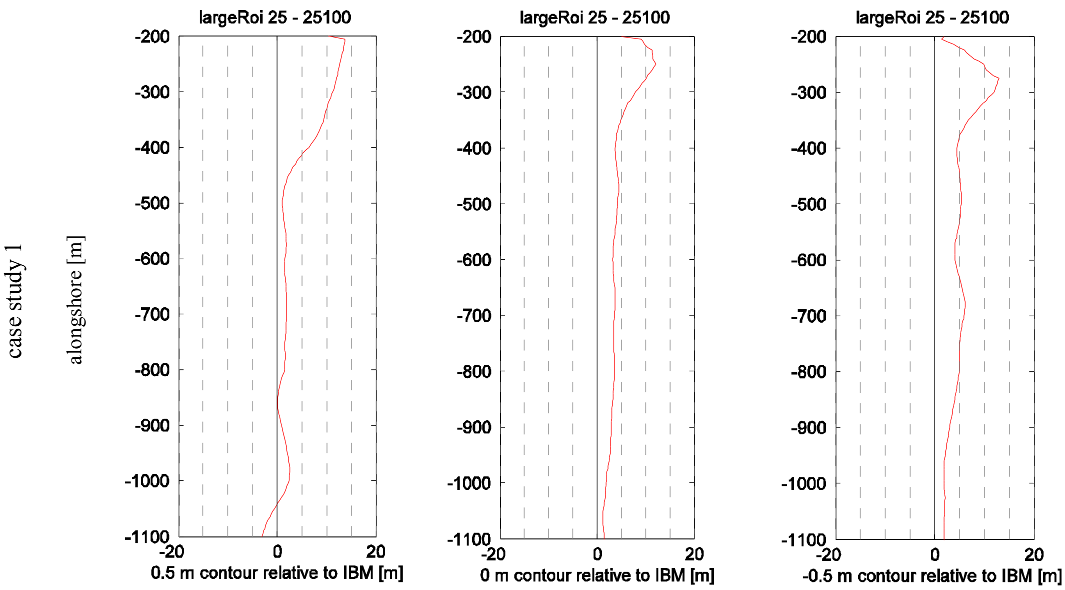

Figure 4.6: ASM countour positions relative to IBM contour positions for the first case study for the three elevation contours. Positive values on the x-axis indicate a more seaward position.

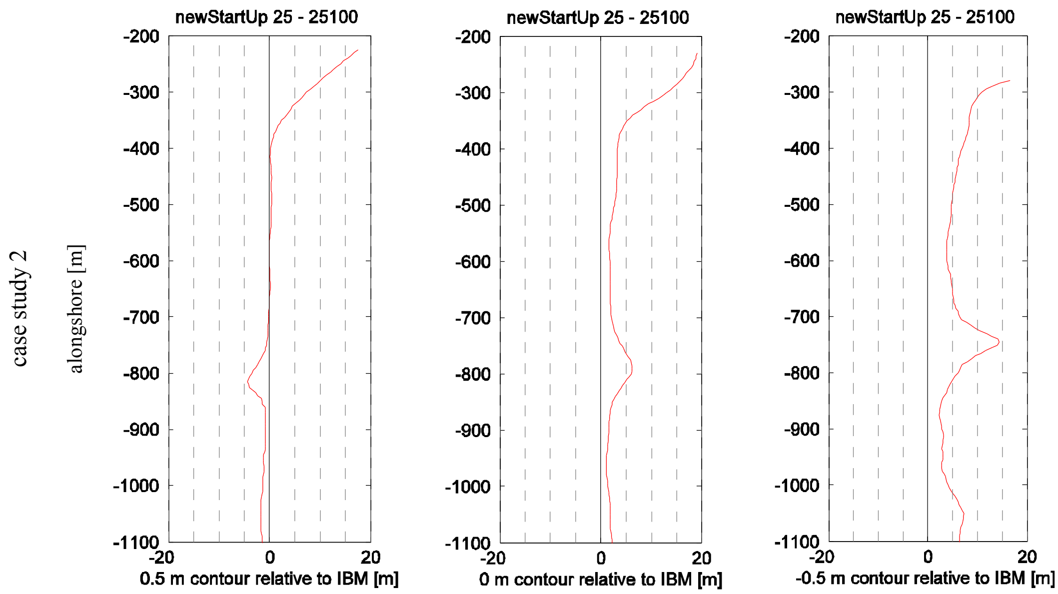

Figure 4.7: ASM countour positions relative to IBM contour positions for the second case study for the three elevation contours. Positive values on the x-axis indicate a more seaward position.

4.5 Findings on the ASM performance and ASM data quality

From the above comparisons the following conclusions are drawn:

- The smallest smoothing scales and the smallest time windows give the smallest rms error with DGPS data. This conclusion justifies the choice for the small smoothing scales of the first bench-mark bathymetry.
- Larger smooting scales and larger time windows result in bathymetries from which CSIs can be extracted well. CSIs derived from such bathymetries better resemble the IBM CSIs than those obtained from bathymetries with smaller smoothing scales and smaller time windows.
- Generally, CSIs derived from bathymetries with larger smoothing scales, are a little more stable and are less prone to small alongshore changes. This can be seen in the comparison of the ASM MICL to the IBM MICL for two smoothing scales (Figure 4.8). The detail introduced by the smallest smoothing scales is not necessarily correct, as smaller smoothing scales do not average out measurement errors as larger scales do. Therefore, the use of large smoothing scales (L_x = 25 m and L_y = 100 m) is advised when data analysis based on CSIs is performed.
- The influence of Z_{dif} on the obtained CSIs seems to diminish if the time window is increased. It was expected that the trade-off between accepting wrong points and rejecting good points would be better visible in the obtained CSIs. Apparently, the detection is good enough and leads to similar results for all values of Z_{dif} over the period of the time window. The only exception is the combination of a value of 0.10 m for Z_{dif} with a time window of only three days.
- As the runs with Z_{dif} s of 0.10 m and 0.50 m have a maximum length of six days (case study 2) it is unclear how Z_{dif} affects the performance of the ASM in the long run. For a value of 0.25 m for Z_{dif} the ASM continued to run for several months (March 17th 2006

till July 14th 2006). It is expected that the performance of the ASM depends less on the value of Z_{dif} if the time window of the second bench-mark bathymetry is set at several days (3 to 6 days).

- CSIs
  - The ASM MICL is located seawards of the IBM MICL by an average of 2 to 3 m. Considering the beach slope and the acceptance criterion used, this change could be the result of detection errors. However, as the changes are fairly consistent over all runs and both case studies, it is considered that the ASM will always detect the MICL seawards of the IBM MICL. This, however, is the result of only two case studies.
  - A drawback of the MICL is that it depends on the quality of the bench-mark bathymetry. One of the problems defined in Section 3.5 is that sand bars are sometimes not accepted. In that case sand bar data are not stored in the database, and the sand bar is not represented in the derived bathymetries. This may lead to underestimation of the intertidal beach volume, to a too much landward calculated MICL postion and may lead to wrong conclusions on beach erosion. Contours are less affected by this particular problem.
  - The ASM contours are all detected seawards of the IBM contours. The seaward shift increases with decreasing contour elevation. The intertidal beach bathymetry obtained with ASM has a gentler slope than one obtained with IBM.

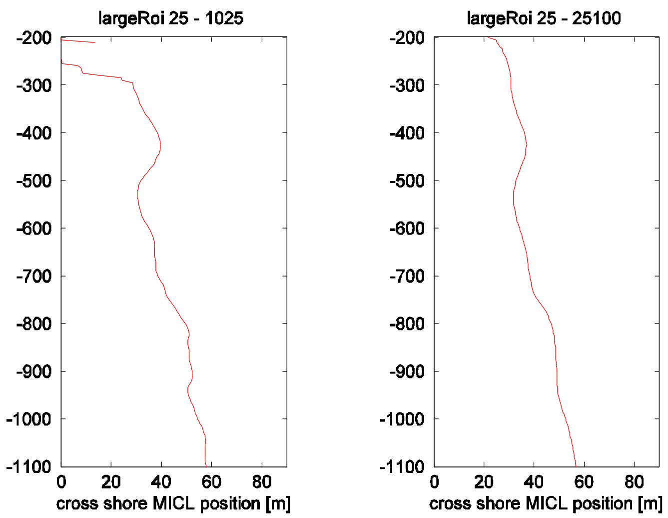

Smoothing scales $L_x = 10$ m, $L_y = 25$ m

Smoothing scales $L_x = 25$ m, $L_y = 100$ m

Figure 4.8: MICL position for two smoothing scales for run 1_largeRoi_25 with a time window of three days.

4.6 Best ASM settings at the Coast 3D site

This section describes what settings can best be used on the Egmond Coast 3D site. This section should be viewed as a guide to future use of the ASM on Egmond beach.

4.6.1 Vertical criterion and bench-mark bathymetry interpolation

What settings for the vertical acceptance criterion and the interpolation of the bench-mark bathymetries can best be used when running the ASM, depends on the purpose of the obtained bathymetry data. This section discusses the interaction between these settings and the connection to the purpose of the data.

Obtain CSIs

If the data is meant to obtain CSIs the findings of of the previous section indicate that the value for Z_{dif} does not affect the outcome, as long as a time window of several days and smoothings scales in the order of 25 m cross-shore and 100 m alongshore are used in the post-processing interpolation.

For the time windows of the bench-mark bathymetries is recommended to use a longer time window for the second bathymetry than for the first bathymetry. The use of larger smoothing scales for the second bench-mark bathymetry is also advised. In this case the second bathymetry can function as a savety net in the quality control, because it probably has less gaps. Based on the small rms errors for the smaller smoothing scales and the shorter time window, the first bench-mark bathymetry can best be obtained with a time window of one day and smoothing scales in the order of 10 m cross-shore and 25 m alongshore. In the double quality check shoreline point are then first compared to a bathymetry of which it is thought it represents the true bathymetry best. The run form March 17th to July 14th 2006 has shown that time windows of 1 day (looking back in time) for the first bench-mark bathymetry and 2 days for the second bench-mark bathymery work well during summer conditions. It was thought that these time windows are too short for shoreline detection in winter conditions. Longer time windows are recommended when detection is expected to be harder, due rough weather conditions. Longer time windows are also recommended when smaller values of Z_{dif} are used, as less shoreline points are accepted by ASM for smaller values of $Z_{dif..}$ The use of short time windows in combination with a small value of Z_{dif} may result in too little shoreline points in the time window to obtain good bench-mark bathymetries.

Obtain most exact measure

The value of Z_{dif} is of importance if the purpose of the use of the ASM is to obtain some points that describe the true bathymetry best at their locations. Based on the comparison of ASM bathymetries to DGPS data it is recommended to use a small value of Z_{dif}, as this gives the smallest rms errors. It was recognised that a value of Z_{dif} of 0.10 m leads to a bathymetry with more gaps. This statement is based on the number of DGPS data points against which the ASM bathymetries were compared (Table 4.6). As less detected shoreline points are accepted when a smaller value of Z_{dif} is used, the bathymetry that is obtained from that data also results in more gaps. For values of Z_{dif} in the order of 0.10 m it is therefore recommended to use longer time windows in the determination of the bench-mark bathymetry, especially for the second one. In this way problems caused by incomplete bench-mark bathymetries are avoided, and the ASM is prevented from collapsing.

4.6.2 Other settings

The settings described in this section do not depend on the purpose of the ASM obtained data, but were found to be good practice in this research.

The landward and seaward shifts were set at 300 m and 100 m respectively. In practice the landward boundary of the region of interest was cut-off at –40 m (see Figure 2.6B), to exclude buildings from the region of interest. The region of interest was thus not moving at the landward side. The run with a value of 40 m for the landward shift had slightly larger rms errors compared to the DGPS data and did not lead to significantly better CSIs.

The beach slope and the value for K_{osc}, both used to calculate the shoreline elevation, were kept at 1:40 and 1.3 respectively, similar to the settings of the IBM.

The storm settings were copied from Cerezo and Harley (Appendix B). From the time of the image wave heights of two days back in time are analysed. If, in that period, any wave occurred with a H_{rms} wave height of 2 m or higher, the vertical acceptance criterion is loosened to 0.80 m. A justification for the H_{rms} wave height of two meters was found in Quartel et al. (2007) who concluded that morphological changes on the intertidal beach are induced by storms that are, amongst others, characterized by a H_{rms} wave height above 2 m. The time window used to look back in time could be linked to the time window of the first bench-mark bathymetry. If, at two days after the storm, the vertical acceptance criterion is sharpened again, one might want to consider checking the newly detected shoreline points first on a bench-mark bathymetry that is composed of post-storm shoreline points only. This would mean that the storm duration criterion (two days in this research) should be half of the time window of the first bench-mark bathymetry.

All ASM settings and their values in this research are listed in Appendix E.4.

5 Application of ASM

5.1 Introduction

In Chapter 4 the performance of the ASM was only compared to IBM for two case studies. In this chapter the performance and application of the ASM in data analysis is studied for periods of time ranging from 1.5 to 4 months. The CSIs introduced in Chapter 4 are used to perform the data analysis.

The ASM was run for three periods:

- Run 1: Summer conditions: March 17th 2006 till July 14th 2006;
- Run 2: Winter conditions: November 20th 2005 till December 28th 2005;
- Run 3: Winter conditions: January 10th 2006 till March 16th 2006.

All ASM runs were started from manually detected shoreline points (using IBM). The ASM settings that are used to detect the shorelines are listed in Appendix E.4.

The first run covers the summer period from March 16th 2006 to July 14th 2006 with mostly fair weather. One minor storm occurred in May, with H_{rms} wave heights above 2 m. In the end of March and the beginning of April 2006 H_{rms} wave heights are above 1.5 m for some time. The wave heigths for this run are given in Figure 5.1. The second and third run cover two storms that are quite similar in both H_{rms} wave height (H_{rms} > 3.5 m) and duration (approximately 3 days). This can be seen in Figure 5.2. The waves were oriented from the northwest for both storms.

In this research bathymetries are interpolated from detected shoreline points for every day. As concluded in the previous chapter, the time window used to interpolate bathymetries shoud be several days and is set at 6 days (3 days forwards and 3 days backwards) in this research. The smooting scales that are used are large (L_x = 25 m, L_y = 100 m), as it was concluded in Chapter 4 that these are best when performing data analysis based on CSIs.

Section 5.2 shows the ASM performance and beach behaviour for summer conditions. For this run, the daily ASM derived CSIs are compared to monthly IBM derived CSIs. The available IBM data for the Egmond Coast3D site camera 1 are listed in Table 5.1. Section 5.3 presents the ASM performance and beach behaviour for the winter conditions. Section 5.4 shortly presents the ASM performance when various succeeding runs are coupled. Finally the conclusions on the application of the ASM in data analysis are presented in Section 5.5.

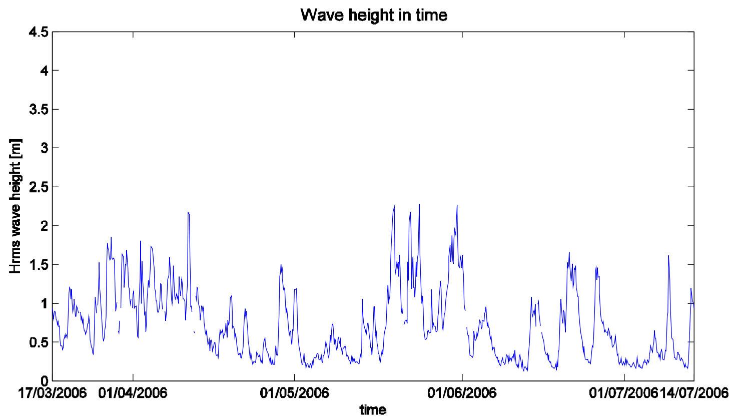

Figure 5.1: H_{rms} wave heigths during run 1. Mind the longer x-axis.

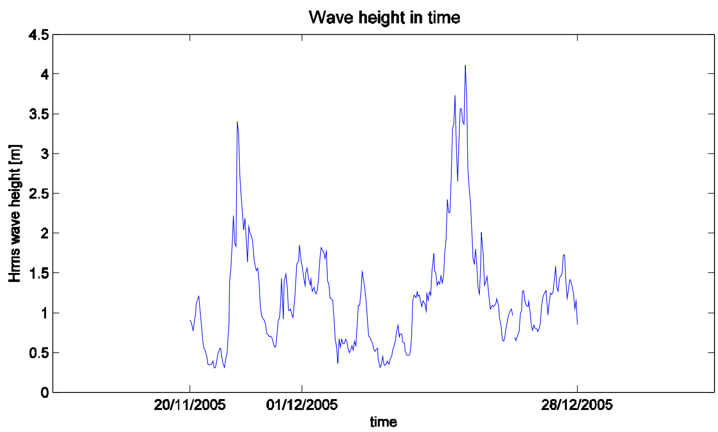

A: H_{rms}wave height for the period of November 11th 2005 till December 28th 2005.

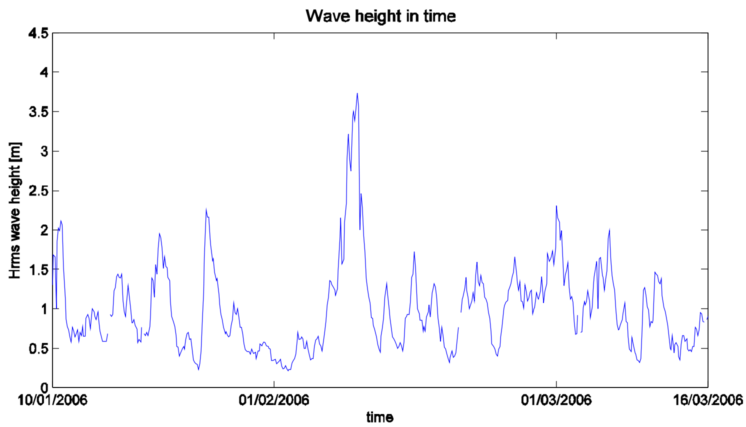

B: H_{rms}wave height for the period of January 10th 2006 till March 16th 2006.

Figure 5.2: H_{rms} wave heights for run 2 and 3. Measured at munitistortplaats.

Table 5.1: IBM data available during the first run of the ASM. The right column lists the time windows that were applied to obtain the IBM bathymetries. From these bathymetries CSIs are derived that are compared to CSIs derived from ASM bathymetries.

IBM data available	Time window
March 17th to 19th	3 days → March 18th
April 9th to 15th	7 days → April 12th
May 7th to 12th	6 days → May 9th
May 15th to 19th	5 days → May 17th
June 16th and 17th	2 days → June 16th
July 13th to 15th	3 days → July 14th

5.2 Summer conditions

5.2.1 Performance ASM: summer conditions: ASM vs IBM CSIs

In this section daily CSIs derived from the first ASM run are compared to the CSIs derived from the monthly IBM bathymetries. Figure 5.3 and Figure 5.4 show the CSIs derived from the ASM and IBM bathymetries for three alongshore locations in time.

As can be concluded from Figure 5.3 the ASM contours and MICL correspond very good with the IBM contours and MICL. The IBM bathymetries are considered to be the best that can be derived with video imagery. The ASM data follows the same trend as the IBM data, but provide detail on a much higher temporal resolution. This higher resolution in time is a great advantage of the ASM compared to the IBM. The good agreement between the IBM and ASM CSI gives trust in the correctness of the ASM data at other moments in time.

The 0 m contour and the MICL show a strong agreement. This is not surprising as the MICL is calculated from the volume between the 0.50 m and -0.50 m contours. The MICL, however, shows some strange peaks each within a few days time. These can be the result of data missing around the -0.50 contour or disappearing / rediscovery of sand bars. Most shifts however coincide with the lack of the -0.50 m contour. This contour is missing at some moments in time because the water level does not reach such low levels on some days. If this occures for a period longer than six days (the time window used in this data analysis) the -0.50 m contour is absent in the obtained bathymetry. This makes the -0.50 m contour less appropriate as a CSI in data analysis.

Although the slope (Figure 5.4) shows very chaotic behaviour, the ASM and IBM slope have more or less the same trend. The agreement between the IBM and ASM slope is however less than was expected from the great agreement between the 0.50 m and -0.50 m ASM and IBM contours. Because of its chaotic behaviour the slope will not be used further as a CSI to study beach behaviour.

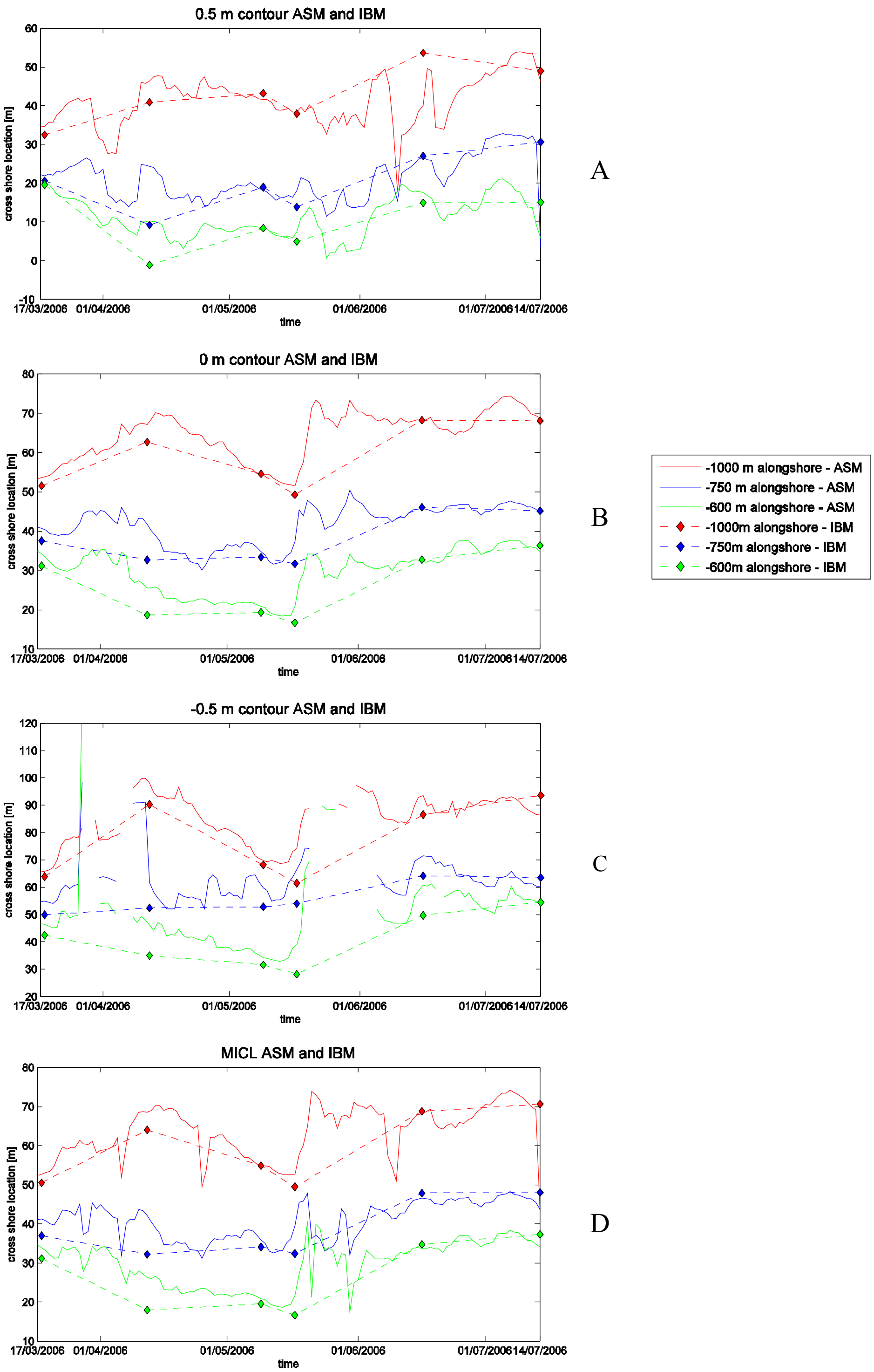

Figure 5.3: CSIs from bathymetries of the ASM summer run and of IBM bathymetries at three alongshore locations. The y-axis is positive in seaward direction.

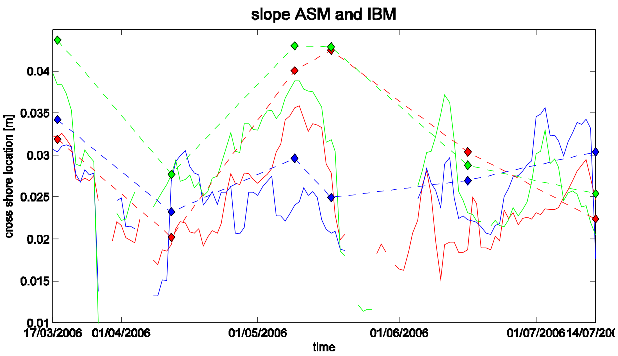

Figure 5.4: Slope derived from bathymetries of the first ASM run and IBM bathymetries at three alongshore locations.

5.2.2 Beach behaviour: summer conditions

From Section 5.3.1 it can be concluded that the 0 m contour can be used best tot study beach behaviour for this run. When compared to the wave data collected during the ASM summer run (see Figure 5.5) the 0 m contour seems to respond to the higher waves in the end of March/beginning of April and the storm in May. On both occasions the 0 m contour shifts seaward. These shifts can be explained from the flattening of the intertidal beach as a response to high energy waves (Aagaard et al., 2005).

Other smaller shifts of the 0 m contour are not obseverved simultaniously for all three alongshore locations and cannot be linked easily to the wave climate. Alongshore differences in response to smaller peaks in the wave climate (such as the one at the end of April) might be explained by differences in slope (Aagaard et al., 2005), the presence of rips, the local shape and height of the subtidal bars (Aagaard et al., 2005; Van Rijn and Walstra, 2002) or by detection errors of the ASM.

Figure 5.6 shows the position of the 0 m contour at all alongshore locations in time. Figure 5.6 shows the development in time of an embayment (-650 m alongshore) and a salient (-900 m alongshore) from a beach that was first aligned more straight (March 18th 2006). The seaward shift at all alongshore locations as a response to the storm in May is also clearly visible. After the storm the alongshore pattern with the embayment and salient continues to exist although less pronounced. This is also visualized in Figure 5.7, that shows the cross-shore position of the 0 m contour for some days. The development from a straighly aligned beach to a beach with an embayment and a salient is clearly visible form March 18th to May 1st. The seaward shift induced by the May storm is also clearly visible (May 13th to May 23rd).

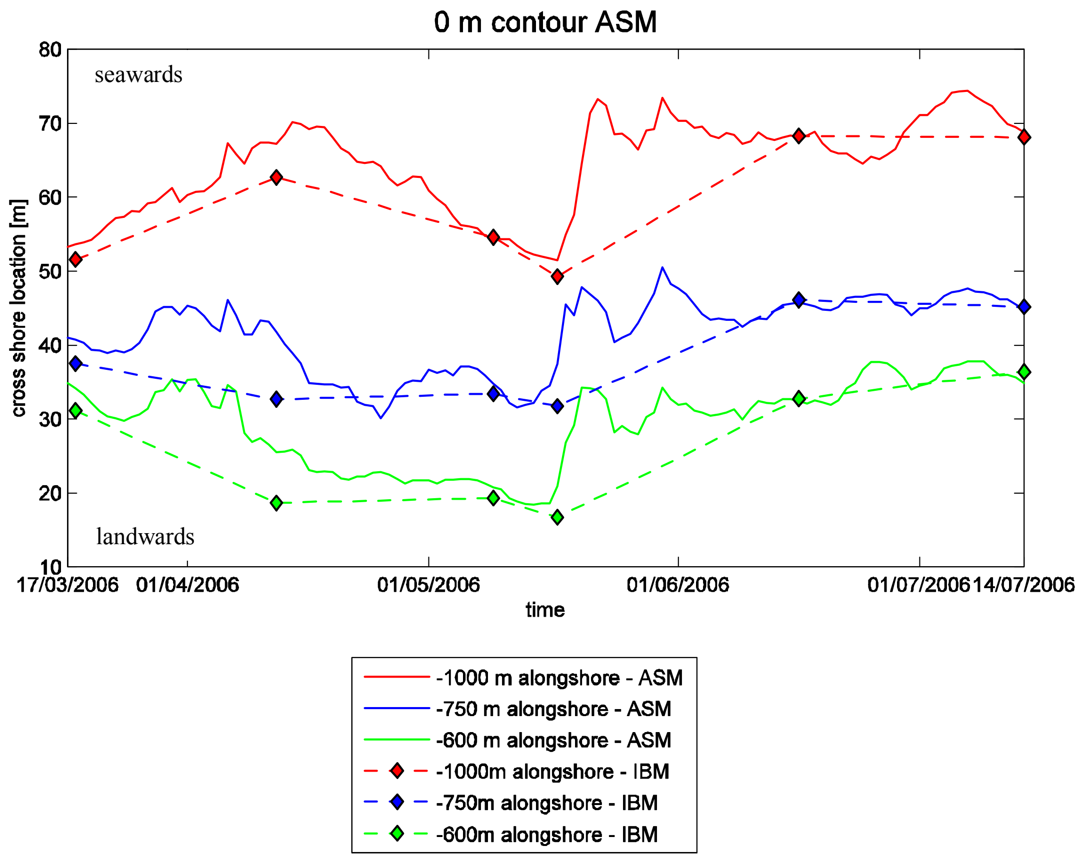

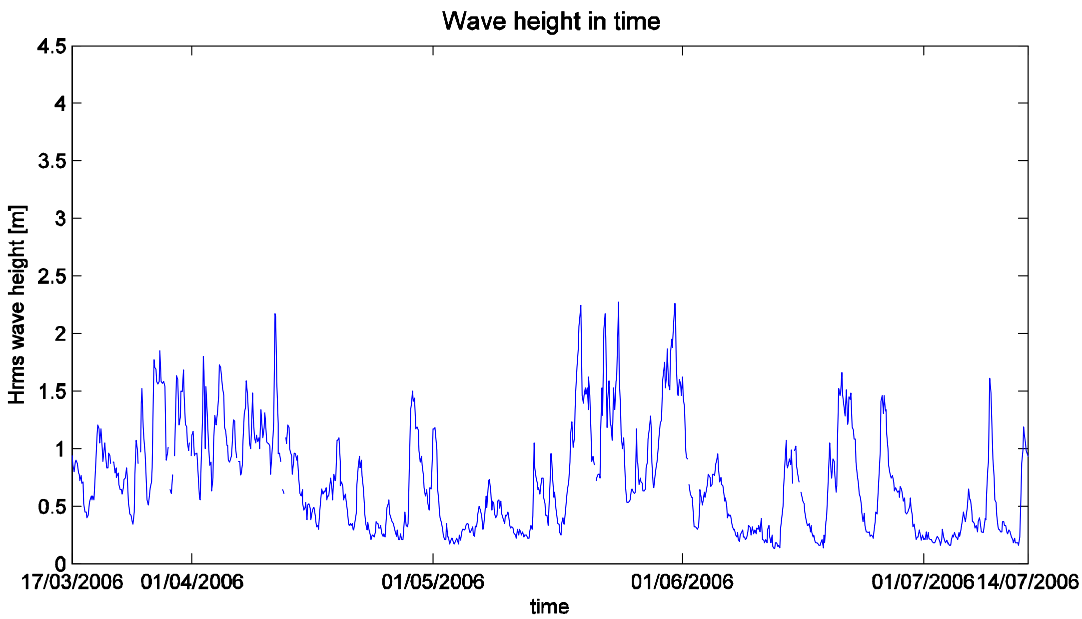

Figure 5.5: Above: cross shore movement of the 0 m contour in time at three alongshore locations for the first run. Below: H_{rms} wave heights measured at munitiestortplaats.

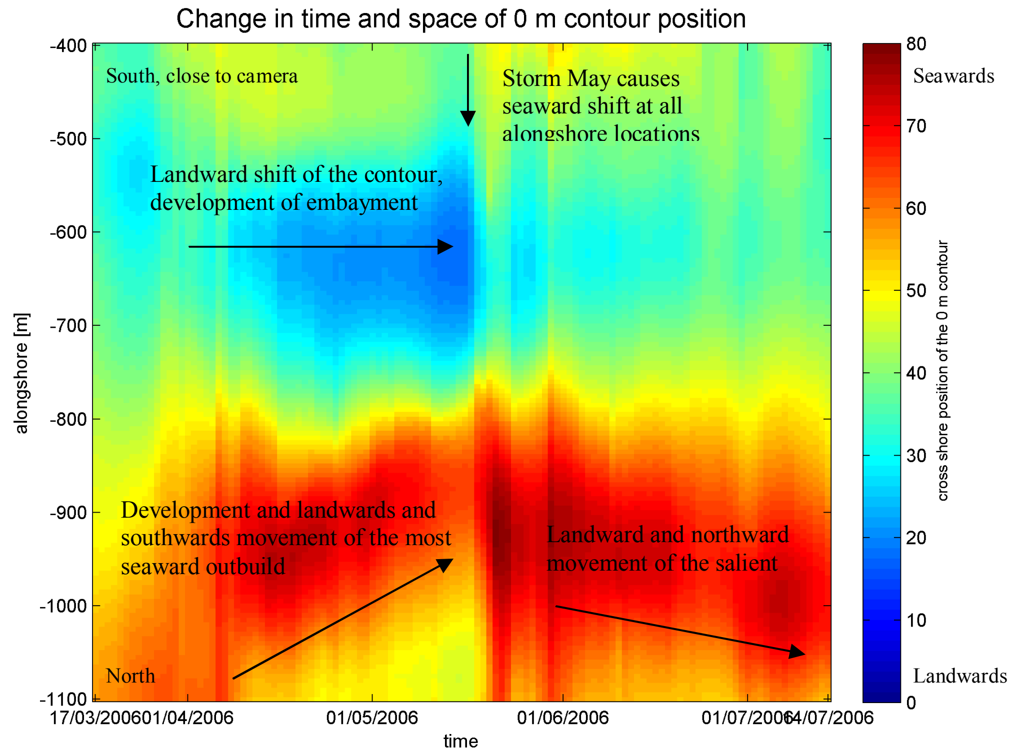

Figure 5.6: Change of the 0 m contour position in time for all alongshore locations for the first run.

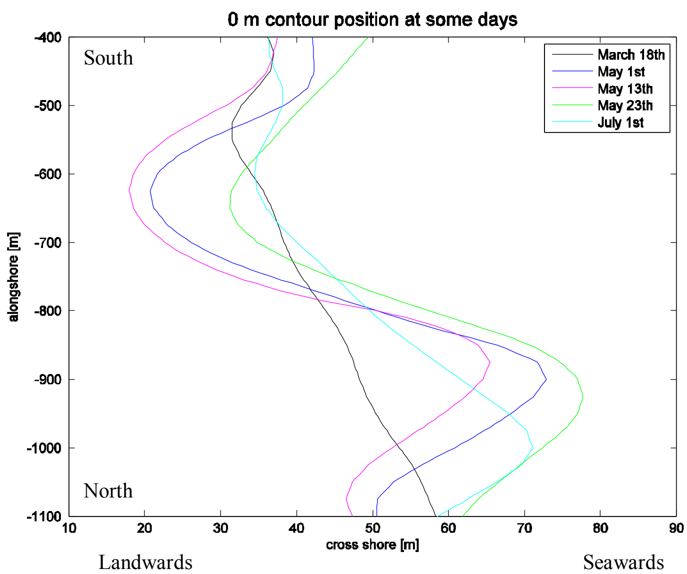

Figure 5.7: Cross shore positioning of the 0 m contour for some days. The 0 m contour shows the development of a salient and an embayment from March 18th till May 1st, and a landwards movement from May 1st till May 13th. The May storm (see Figure 5.5) causes a seaward shift of the 0 m contour at all alongshore locations. After May 23rd the beach seems to straighten again a little, with nortward migration of the most seaward outbuild.

5.3 Winter conditions

5.3.1 Performance ASM: winter conditions

Section 5.2 showed that the ASM derived CSIs corresponds very well with the IBM derived CSIs and that during summer wave-energy conditions the 0 m contour is a CSI that can adequately describe the beach behaviour on a daily / weekly base. This section presents the CSIs that were obtained for the runs with winter conditions.

CSIs for the November to December 2005 run

Figure 5.8 shows the CSIs as derived from the bathymetries of the second ASM run. Because of the higher water levels during this period the -0.50 m and 0 m contour are not always present in the obtained intertidal beach bathymetries. The MICL that is calculated from the intertidal beach volume between 0.50 m and -0.50 m, is not very trustworthy as especially the lower elevations are missing in the obtained bathymetries. Overall the 0.50 m contour seems to be the only CSI that can be used for this run to study beach behaviour.

CSIs for the January to March 2006 run

Figure 5.9 shows the CSIs that were derived from bathymetries of the third ASM run. Overall the CSIs could be derived better than for the second run, but still the -0.50 m and MICL show some strange behaviour. For this run the 0 m contour seems to be the best CSI to study beach behaviour, as this CSI does not show untrustworthy shifts.

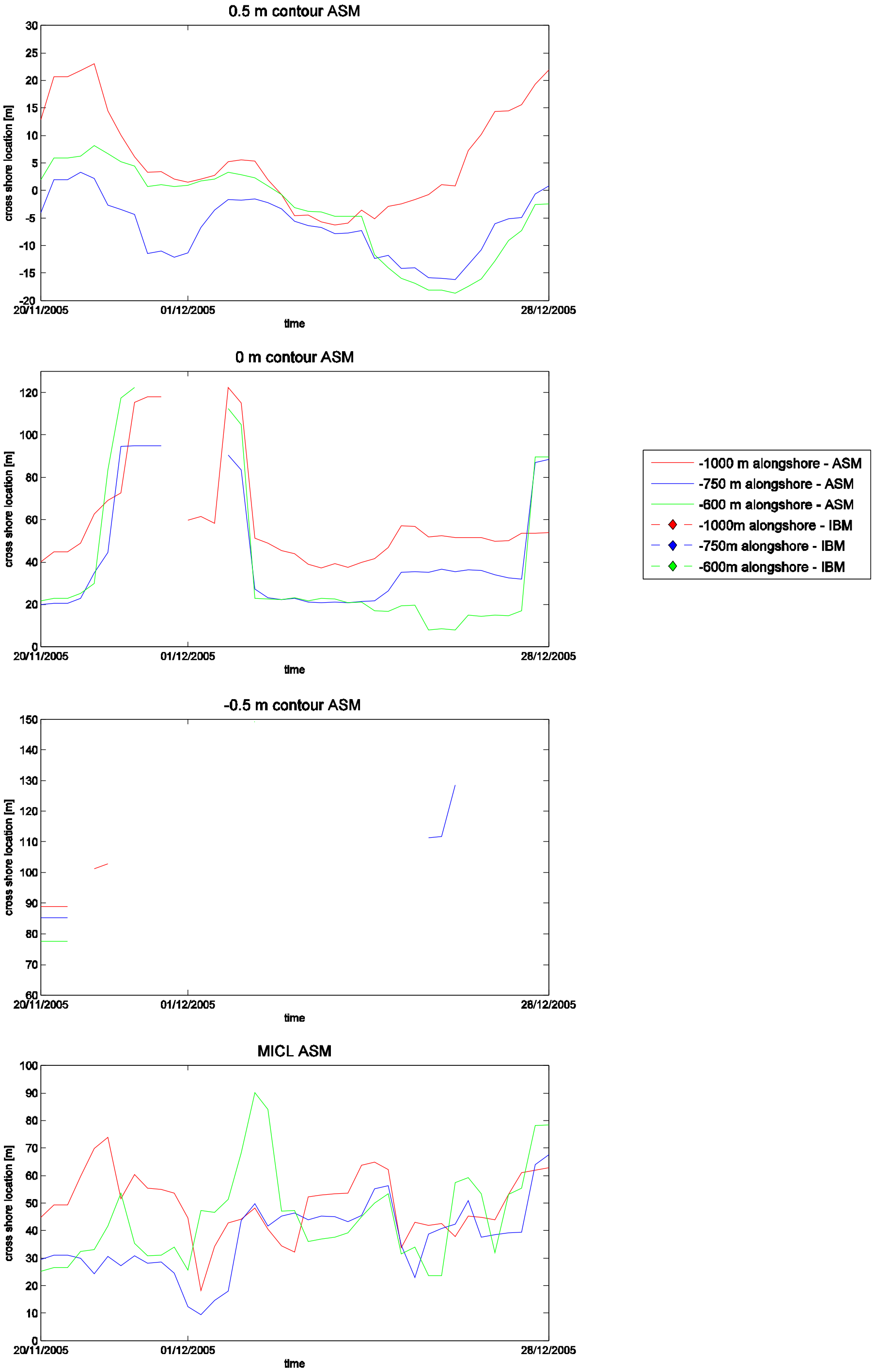

Figure 5.8: CSIs from bathymetries of the second run. The -0.50 m contour is hardly present in the intertidal bathymetries because of higher water levels. The 0 m contous was also not always visible for the same reasons. The MICL seems rather shaky and is not very trustworthy, as it is calculated from the intertidal beach volume between 0.50 and -0.50 m. The y-axis is possitive in seaward direction.

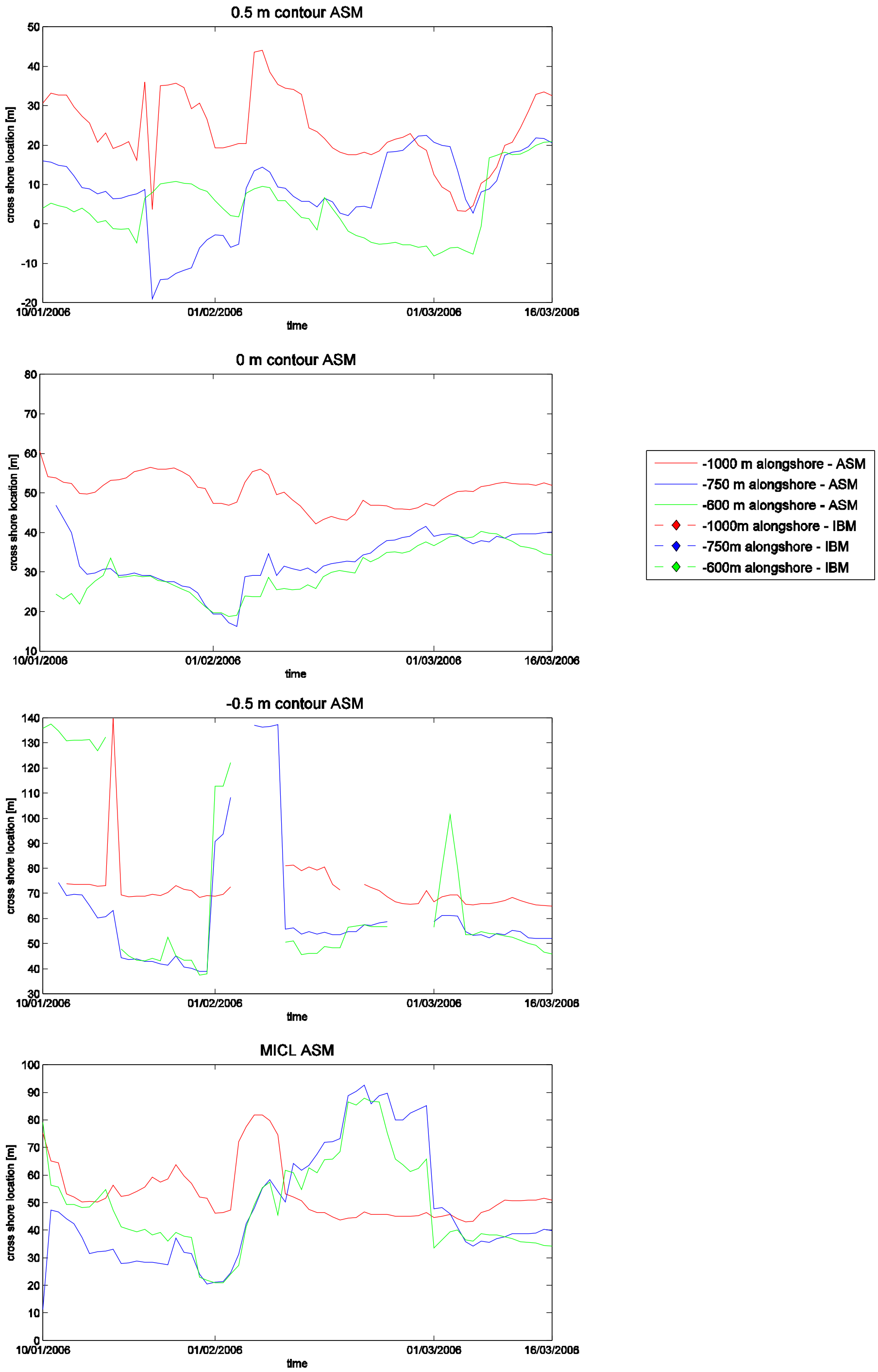

Figure 5.9: CSIs from bathymetries of the third run. The y-axis is positive in seaward direction. The -0.50 m contour shows some sudden and untrusworthy shifts and is not always present. The 0 m contous shows a rather continuous behaviour at the three plotted alongshore locations. The 0.50 m contour seems rather good except for the sudden shifts at -1000 and -750 m alongshore at the end of Janurary. The MICL also shows some sudden shifts.

5.3.2 Beach behaviour: winter conditions

November to December 2005

Figure 5.10 shows the 0.50 m contour line and the measured wave heights for the second run. No obvious direct relation between the 0.50 m contour position and the H_{rms} measured wave height could be discovered at all three alongshore locations. However, the two storms (November and December) seem to cause a landward shift. This shift is not observed at -1000 m alongshore for the December storm. What causes these differences is unclear, but it could be due to differences in the nearshore morphology (e.g. location and height of the subtidal bars). In the last week of December a strong seaward shift of the 0.50 m contour is observed. It is expected that this shift is driven by the lower wave heigths. However, other periods with lower wave heights do not show sua a strong seaward shift. This may be because of differences in nearshore morphology or perhaps the wave direction.
If the behaviour of the 0.50 m contour is studied at all alongshore locations, some landward shifts of the 0.50 m contour, induced by the storms are observed (see Figure 5.11).

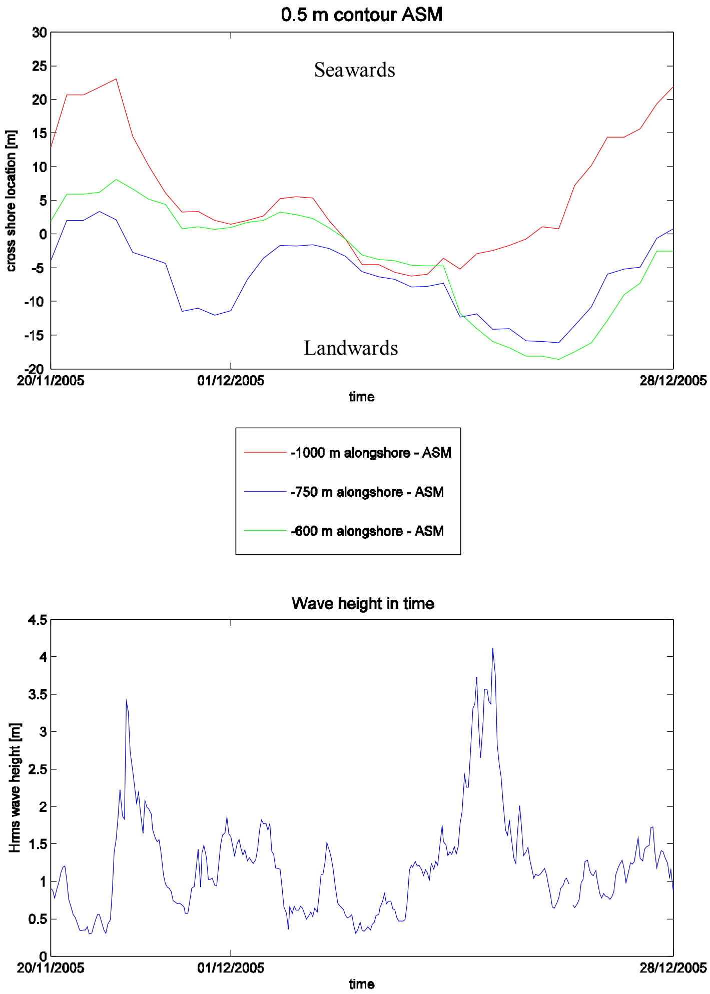

Figure 5.10: Above: cross shore movement of the 0.50 m contour in time at three alongshore locations for the second run. Below: H_{rms} wave heights measured at munitiestortplaats.

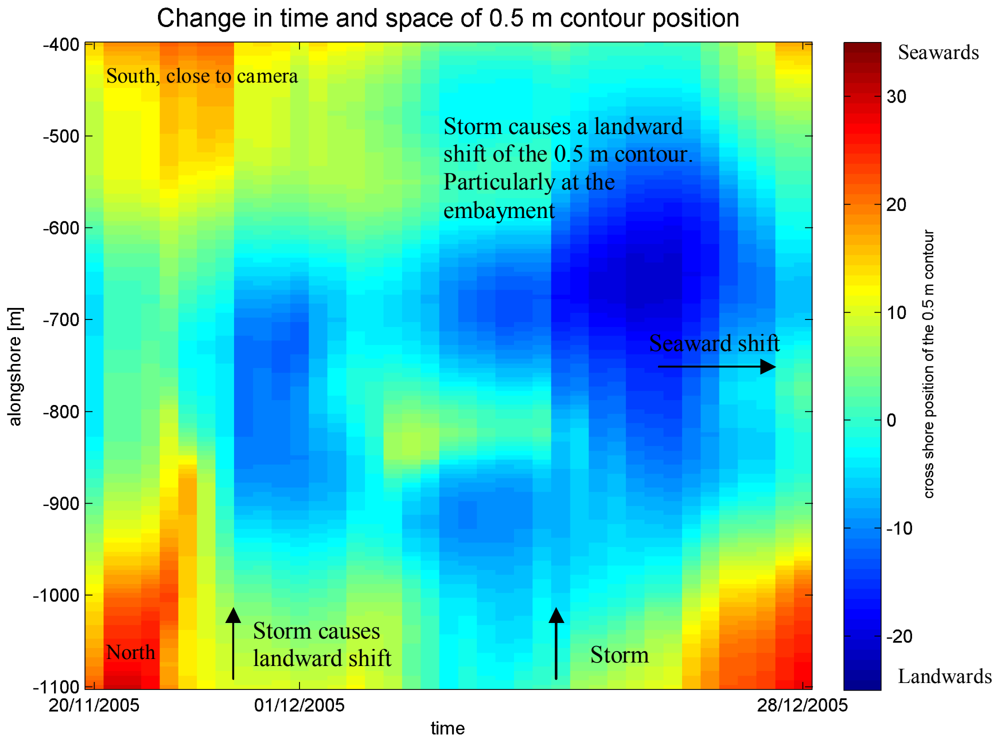

Figure 5.11: Change of the 0.5 m contour position in time for all alongshore locations for the second run. The cross shore axis is positive in seaward direction.

January to March 2006

Figure 5.12 shows the 0 m contour position at three alongshore locations and the measured H_{rms} wave heights for the third run. Concluding from Figure 5.12 there seems to be a seaward shift (5 to 12 m) of the 0 m contour induced by the storm in February. A seaward shift of the 0 m contour was also observed for the ASM summer run. However, during the summer run, the storm induced seaward shift is much larger (15 to 20 m). So, although the storm wave heights of the third run are higher, the impact is smaller. This difference may be explained by the assumption that the beach in February, at the end of the winter season, has a 'winter profile', induced by previous stomrs, on which a new storm has less influence. The May storm in the first ASM run follows a period of relatively nice weather, which has lead to a 'summer profile' on which a storm can have more impact.

Figure 5.13 shows the behaviour of the 0 m contour for all alongshore locations. Like for the summer run the storm seems to induce a sudden seaward shift at all alongshore locations. After the storm a continued seaward shift is observed. Northward of the -950 m alongshore first a landwards shift is observed after the storm period. What causes the landward shift at that locacation is unknown. It could be either real different beach behaviour at those alongshore locations, caused by morphologic differences of e.g the nearshore zone, or the result of detection errors.

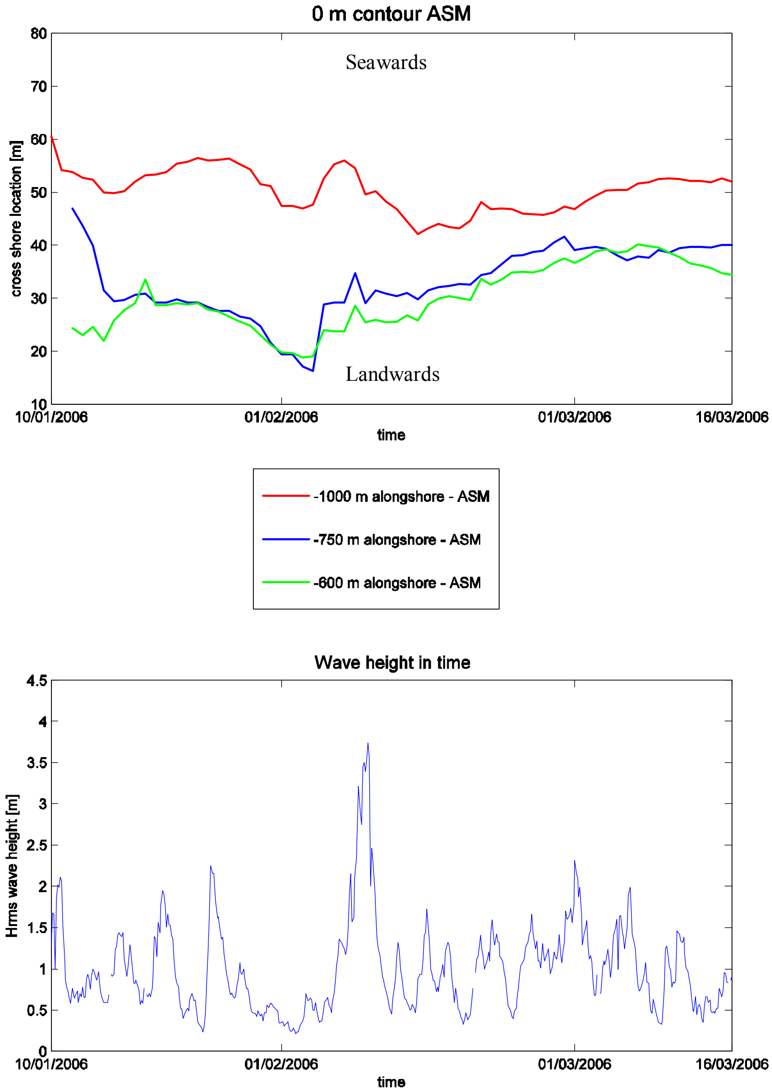

Figure 5.12: Above: cross shore movement of the 0 m contour in time at three alongshore locations for the third run. Below: H_{rms} wave heights measured at munitiestortplaats.

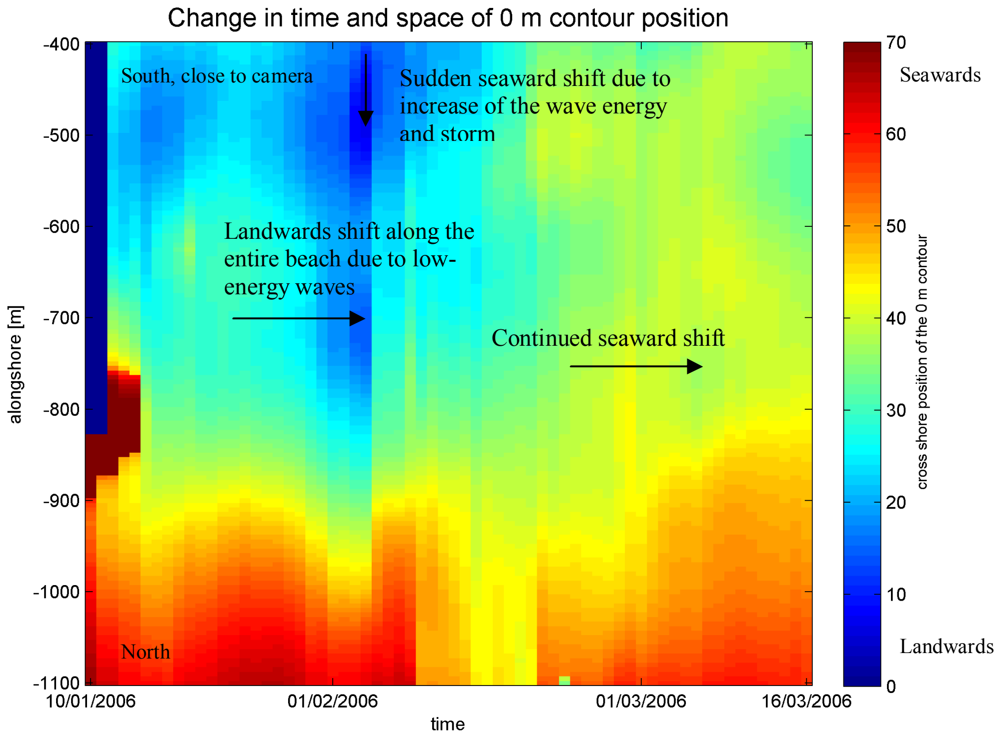

Figure 5.13: Change of the 0 m contour position in time for all alongshore locations for the third run. The cross shore axis is positive in seaward direction.

5.4 ASM performance for succeeding runs

Together the runs presented in this chapter, cover the period from November 20th 2005 to July 14th 2006. From December 29th 2005 to January 9th 2006 data is missing from this period, because of missing images. To study the performance of the ASM for succeeding runs the transitions of the 0 m contour, the 0.50 m contour and the MICL from one run to another are studied (see Figure 5.14).

The transition of the 0 m contour between the third and first run is very smooth. The transition between the second and third run is not good at -750 m and -600 m. At -1000m the transition seems reasonable, but it is not very clear, as data in between the two runs is missing. The transitions of the 0.50 m contour between the second and third and the third and first runs seem smooth at all alongshore locations. The transition of the MICL between the third and the first runs is smooth at all alongshore locations. Between the second and the third run, the transition between the MICL does not seem smooth, but this could merely be the result of the spikiness of the calculated MICLs.

The overall smooth transitions indicate that the performance of the ASM, concerning CSIs, between a longer period of running and a newly started run is similar. This was also concluded in Chapter 4 based on the comparison between the MICLs of the two runs in Figure 4.4 (upper and lower right).

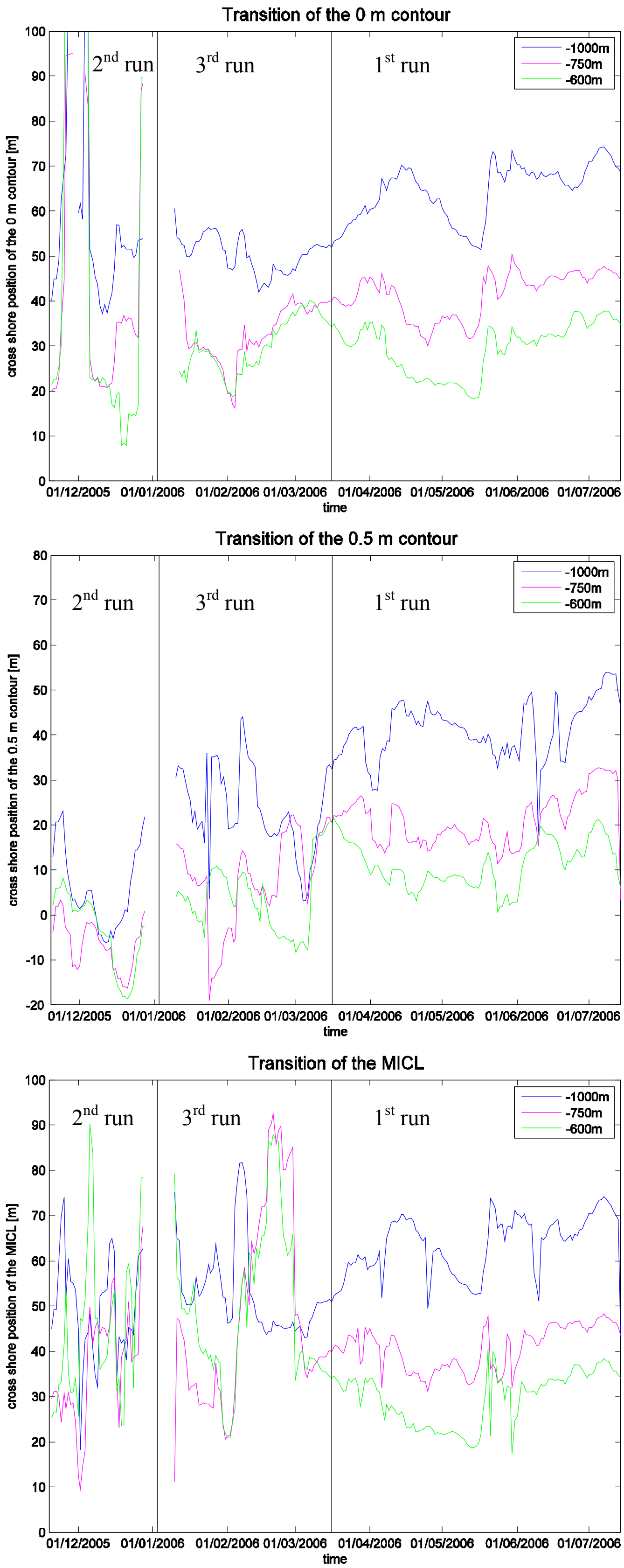

Figure 5.14: Transition between the 0 m contour, the 0.50 m contour and the MICL derived from the three runs. All y-axis are positive in seaward direction.

5.5 Findings on the application of the ASM

From the above comparisons between CSIs that were derived from ASM and IBM bathymetries and from the application of ASM data in studies on the beach behaviour the following conclusions are drawn.

- CSIs of ASM bathymetries compare very well with CSIs from IBM bathymetries, but they provide much more detail on the beach behaviour on the time scale of days to weeks. The ASM CSIs clearly show that the beach responds directly to changes in H_{rms} wave heights. This direct response could not be studied with the monthly IBM data.
- Both alongshore beach behaviour (e.g. the development and migration of the salient in the first run) and cross-shore beach behaviour (e.g. the seaward shift of the 0 m contour at all alongshore locations as a response to the storm) can be studied from ASM bathymetries.
- It was not possible to obtain one CSI that could be used for all three runs. This may hamper year-round studies of the beach behaviour.
- Differences in response of the beach at different alongshore locations and differences in response of the beach to storms between summer and winter conditions were observed. These differences could not be explained from the CSIs alone. More information on the entire coastal morphology is required to explain these differences. Combining intertidal beach information with knowledge of the position and height of nearshore bars may improve our understanding of the beach response to changes in wave heights. This allows for obtaining data on many storms, which in turn allows for classification of these storms based on the beach response.
- The three periods that were studied suggest that the 0 m contour shifts seawards due to higher H_{rms} wave heights and landwards during lower wave-energy conditions. The 0.50 m contour seems to respond just the other way around: landward movement during high wave-energy conditions and seawards movement during lower H_{rms} wave heights, although the latter was not always observed. These observations agree mostly with conclusions of other studies (Aagaard et al., 2005; Cohen and Brière, 2007; Quartel et al., 2007), but longer periods of time and more storms should be studied to obtain a full understanding of the intertidal beach behaviour.

6 Discussion

The performance of the ASM has been greatly improved. The test runs in Chapter 5 have shown that the ASM is capable of detecting the shoreline for both summer and winter conditions for very long periods (1.5 to 4 months for the various runs) without human support. This chapter provides discussions on the detecton of shoreline points in this research, on the use and limitations of ASM data and on the utilization of ASM at other Argus sites.

6.1 On the detection of shoreline points in this research

Detection method

As the Dutch beach was considered in this research, only the PIC detection method was used for shoreline detection. Many improvements made to the ASM are related to the use of the PIC method. An example of such an improvement is the definition of the region of interest. The color criterion used by the PIC detection method is determined on the pixels colors within this region. Furthermore, only pixel within the region of interest can currently be detected as the shoreline by the PIC method. Therefore a good definition of the region of interest is vital to the performance of the ASM when the PIC detection method is used.

Interpolation method of bench-mark bathymetry

For all runs only the loess interpolation was used to obtain the bench-mark bathymetries. According to Plant et al. (2002), the loess interpolation is an appropriate interpolation method to obtain bathymetries. The loess interpolation indeed showed to provide good results, and therefore no other interpolation methods have been tested.

Calibration of settings

The calibration that was performed in Chapter 4 mainly focusssud on the value of the vertical acceptance criterion that should be used in the ASM. The effect of different landward shifts on the determination of the region of interest and the ASM performance was only investigated for one case study. Of the other parameters, such as the seaward shift or the time window of the bench-mark bathymetries, the impact has only been reasoned about. Their influence on the performance of the ASM and the obtained bathymetries are not as well investigated as the influence of Z_{dif}. Z_{dif} itself seems to have minimal influence on the obtained bathymetries if a time window of several days is used in the post processing interpolation.

Quality control

The quality control on the detected shoreline points is rather rigid: a shoreline point is either rejected or accepted. Once a shoreline point is accepted it is treated, in later time steps and in data analysis, as being absolutely true. All points that are stored in the database are treated equal, for example in obtaining the bench-mark bathymetry of the next time step. In Section 3.6.3 a solution to this problem was proposed.

6.2 On the use and limitations of ASM data

6.2.1 Visible time and spatial scales

The conclusions of Chapter 4 were that for data analysis based on CSIs time windows of several days and smoothing scales in the order of 25 m cross-shore and 100 m alongshore should be used. The use of a time window of several days implies that short-term beach changes on a daily time scale are not clearly visible. On a weekly time scale however, where there is no overlap in the data, beach changes are clearly visible. The use of large smoothing scales implies that small features are not visible, as they are averaged out. According to Plant et al. (2002) the rule of thumb on the shortest visible length scales for loess interpolation are given by equation (6.1).

$$L \leq 0.5 L_0 \tag{6.1}$$

Where L is the smoothing scale and L_0 is the shortest visible length scale on the interpolated bathymetry. This means that for the largest smoothing scales used in this research (L_x = 25 m; L_y = 100 m) features with length scales of 50 m in cross-shore direction and 200 m in alongshore direction are visible. Examples of these features are the salients and embayments that were recognized by Aagaard et al. (2005) and Cohen and Briere (2007). Changes on these large spatial scales normally correspond with large temporal scales. However, the largest morphological changes are known to happen during storm events. As the ASM allows for identification of morphologic changes on time scales in the order of days to weeks, changes on a large spatial scale can be studied well on the time scale of storm events. The results of Chapter 5 show that this is indeed possible, and that the beach behaviour can be linked reasonable well to the main changes in H_{rms} wave heights.

6.2.2 ASM vs. DGPS

The data derived from ASM detected shoreline points showed to correspond well with the DGPS data. For bathymetries, derived with a time window of three days and smoothing scales of 25 m cross-shore and 100 m alongshore, the rms errors were in the order of 0.34 to 0.55 m for various ASM runs. The IBM bathymetries showed an rms error of 0.31 m for these post-processing interpolation settings. Unfortunately, the ASM data could thus far only be compared to DGPS measurements of one day (March 17th 2006).

ASM obtained data have some advantages over DGPS obtained data:

- ASM data have a much higher resolution in time and space. This allows for the study of beach changes that are not well covered by traditional DGPS measurements. Especially on the shorter time scale of weeks the ASM obtained data provides great advantages. The advantages on smaller spatial scales (1 to 10 m) is less, as the measurement error of the ASM is too large on those scales.
- Because DGPS is often less densely collected than ASM data, interpolation to a grid can introduce more errors that it can with dense ASM data. Separate DGPS measurements can indeed be better than ASM measurements, but, depending on the sampling density, ASM and DGPS interpolated bathymetries might equally well describe the true bathymetry.
- ASM data can be obtained daily at very low costs.

DGPS data also have some advantages over ASM obtained data. These are:

- During DGPS measuring campaigns interesting features can be measured on purpose, while with video detection the measured locations depend on the shoreline locations.
- DGPS measurements can be used to measure beach changes on smaller (< 50 m x 200 m) spatial scales that are not well sampled by the ASM.
- DGPS measurements are not limited by low and high water. DGPS measurements can be performed outside the intertidal beach.

6.2.3 ASM vs. IBM

The comparison of ASM and IBM bathymetries has only been performed based on coastal state indicators (CSIs). Although the ASM and IBM derived CSIs are very much alike, they do not give a complete indication of the true differences between the obtained bathymetries. The comparison merely shows that the ASM bathymetries could be used to gain trustworthy CSIs, that could be used to study beach changes. Comparison of IBM and ASM bathymetries by subtraction might give some insight in the spatial spread of the differences, and may indicate whether the differences between ASM and IBM bathymetries are different at alongshore locations close to and further from the camera.

6.2.4 Use in research and management

The ability of the ASM to obtain daily bathymetries for a longer period of time has been shown in Chapter 5. From the daily bathymetries CSIs can be derived. For each of the runs in Chapter 5 a CSI was found that could be used to study the beach behaviour for the time period of the run. However, these CSIs were not the same for all runs. For the first and third run the best CSI was the 0 m contour, while it was the 0.50 m contour for the second run. For the second run the 0 m contour could not be well obtained. Incomplete bathymetries, due to high water levels at that elevation and general bad detection during this run, are the most probable cause for this problem. Year-round studies of the beach behaviour might thus need to be performed by means of various CSIs. Further tests with ASM obtained bathymetries are needed for to be more conclusive on this matter.

The 0 and 0.50 m contours showed a clear response of the beach to changes in wave energy. This, combined with the fact that for the first run the manually and automatically obtained bathymetries correspond well and provide a similar trend in the movement of the 0 m contour, gives trust in the use of the ASM for management and research applications. Some examples of research applications are:

- The study of beach response to storms and the subsequent beach recovery.
  Thus far, research on storm impact has only been performed on a small number of storms. The ASM enables the collection of many pre- and post-storm bathymetries, to study storm impact. The ASM also enables the study of post-storm beach behaviour, as daily bathymetry data can be easily obtained for longer periods of time.
- Direct and long term beach response to nourishments.
  The impact (accretion and erosion) of nourishments on the beach can be monitored by using ASM bathymetries. The design of nourishments may benefit from increased knowlegde on the impact of nourishments.
- The impact of the Ecobeach project (Brière et al., 2008);
  The Ecobeach project is expected to lead to a widening of the beach through installation of a drainage system. Brière et al. (2008) recommend the continuation the monitoring to about a minimum of two years after the installation of the drainage system. By means of ASM obtained bathymetries the effect of the Ecobeach project could be monitored.
- Studies on long-term beach development (alongshore and cross-shore)
  Alongshore and cross-shore behaviour of the beach could be studied from ASM bathymetries for longer periods of time. Because daily information is available, non-linear trends in seasonal and yearly beach behaviour become visible.
- Support of numerical models
  Numerical models may benefit from daily bathymetries by updating and checking their outcomes to the ASM obtained bathymetries.

It should be noted that behaviour of smaller morphological features (<50 cross-shore and 200 m alongshore) cannot be studied well from ASM obtained bathymetries (Section 6.2.1).

In management applications the ASM obtained bathymetries could be used as an addition to the yearly Jarkus measurements. Those only provide information on the beach at every 250 m alongshore. The ASM showed to be able to obtain daily information on a smaller spatial scale. Local erosion treats could be better identified from ASM obtained data. Decisions on and the timing of nourishments, that are currently mainly based on the location of the yearly MCL[8] and on expert judgement, can be better substantiated when information derived from Argus images is used.

6.3 On the utilisation of ASM on other Argus sites

In this research the ASM has only been run for one camera on one Argus site (Coast 3D, camera 1). It is expected that the settings proposed for the Coast 3D site camera 1 also apply for the other cameras the Dutch Argus sites, as they all cover similar beaches. However, for other Argus sites, detection related parameters might need to be set differently. This section discusses what settings need attention when ASM is first applied at another Argus site.

The detection and elevation models might need to be changed to models that are appropriate for the monitored beach. The detection models described in Appendix C have all been developed for different beaches. One of these models could be used, or a new detection method could be developed. The parameters needed to calculate the shoreline elevation, beach slope and K_{osc}, should be calibrated for the beach site. Offshore wave data and offshore elevation data need to be available to calculate the shoreline elevation.

If the detection model needs a region of interest, the settings related to the determination of that region (if a moving region of interest is used) need to be calibrated. The quality control of the detected shoreline points should be reconsidered. Is a vertical acceptance criterion appropriate, or should a region of acceptance be used, as in Plant's version of the ASM (Section 2.3.1). The value for the acceptance criterion should also be calibrated.

For the determination of the bench-mark bathymetries the smoothing scales and the time window need to be considered. Smoothing scales could be smaller when the tidal range is smaller or when the beach is steep (because shoreline points are then closer together). On beaches with a larger tidal range or a flatter slope, the smoothing scales might need to be larger. The time window of the bench-mark bathymetries is also of importance. On beaches with a diurnal tidal cycle the time window may need to be larger than on beaches with semi-diurnal tidal cycles.

Settings related to the Argus station (siteID, name) and camera (camera number, image range) of course always have to be changed if the ASM is applied elsewhere.

8. Momentary coastline, derived from Jarkus measurements.

7 Conclusions and recommendations

This final chapter provides an overview of the conclusions and recommendations. It provides answers to the research questions and gives an overview of the steps that could be taken in further research.

7.1 Conclusions

In this section the conclusions are presented per objective. The objectives were presented in the Introduction.

7.1.1 Objective 1: improved performance and usability of ASM

Problems and improvements

The version of the ASM that was the starting point of this research collapsed after a few days of data collection on the Dutch beach. The complexity of the Dutch beach and the weather conditions played a part in this collapse, but the most important problem was the declining number of detected and stored shoreline points in time. The ASM needs sufficient (self detected) shoreline points to be able to derive a good bench-mark bathymetry. This bathymetry is used to obtain a region of interest and to perform a quality check on the newly detected shoreline points. A declining number of shoreline points in time, initiated for example by a day of bad weather or bad detection in general, could induce a downward spiral that led to even less data points in time and finally to the collapse of the ASM. The solutions proposed all focused on avoiding this downward spiral. The improvements that added most to the performance of the ASM are the extension of the region of interest, the avoided zigzagging of the regions of interest, and the double quality check on the detected points.

Improved usability

The usability of the ASM was improved by introducing a new set-up that allows flexible use of the tool on various beaches and even in laboratory settings. The new set-up calls various routines one by one that perform the different steps needed in shoreline detection. Each routine can be replaced by a routine that performs the same step, but in a different way. The PIC detection model could e.g. be replaced easily by another shoreline detection model.

Man-hours saved

The current version of the ASM has detected shorelines for a continuous period of 4 months in a summer period (March 17th 2006 to July 14th 2006) and for two continuous winter periods of 1.5 and 2 months (Noverber 20th 2005 to December 28th 2005 and January 10th 2006 to March 16th 2006). All ASM runs were terminated manually, the ASM did not collapse. The ASM, with the settings used in this research, currently takes 3.5 to 4 minutes to map the shoreline on one image. In case of half-hourly images and 12 daylight hours, this means that it takes the ASM approximately 1,5 hours to map the shorelines of one day for one camera. It takes longer to obtain shorelines by ASM than it takes to obtain them manually by IBM, which requires 30 to 60 minutes per day per camera. However, the ASM runs automatically making all human effort redundant.

The biggest advantage of the improved ASM is that the intertidal beach bathymetries can now be obtained on a daily to weekly time scale, without the need of expensive and time-consuming human efforts. For the run of 4 months (120 days) it would have taken at least 60 man-hours to obtain the daily bathymetries. These man-hours are now saved by the use of the ASM.

7.1.2 Objective 2: quality, use and limitations of ASM data

Quality of ASM data

The automatic quality control on the detected shoreline points raised questions on the quality of the ASM obtained bathymetries and on the use and limitations of the ASM bathymetries in data analysis. To study the quality of the ASM shoreline data, the obtained bathymetries were compared to DGPS measurements and IBM bathymetries.

Compared to DGPS data the ASM data show rms errors between 0.24 and 0.55 m. ASM bathymetries obtained with the smallest smoothing scales (10 m cross-shore and 25 m alongshore) and the shortest time window (1 day) for the loess interpolation show the smallest rms errors. Generally, the rms errors increase for larger smoothing scales and a longer time window. The rms errors, calculated for a bathymetry with a time window of 3 days and smoothing scales in the order of 25 m cross-shore and 100 m alongshore, range between 0.34 and 0.55 m. IBM obtained bathymetries show, as expected, the smallest rms errors with DGPS data (0.25 to 0.32 m).

For two case studies ASM and IBM bathymetries were compared by means of coastal state indicators (CSIs). The CSIs considered were the momentary intertidal coastline (MICL), several elevation contours and the slope. The ASM was run with different values for the vertical acceptance criterion (Z_{dif}): 0.10 m, 0.25 m, 0.50 m. Overall, CSIs derived from ASM bathymetries with large smoothing scales (25 m cross-shore and 100 m alongshore) and large time windows (3 to 6 days) show the best agreement with CSIs derived from IBM bathymetries. In general, the influence of the value of Z_{dif} on the derived CSIs was not clearly visible.

Generally, the ASM derived MICL lay 2 to 4 m seaward of the IBM derived MICL. This is probably the result of the seaward shifts of the –0.50 m, 0 m and +0.50 m NAP contours, which showed a seaward shift of 4 to 5 m, 2 to 3 m and 0 to 1 m respectively. Generally, the seaward shift was larger for lower elevation contours. These shifts also result in a gentler slope for the ASM bathymetries. The seaward shift of the elevation contours is thought to be the result of the detection and acceptance of shoreline points that are located seawards of the true shoreline. It seems that this problem is stronger at lower water levels, explaining the larger seaward shift of the lower elevation contours.

Use and limitations of ASM bathymetries

The smoothing scales and the time window that are used in the interpolation of the bathymetries affect the spatial scales and the time scale that can be studied with the obtained bathymetries. Use of larger smoothing scales implies that small-scale features on the beach cannot be studied. Features at the alongshore scale of 200 m and the cross-shore scale of 50 m can well be studied when smoothing scales of 25 m cross-shore and 100 m alongshore are used. The use of time windows of several days implies that true day-to-day CSIs cannot be well obtained from ASM data. The need for time windows of several days results from a lack of shoreline data on days with bad detection and the daily fluctuations in high and low water. Longer time windows (3 to 6 days) generally supply useful bathymetries. Beach changes on a time scale of several days to a week can thus well be studied using ASM data. The development of embayments and salients and the response of the beach to storms are examples of the spatiotemporal scales that can be studied with ASM data. This was clearly shown in Chapter 5, where the CSIs derived from daily ASM bathymetries, with a time window of six days, provided a more detailed insight into the beach response to changing H_{rms} wave heights than the monthly IBM derived CSIs could.

Applications in research and management

The daily bathymetries, that can become available because of the improved version of the ASM, provide opportunities for both research and management. The high resolution in time allows for the study of storm impact. Because intertidal bathymetries can now become available over longer periods of time, the number of storms that can be studied increases. The longer time series also support research on beach recovery and seasonal changes. The impact of beach and nearshore nourishments is another subject that could be monitored from ASM bathymetries. This may support the design and timing of the nourishments. The daily ASM bathymetries provide better insight into localized threats and non-linear beach behaviour. The ASM data can be used as an addition to the yearly Jarkus measurements and, in that way, support management decisions.

7.2 Recommendations

This section lists the recommendations on the use of the ASM data in research and management and suggestions for further research.

Use of ASM data in research and management

- It is recommended to use the advantage of being able to easily obtain daily bathymetries for very long periods of time in studies on beach behaviour. Some examples of research applications, also listed in Section 6.2.4, are the study of storm impact and subsequent beach recovery, seasonal changes and the impact of nourishments.

- For managements purposes, CSIs derived from the ASM data can be used as indicators of beach evolution. Relative beach erosion and accretion can well be monitored using ASM data. The ASM data can be used as an addition to the yearly Jarkus measurements both in time and space. On the spatial scale ASM data can be used to fill the space in between the Jarkus transects. This helps to avoid missing erosion hotspots. This was already acknowledged by Wijnberg et al. (2004) that based their conclusion on manually obtained monthly bathymetry data. On the temporal scale, the ASM data can be used to study beach change in between the yearly measurements. ASM data allows monitoring on smaller spatiotemporal scales than is possible with Jarkus measurements alone.
- The MICL position, as calculated in this research, is easily affected by the presence of sand bars in the obtained bathymetry. If no sand bar is present in the obtained bathymetry, this does not necessarily imply that it is absent in reality. This research showed that the ASM sometimes does not correctly detect the sand bars. This would lead to a lower calculated beach volume and thus to a too much landward located MICL. Use of only the MICL for monitoring purposes may therefore result in wrong conclusions on erosion and accretion. It is advised to also use contours from ASM obtained bathymetries to monitor beach evolution.

Suggestions for further research

- The data derived with the ASM should be compared to DGPS data of more than one day. Currently, only ASM data of March 17th 2006 was compared to DGPS data.
- CSIs derived from ASM bathymetries should be compared to CSIs of IBM bathymetries for more days. Currently only six days are compared.
- The ASM and IBM bathymetries should be compared by considering spatial differences by means of substraction. This provides insight into where the differences are largest. This may help in further improving the ASM.
- The influence of other settings on the obtained bathymetries should be tested more thoroughly. It would be especially interesting to know how the ASM performs for larger smoothing scales for the first bench-mark bathymetry. Currently, due to the small smoothing scales that were used in this research, interpolation of this bathymetry takes most of the time the ASM needs to detect shorelines.
- The suggestions for further improvements in Section 3.6 should be implemented and tested. For the proposed criterion it would be interesting to know if it reduces the number of wrongly accepted and rejected points. Furthermore, the influence of the 'measure of trust', on the performance of the ASM and on the obtained ASM bathymetries needs to be investigated.
- The performance of the ASM under storm conditions needs to be researched further for heavier and longer storms. Also storm settings ($Z_{dif,storm}$, $H_{rms.storm}$ and the storm duration criterion (Section 2.3.1)) for the Dutch beach need to be obtained. A suggestion for $H_{rms,storm}$ is 2 m. Quartel et al. (2007) found morphological response of the intertidal beach for H_{rms} wave heights above 2 m. This value was used in this research.
- Sand bars that are not detected are not necessarily absent. The MICL is susceptible to this 'disappearance' of sand bars. Contours are less influenced by this problem. During this research a large correlation was seen between the MICL and the 0 m NAP contour

during the summer run of the ASM (March 17th 2006 to July 14th 2006). It is therefore recommended that the correlation between the MCL and the 0 m NAP contour is studied, to see if the 0 m contour can also be used to describe erosion and accretion adequately. Wijnberg et al. (2004) already found a good correlation between the MICL and the MCL.

- The reliability of ASM data should be studied further, to investigate if it can support coastal management decisions. So far the ASM data should only be used as an indication to beach erosion or accretion.

8 References

Aagaard, T., Kroon, A., Andersen, S., Møller Sørensen, R., Quartel, S., Vinther, N., 2005. Intertidal beach change during storm conditions; Egmond, The Netherlands. Marine Geology 218, pp. 65-80.

Aarninkhof, S.G.J., Roelvink, J.A., 1999. Argus-based monitoring of intertidal beach morphodynamics. In Proc. of Coastal Sediments Conf., Long Island (NY), USA, 2429-2444.

Aarninkhof, S.G.J., 2003. Nearshore bathymetry derived from video imagery. PhD Thesis, Delft University of Technology.

Aarninkhof, S.G.J., Turner, I.L., Dronkers, T.D.T., Caljouw, M., Nipius, L., 2003. A video-based technique for mapping intertidal beach bathymetry. Coastal Engineering 49, 275-289.

Aarninkhof S.G.J., Morelissen, R., Cohen, A.B., 2007. The Argus Runtime Environment: Guidelines on Installation and Use. WL|Delft Hydraulics, Marine and Coastal Management.

Brière, C., Cohen, A., Van den Boogaard, H., Arens, S., 2008. Ecobeach Monitoring project Phase II. WL|Delft Hydraulics.

Cohen, A.B., Briere, C., 2007. Evaluatie van de uitgevoerde suppleties bij Egmond op basis van Argus video waarnemingen. WL|Delft Hydraulics, Marine and Coastal Management.

Davidson, M., Van Koningsveld, M., De Kruif, A., Rawson, J., Holman, R., Lamberti, A., Medina, R., Kroon, A., Aarninkhof, S., 2007. The CoastView project: Developing video-derived Coastal State Indicators in support of coastal zone management. Coastal Engineering, 54, 463-475.

Geologisch, 2008. http://www.aardrijkskunde.org/topo/images/nederland_contour.gif

Google Maps. http://maps.google.com

Holland, K.T. and Holman, R.A., 1997. Video Estimation of Foreshore Topography Using Trinoculare Stereo. Journal of Coastal Research, 13 (1), 81-87.

Holland, K.T., Holman, R.A., Lippman, T.C., Stanley, J., Plant, N.G.., 1997. Practical Use of Video Imagery in Nearshore Oceanographic Field Studies. IEEE Journal of Oceanic Engineering 22(1), 81-92.

Kroon, A. , De Boer, A.G., 2002. Horizontal flow circulation on an intertidal beach.In Van Rijn, L.C., Ruessink, B.G., Mulder, J.P.M. Coast3D - Egmond. The behaviour of a straight sandy coast on the time scale of storms and seasons. Process knowledge and guidelines for coastal management. Amsterdam: Aqua Publications. pp. D-1 – D-16.

Kroon, A., Davidson, M.A., Aarninkhof, S.G.J., Archetti, R., Armaroli, C., Gonzalez, M., Medri, S., Osorio, A., Aagaard, T., Holman, R.A., Spanhoff, R., 2007. Application of remote sensing video systems to coastline management problems. Coastal Engineering 54, 493-505.

Madsen, A.J. and Plant, N.G., 2001. Intertidal beach slope predictions compared to field data. Marine Geology 173, 121-139.

NCSU, 2008. http://www.ncsu.edu/scivis/lessons/colormodels/color_models2.html

Nipius, L., 2002. Evaluation of Nourishments at Egmond. MSc thesis, Delft University of Technology, departement of Civil Engineering and Geosciences, division of Hydraulic and Offshore Engineering.

Plant, N.G., Holman, R.A., 1997. Intertidal beach profile estimation using video images. Marine Geology 140, 1-24.

Plant, N.G., Holland, K.T., Puleo, J.A., 2002. Analysis of the scale of errors in nearshore bathymetric data. Marine Geology 191, 71-86.

Plant, N.G., Aarninkhof, S.G.J., Turner, I.L., Kingston, K.S., 2007. The performance of shoreline detection models applied to video imagery. Journal of Coastal Research 23, 658-670.

Plant, 2008. Personal correspondance.

Quartel, S., and Grasmeijer, B.T., 2007. Dynamiek van het strand bij Noordwijk aan Zee en Egmond aan Zee en het effect van suppleties. Rapport: CR-2007-01. Utrecht University, Faculty of Geosciences.

Quartel, S., Ruessink, B.G., Kroon, A., 2007. Daily to seasonal cross-shore behaviour of quasi-persistent intertidal beach morphology. Earth Surf. Process. Landforms 32, 1293-1307.

RIKZ, 2001. Zoutkrant. July 2001(2).

Smit, M.W.J., Aarninkhof, S.G.J., Wijnberg, K.M., González, M., Kingston, K.S., Southgate, H.N., Ruessink, B.G., Holman, R.A., Siegle, E., Davidson, M., Medina, R., 2007. The role of video imagery in predicting daily to monthly coastal evolution. Coastal Engineering 54, 539-553.

Storlie, C.B. and Helton, J.C., 2008. Multiple predictor smoothing methods for sensitivity analysis: Description of techniques. Reliability Engineering and System Safety 93, 28-54.

Van Koningsveld, M., Davidson, M., Huntley, D., Medina, R., Aarninkhof, S., Jiménez, J.A., Rigdewell, J., De Kruif, A.,2007. A critical review of the CoastView project: Recent and future developments in coastal management video systems. Coastal Engineering 54, 567-576.

Van Rijn, L.C., and Walstra, D.J.R., 2002. Basic features of morphodynamics at the Egmond site on the short-term time scale of storms. In Van Rijn, L.C., Ruessink, B.G., Mulder, J.P.M. Coast3D - Egmond. The behaviour of a straight sandy coast on the time scale of storms and seasons. Process knowledge and guidelines for coastal management. Amsterdam: Aqua Publications. pp. I-1 – I-16.

Van Rijn, L.C., Ruessink, B.G., Mulder, J.P.M., 2002. Coast3D - Egmond. The behaviour of a straight sandy coast on the time scale of storms and seasons. Process knowledge and guidelines for coastal management. End document March 2002. Amsterdam: Aqua Publications. ISBN 90-800356-5-3. EC MAST Project No. MAS3-CT97-0086, March 2002.

Wijnberg, K.M., Aarninkhof, S.G.J., Van Koningsveld, M., Ruessink, B.G., Stive, M.J.F., 2004. Video monitoring in support of coastal management. Proc. of 29th Int. Conf. on Coastal Engineering, Lisbon, Portugal.

Wright, L.D. and Short A.D., 1984. Morphodynamic variability of surf zones and beaches: a synthesis. Marine Geology 56, 93-118.

A Egmond beach

A.1 General

Egmond beach is located on the Holland coast. This is the central part of the Dutch coast between Den Helder in the North and Hoek van Holland in the South (see Figure A.1).

The width of Egmond beach varies between 100 and 200 m from dune foot to the low water line. The grain diameter varies between 250 and 350 µm and is coarsest on the intertidal beach (Van Rijn et al., 2002). The intertidal beach is characterized by the presence of swash bars with heights ranging between 0.1 and 1 m. Swash bars develop at the low water line and migrate onshore due to swash processes during low to moderate wave-energy conditions. Their dimensions vary between 20 to 50 m cross-shore and 100 to 500 m alongshore. Through troughs, where the maximum flow velocity is 0.6 m/s the sediment is transported alongshore. Off shore directed sediment transport takes place through the rip channels that intersect the swash bars (see Figure A.2). This horizontal circulation is driven by an alongshore gradient in mean water level due to differences in wave-induced set-up, which is higher over the bar than over the rip channel (Kroon and De Boer, 2002). Net onshore sediment transport is in the order of 0.3 to 1 m^3/m/day. During storms the dominant transport process is directed offshore, driven by undertow. During these high wave-energy conditions the swash bars are destructed, leading to a flattening of the beach (Van Rijn et al., 2002).

The nearshore part of the Egmond coast is characterized by two subtidal bars, which evolve in a cyclic manner. The outer bar (most seaward) lies below the mean water depth of –3.5 to –4 m NAP and has a straight pattern. The intter bar lies below a mean water depth of –1.5 to –2.5 m NAP and has an irregular pattern. The cross-shore distance between the two bars is approximately 300 m. This distance is rather constant in time (Van Rijn et al., 2002).

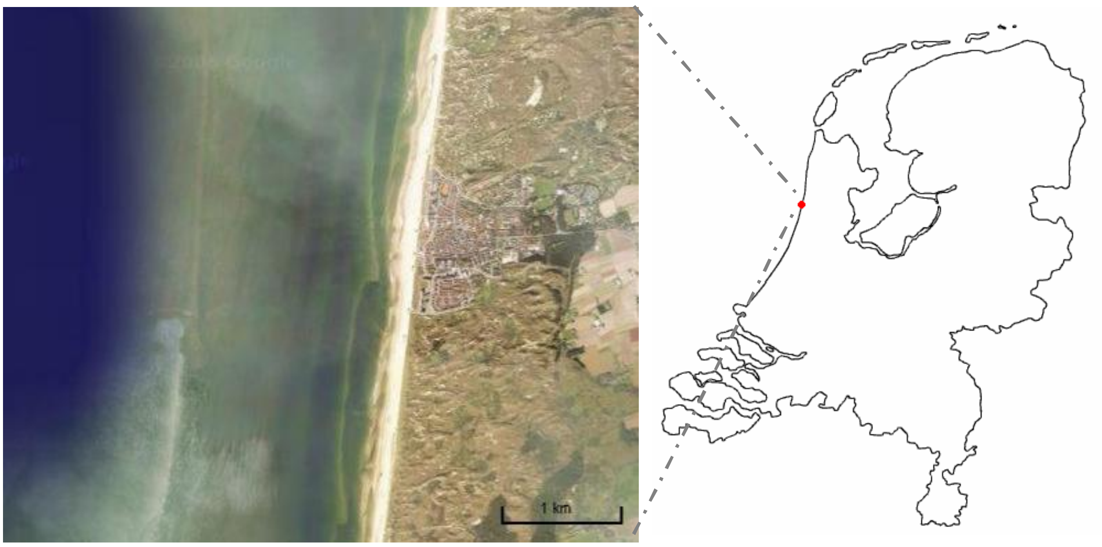

Figure A.1: Egmond beach (left) (Google Maps, 2008); Netherlands (right) (Geologisch, 2008)

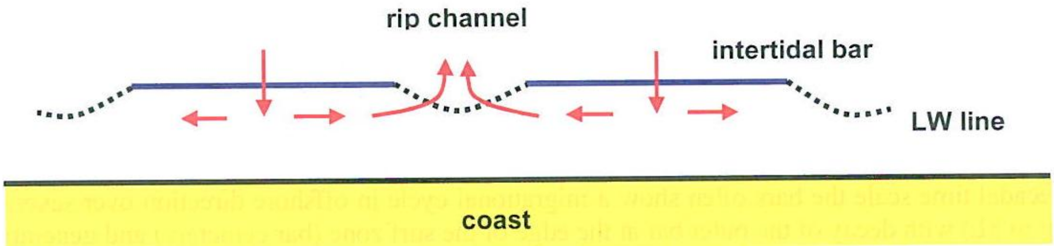

Figure A.2: Horizontal circulation during low wave-energy conditions. The water flows over the intertidal bar, then flows alongshore through the the trough and finally offshore through the rip channel. The net onshore sediment transport during fair weather is 0.3 to 1 m^3/m/day (Van Rijn et al., 2002).

Historical maps of Egmond show structural erosion of the Egmond beach. The shoreline retreat was about 1m/year between 1600 and 1750 and about 0.5 m/year from 1750 to 1990 (Van Rijn et al., 2002). From 1990 on, the shoreline retreat was kept under control by nine beach nourishments and two nearshore nourishments (Cohen and Briere, 2007).

A.2 Environmental conditions

Van Rijn et al. (2002) classified the Holland coast as a mixed energy coast, meaning that both wind waves and the tide act on the sandy sediments and that both induce a morphological response.

The Egmond coast experiences an asymmetrical tide, with approximately 4 hours flood and 8 hours ebb. The tidal range is 1.65 m on average, with a maximum during spring tide of 2 m and 1.4 m during neap tide. The tidal currents are directed northwards during the flood hours and directed southwards during the ebb period.

The yearly average wave height is 1.2 m. During the winter months (November to January) the average wave height is 1.7m; during the summer months (April to August) the average wave height is 1.0 m. The wave rose in Figure A.3 shows the H_{rms} wave heigths measured by various wave stations[9] from January 1st 1998 to August 31st 2007.

A.3 Research on Egmond intertidal beach

The evolution of the Dutch coast has been monitored since 1965 (Jarkus database). Each year the bottom profiles are measured to depths of -6 m NAP with an alongshore spacing of 250 m (Van Rijn et al., 2002). To allow research on smaller time and spatial scales, additional measuring campaigns have been held. This section describes the conclusions of

9. From 1998 to 2002 the first preferred wave buoy was at the IJmuiden Pier, from 2003 to 2007 the preferred wave buoy was Munitiestortplaats. In both cases the second perferred wave buoy was Eierlandse Dam.

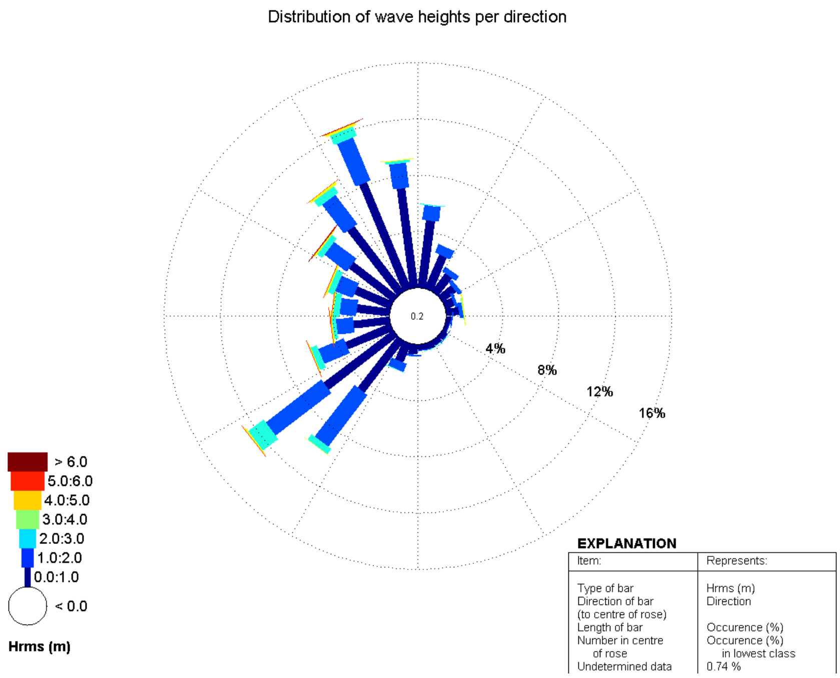

Figure A.3: Wave rose for Egmond beach for the period January 1st 1998 to August 31st 2007 measured by various wave stations.

some studies that focused on the (intertidal) beach behaviour on the time scale of storms and seasons.

Aagaard et al. (2005) analyzed the morphologic response of the intertidal beach of Egmond to three storms occurring within six days in the fall of 2002. One of their objectives was to study the spatially inhomogeneous beach response. They recognized that Egmond beach is an intermediate beach (between reflective and dissipative), based on the discriminator of Wright and Short (1984).

$$\Omega = \frac{H_b}{w_s T} \qquad \text{A.1}$$

Where H_b is the breaker height, w_s is the fall velocity of the sediment and T is the wave period. For Egmond beach a value for Ω of about 3 was calculated. Egmond beach is characterized by dissipative salients and reflective rip embayments. Aagaard et al. (2005) found a different response to storms for the salients and the embayments. The mean slope of the embayments prior to the storms was approximately 1/23 and changed to 1/30. The net erosion was 15.1 m^3/m and the 0-m-contour shifted 5 m seaward. At the salient the slope was gentler to begin with and remained unchanged at a mean value of 1/31. The erosion was only 3.8 m^3/m.

Aagaard et al. (2005) give two possible reasons for the difference in erosion of the embayments and salients. The first reason is the combination of larger undertow during high-tide and higher sediment concentrations due to plunging waves at the embayments. Undertow velocities scale with the radiation stress gradient, that in turn depends on wave height and beach slope. At the rip embayments the inner bar is lower, allowing higher waves to reach the steeper beach, leading to higher undertow velocities at the embayments than at the salients. Because the beach is steeper at the embayments the waves plunge instead of spill, entraining more sediment. The second reason could be the smaller net onshore directed sediment fluxes during low tide. At steeper beaches the backwash has a higher velocity, favouring transport by backwash over uprush transport or diminishing the effect of uprush transport.

Based on 5-week beach and nearshore measurements (18 October 1998 till 12 November 1998) Van Rijn and Walstra (2002) concluded that the location of the rip channels indicates locally smaller beach volumes and correlates with lower inner bar crest levels. Where the inner bar is well-developed the beach volume is larger, because wave energy is dissipated more. As the inner bar crest level is continuously changing, the beach volume is constantly adapting to a new equilibrium. Van Rijn and Walstra (2002) found that the beach volume is at its mean value when the inner bar has a height of -1.5 m NAP. With a 1 m rise/fall of the inner bar level, the beach volume accretes/erodes 30 m^3/m. They find that during storm months the daily beach volume change varies between 1 and 3 m^3/m/day.

The correlation that Van Rijn and Walstra (2002) found between inner bar crest level and intertidal beach volume is not supported by Quartel and Grasmeijer (2007). They could not find any relation between the beach volume and the crest level of the inner bar. Clearly, there is no agreement on the impact of the inner bar crest height on beach behaviour. A difference between both studies is that Quartel and Grasmeijer (2007) used monthly measurements, while Van Rijn and Walstra (2002) used daily measurements.

Using Argus images Cohen and Briere (2007) studied the effect of two storms on Egmond beach. One storm took place in 2003, at that time the last nourishment was performed in 2000. The other storm took place after a nearshore and beach nourishments of 2004 and 2005 respectively. The two storms were comparable: both occurred after a two-week period of calm weather and wave height and wind direction were approximately the same. Cohen and Briere (2007) concluded that a non-nourished beach flattens as a result of a storm and that a nourished beach steepens. The steepening especially took place at the hotspot.

Based on monthly bathymetries derived from Argus images Cohen and Briere (2007) recognised the embayment south of Egmond as an erosion hotspot. They concluded that the beach of Egmond, after nourishments, on the long time scale returns to an alongshore profile with an erosion hotspot south of Egmond.

Quartel et al. (2007) monitored the intertidal bar and trough system on the beach of Noordwijk daily for a period of 15 months to study the daily to seasonal cross-shore behaviour. The bars and troughs on the intertidal beach were identified on low water Argus images. The landward boundaries of the bars and troughs show a sawtooth motion of gradual landward migration followed by abrupt seaward shifts. These abrupt shifts were caused by storm events which lasted longer than 30 hours with average H_{rms}wave heights above 2 m and which had an offshore surge level of more than 0.5 m. The intertidal beach showed a response to these storms if the trough was small (< 20 m wide).

B Research by Cerezo and Harley

This appendix contains the documentation of the work performed by Cerezo and Harley in 2006. Their work was not publiced, but nontheless very useful for this and future research.

B.1 Cerezo and Harley (2006)

THE ARGUS RUNTIME ENVIRONMENT : AUTO SHORELINE-PICK

INTRODUCTION

This document summarises the work spent by Antonio Cerezo and Mitchell Harley on the implementation of a program (initially developed by Nathaniel Plant) that enables shorelines in Argus images to be picked automatically (‘autoShorelinePick’). It outlines the overall program routine, the additions made, problems encountered and finally some comparisons of outputs to high-accuracy survey data.

FINDSHORE_COMMAND : MAIN ROUTINE

The overall rationale to the program is that a bathymetry is created from recent (both past and future) shorelines, which is used to either reject or accept shoreline points picked by the IBM. Any point that is greater than a vertical distance ‘Zstd’ from the bathymetry is rejected. Additional rejection criteria were also added to the program, which is discussed later.

The routine is executed by the function ‘findshore_command’. This function requires the input of one array of image times that the user wants to find the shorelines of. This executes the following loop (functions called are in bold):

- LOADS IMAGE SETTINGS AND GLOBAL VARIABLE SHORELINE_DATA **(FINDSHORE_CREATE_SHORELINEDATA)**
- LOADS WAVE AND TIDE DATA **(DBGETEUROWAVE/ DBGETEUROTIDE)**
- FINDS VERTICAL ELEVATION OF THE SHORELINE **(GETETASWASH)**

- LOADS IMAGE DATA
  (FINDSHORE_LOAD_IMAGEDATA)
  - Looks for the planview of the image or make a new one
    (FINDSHORE_UPDATE_IMAGES)
  - Loads planview image details

- LOOPS THROUGH IMAGES WITHIN 'ITIME' ARRAY
  (FINDSHORE_ACIMAGELOOP)
  - Creates a bathymetry made of all the shorelines stored in the database within a certain time period
    (FINDSHORE_UPDATE_BATHY)
  - Gets Region of Interest from IBM userSettings
  - Creates the new variable 'data' to use it in the doFindWL_AC routine
  - Gets horizontal coordinates of the Shoreline
    (DOFINDWL_AC)
  - Compares Shoreline estimates to the bathymetry and rejects "bad" points. Image of shoreline stored in Results folder
    (FINDSHORE_COMPARE_XY)

- SAVES THE SHORELINE INTO THE DATABASE (PROVIDED THAT SHORELINE IS ACCEPTED)

<u>PROGRAM ADDITIONS</u>

Several additions were made to the model to improve its performance. These include additional rejection criteria, the option for a shifting ROI, the option for linear interpolation and the ability to deal with post-storm conditions.

Additional Rejection Criteria

After accepting or rejection points based on the 'Zstd' rejection criteria, the model contains two additional criteria. Firstly, if there are too few good points picked the model rejects the shoreline altogether. Secondly, if the ratio of good points to total points fond is less than a third, then the shoreline is also rejected altogether.

Linear Interpolation

If the hanning interpolation method works poorly (or not at all), then there is now an option to use linear interpolation.

Shifting ROI

Due to the fact that very few 'good' shorelines were being picked at Jvspeijk and at Camera 5 of Narrabn, the program now includes the option to have a shifting ROI. There are two ways that this is achieved. Firstly, the ROI is defined by the contour of the calculated elevation on the calculated bathymetry. The ROI is then a box around this contour, with both seaward and landward offsets. Alternatively, a user-defined ROI shape can shift in the cross-shore direction according to the calculated elevation and the beach slope of the site. The maximum and minimum shoreline boundaries are also defined and are factored into the ROI calculation.

Post-storm conditions

After a storm (defined as Hrms wave heights above a certain height), the bathymetry is unlikely to be similar to previous bathymetries. To accommodate this in the model, the Zstd rejection criterion is loosened for a period of 2 days after a storm, so that new shorelines can be found. However, the shorelines stored during this time should be checked as they may be erroneous.

<u>DESCRIPTION OF IMPORTANT PROGRAM INPUTS</u>

The program requires the input of several parameters, which is mainly done in the file 'findshore_create_shorelinedata'. The most important ones are discussed below.

SHORELINE_DATA.Zstd

This is the most important parameter as it determines which shoreline points are rejected. If this parameter is too large, 'bad' shoreline points will be accepted. Alternatively, if it is too small, no points will be accepted at all. At the same time, the Zstd parameter also has to be sufficiently large to accommodate any changes in bathymetry at daily time scales. After testing on Narrabeen images, a suitable Zstd was found to be 0.3 m. At Jvspejk, approximately 0.5m was more appropriate.

SHORELINE_DATA.Zstorm

This parameter defines the Zstd during post-storm conditions, where it is loosened to accommodate the fact that the bathymetry has probably changed. For Narrabeen, this was set to 0.8m.

SHORELINE_DATA.stormwave

This is the Hrms wave height above which storm conditions occur. For Narrabeen, this was set to 1.5m.

SHORELINE_DATA.LT

This determines how far in the past and future the program takes shorelines from to create a bathymetry. For Camera 1 at Narrabeen, where the bathymetry changes are small on daily time scales, this was set to 5 days. For Camera 5, where the bathymetry is more dynamic, this was set to 2.5 days.

SHORELINE_DATA.interp

This determines the interpolation method used. If you want linear interpolation, this is set to 'linear'. Otherwise, the interpolation will be hanning.

SHORELINE_DATA.eithersideROI

If you want to use a shifting ROI rather than a fixed one, then this parameter is set to 1. Otherwise it is set to 0.

PROBLEMS ENCOUNTERED

Bathymetry

Because the calculated bathymetry determines the rejection criteria, it is essential that the calculation is sound. Initially, the hanning interpolation method yielded very poor results upon comparison to surveyed bathymetries. This error was traced to the use of an old version of the 'scalecinterp' function. Updating this function to the latest version fixed this problem.

Another problem with the bathymetry is that at Narrabeen – where the beach is curved - the coordinates are not aligned directly in the cross-shore – longshore directions. Hence the cross-shore and alongshore scale smoothing parameters must be equal, otherwise the bathymetry will be distorted. Additionally the Narrabeen beach curvature means that points outside the image are calculated and may give the impression that the bathymetry looks bad. However in the ROI, the bathymetry appears to be correct.

Multiple-camera merge

Another problem found in the program was the difficulty in working with plan images instead of oblique ones. Using plan images based on one camera only, the resolution was sufficient (1m) to detect shorelines effectively. Difficulties however arose when detecting shorelines based upon multiple-camera merge images. Firstly, there was an issue with the cameras not being synchronised (the offset was almost 20 minutes in some cases), resulting in a discontinuous merge image. Secondly, the resolution was not sufficient to find shorelines in a complete merge image. Owing to this, the working program is limited to single camera images for the time being.

Shifting ROI

For the time being, the shifting ROI option is still in its developmental phase. For the shifting ROI based upon the contour criteria, testing on Narrabeen images has showed that it works for the majority of the time. There are however occasions where the ROI calculation fails. As the calculation is based upon a contour line on the bathymetry, the times when it fails is mainly due to a poor contour calculation. As this is generally the result of a poor bathymetry calculation anyway, this should cause the automatic shoreline detection to fail anyway. For the shifting ROI based upon a fixed user-defined shape, the problems are that it requires parameters set for each camera at each site, which makes it less automatic.

General shoreline detection problems

Aside from the problems discussed above, there are general shoreline detection problems resulting from the poor quality of the Argus images. This is particularly the case at Jvspeijk, where a good shoreline is yielded only one in every four images. This is compared to camera 1 at Narrabeen, where about 90% of images obtained good shorelines. Therefore, Narrabeen Camera 1 is recommended as an ideal test site for this program.

COMPARISON WITH SURVEY DATA

The autoShorelinePick program was run on Narrabeen Camera 1 for one month from August to September, 2005. This enabled an output bathymetry from the program to be compared to an *in-situ* survey using RTK-GPS on the 19th of September, 2005. Results from this comparison were surprisingly good, as indicated in Figure 1. When subtracting the two bathymetries, the results show that the error in the Argus bathymetry for this day is bounded by ± 0.3 m.

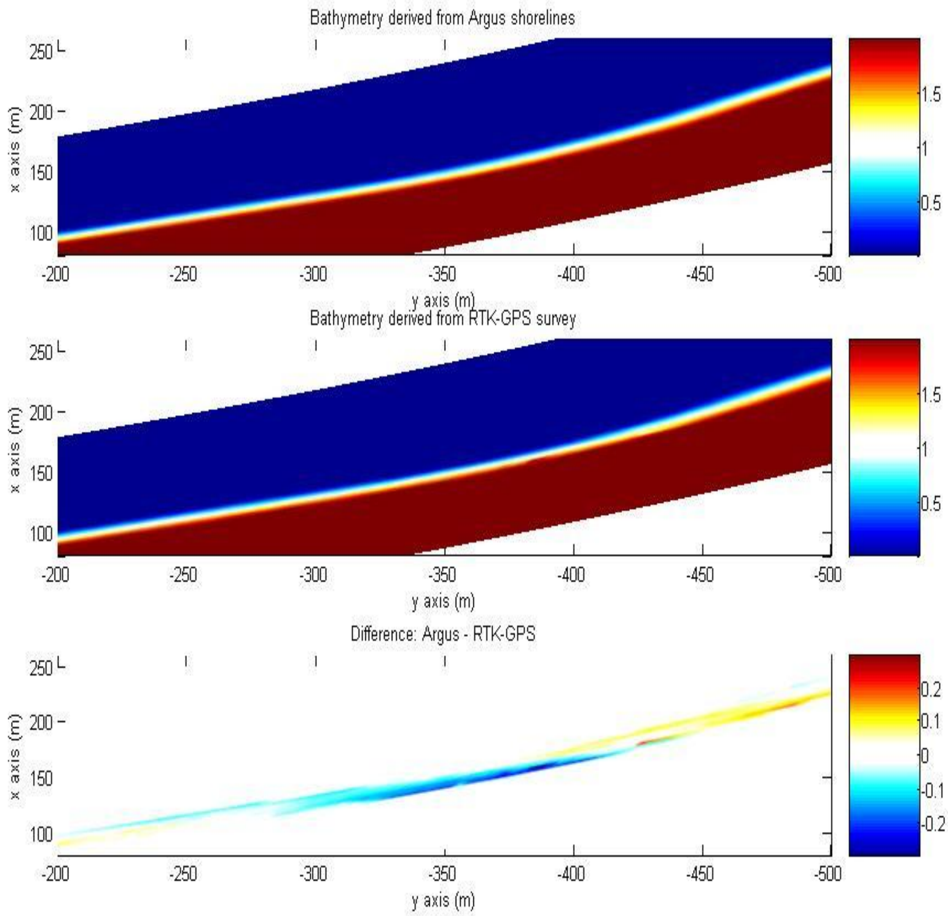

B.2 Cerezo (2006)

<u>THE CASE OF JVSPEIJK</u>

For the particular case of Jvspeijk, there were several surveyed bathymetries available since 1999 to 2001. The one for September 15th 2000 was chosen to contrast the ‘autoShorelinePick’ results with real data. The reason was that it had not bad weather conditions for shorelines picking, unlike the rest of the available days.

Several cases were studied to perform the contrast between real data of September 15th 2000 and the resultant bathymetry of the auto-shorelines picked for the same day. All of these cases were for camera 1 of Jvspeijk.

The results are given here by means of three graphics and the rms error between real data and the obtained bathymetry. The first figure shows the resultant bathymetry after the loess-interpolation of the auto-shorelines picked in each case. The second graphic shows the surveyed bathymetry. The differences between these two graphics are finally shown in the last one, bounded with maximum and minimum tide shorelines (lines in red). It is important to note that coordinates of 'y' axis are in reality negative.

Case 1: Auto-shoreline bathymetry obtained with a manual initial bathymetry of one week.

In this first case - to start with - a manual initial bathymetry was picked from September 12nd 2000 to September 18th 2000. After this, the 'Autoshoreline' program was run to look for shorelines in September 15th 2000; showing the following results:

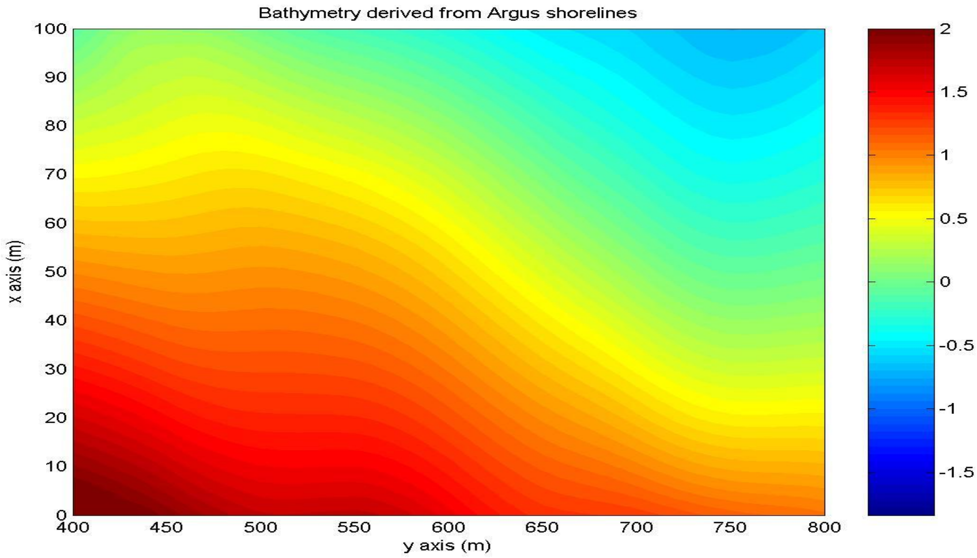

Figure 1: Bathymetry derived from Argus autoshorelines for Case 1.

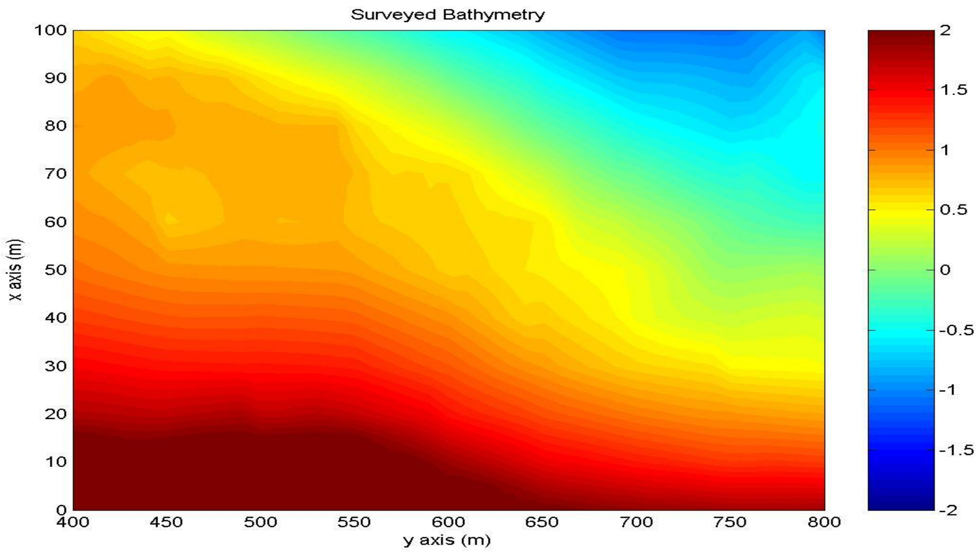

Figure 2: Surveyed bathymetry.

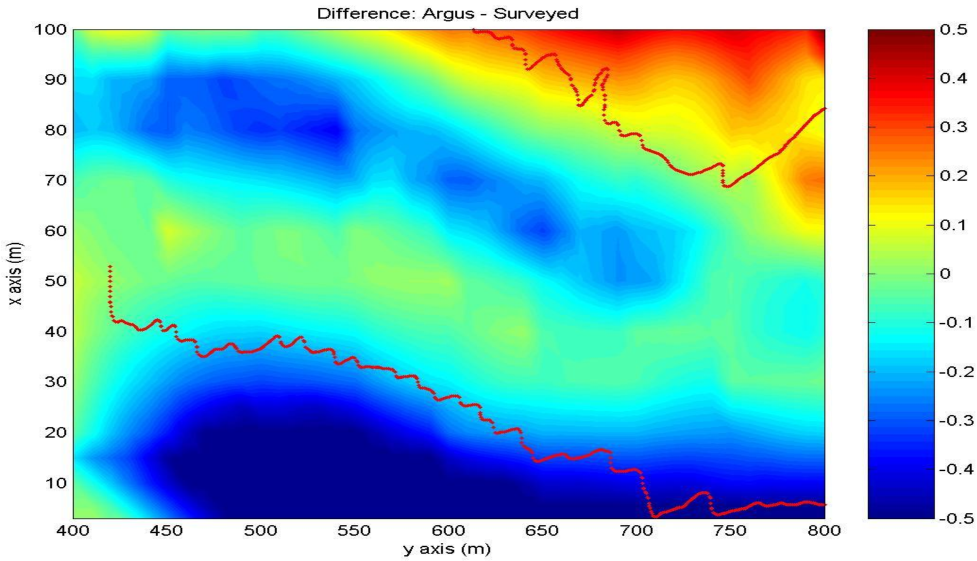

Figure 3: Difference between Argus and surveyed bathymetries for Case 1.

The last figure shows that the final differences in the intertidal beach are in the range of ± 20 cm; which is actually really good. For this case, the rms error is 22.78 cm.

<u>Case 2: Auto-shoreline bathymetry obtained with a manual initial bathymetry from September 2nd 2000, and then run day after day until September 15th 2000.</u>

In the second case, a manual initial bathymetry was made for September 2nd 2000. Afterwards the program was executed from the following day until September 15th 2000. The shorelines of this last day were interpolated in order to obtain the represented bathymetry in the following picture:

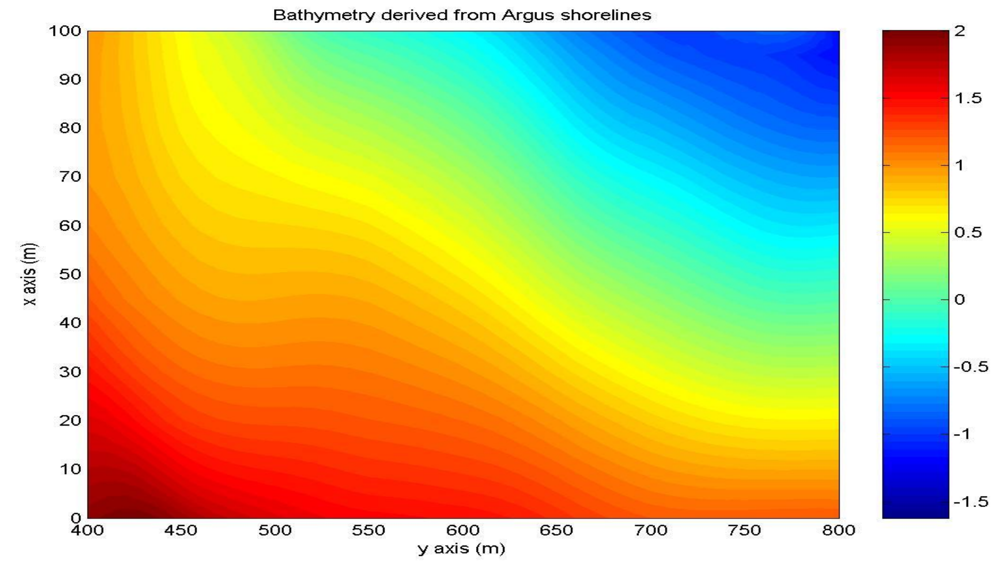

Figure 4: Bathymetry derived from Argus autoshorelines for Case 2.

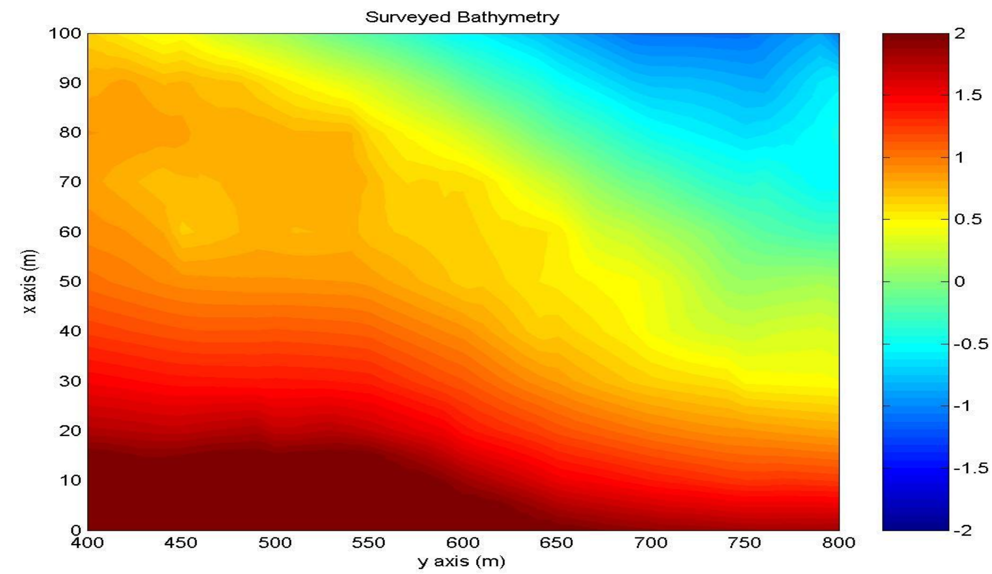

Figure 5: Surveyed bathymetry.

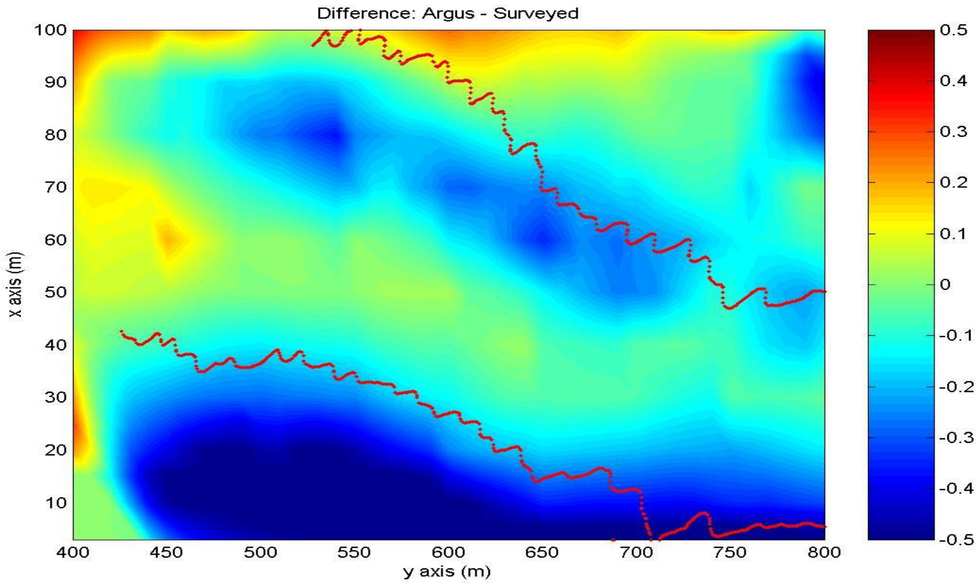

Figure 6: Difference between Argus and surveyed bathymetries for Case 2.

Looking at this last image we can see that the maximum offsets with the surveyed bathymetry are again in ± 20 cm. Even starting with an initial bathymetry of one only day, the good results the program generates are again absolutely shown. For this case, the rms error is 20.76 cm.

<u>Case 3: Comparison between the manual initial bathymetry for September 2nd 2000 and the surveyed bathymetry for September 15th 2000.</u>

In this case, the manual initial bathymetry for September 2nd 2000 and the surveyed bathymetry for September 15th 2000 are compared, in order to check whether the outputs are better or worse than the outputs obtained in the previous case.

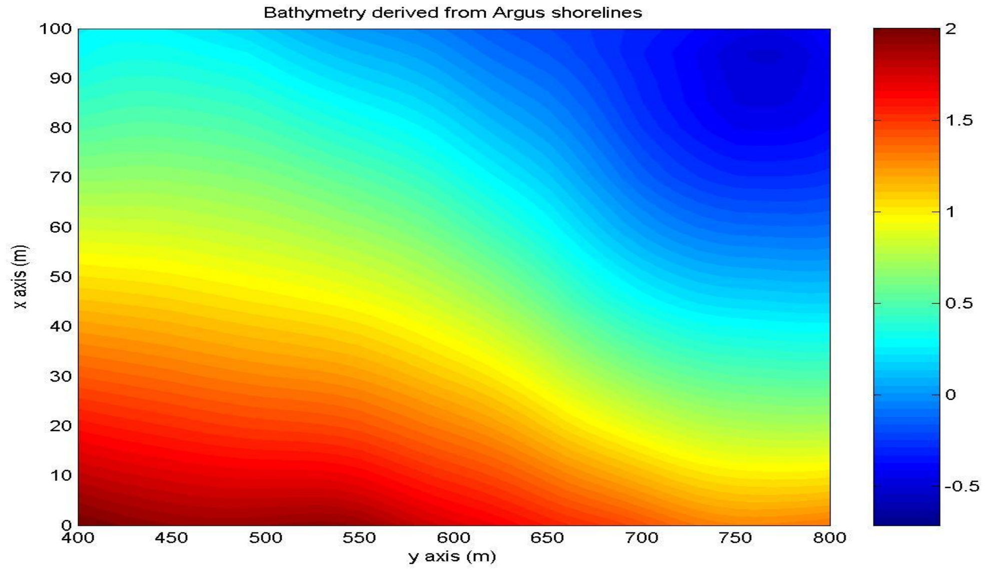

Figure 7: Bathymetry derived from Argus autoshorelines for Case 3.

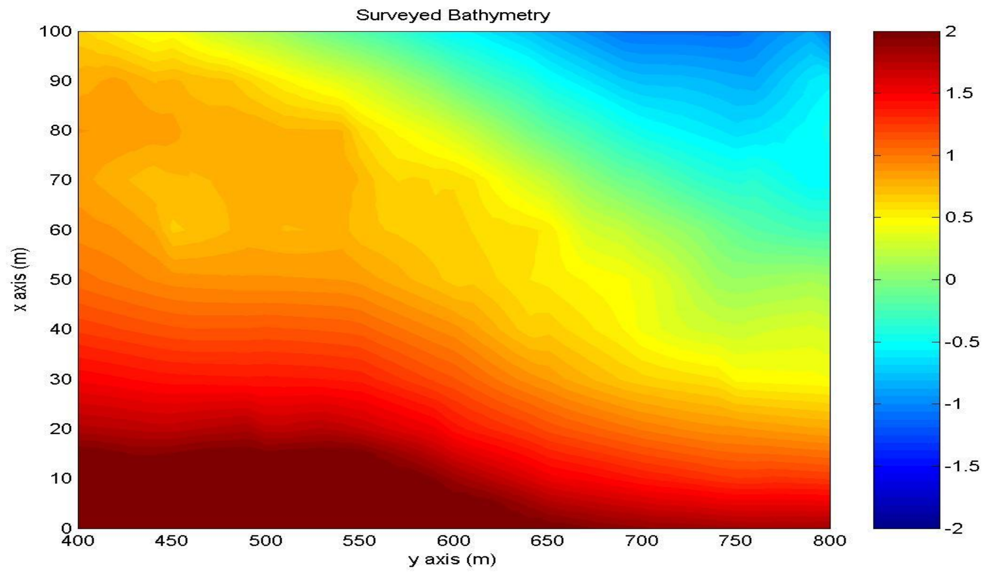

Figure 8: Surveyed bathymetry.

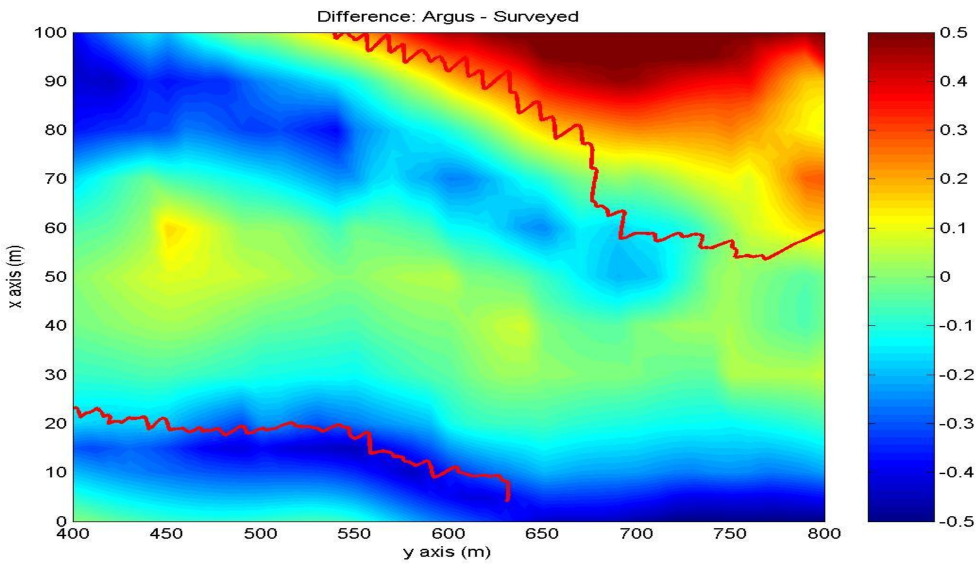

Figure 9: Difference between Argus and surveyed bathymetries for Case 3.

As we can see, differences are again within the same boundaries. Therefore - after running the program since September 2nd 2000 - we can conclude that the outputs for September 15th 2000 are not less accurate than the initial bathymetry. For this case, the rms error is 18.40 cm.

Case 4: Comparison between a manual initial bathymetry for September 15th 2000 and the surveyed bathymetry for the same day.

As a final case, the surveyed bathymetry is compared with a manual initial bathymetry for the same day, which is supposed to be the most accurate one.

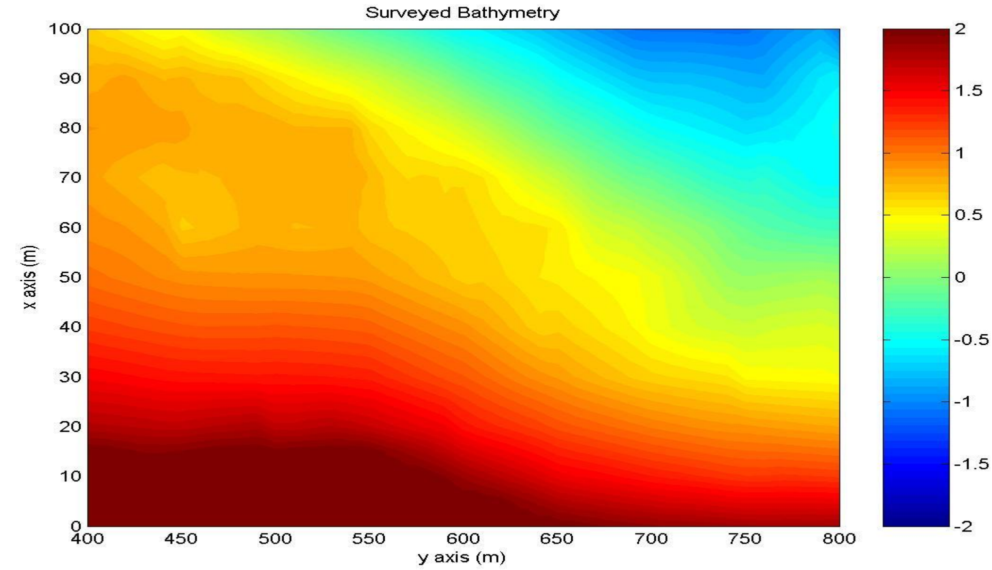

Figure 7: Bathymetry derived from Argus autoshorelines for Case 4.

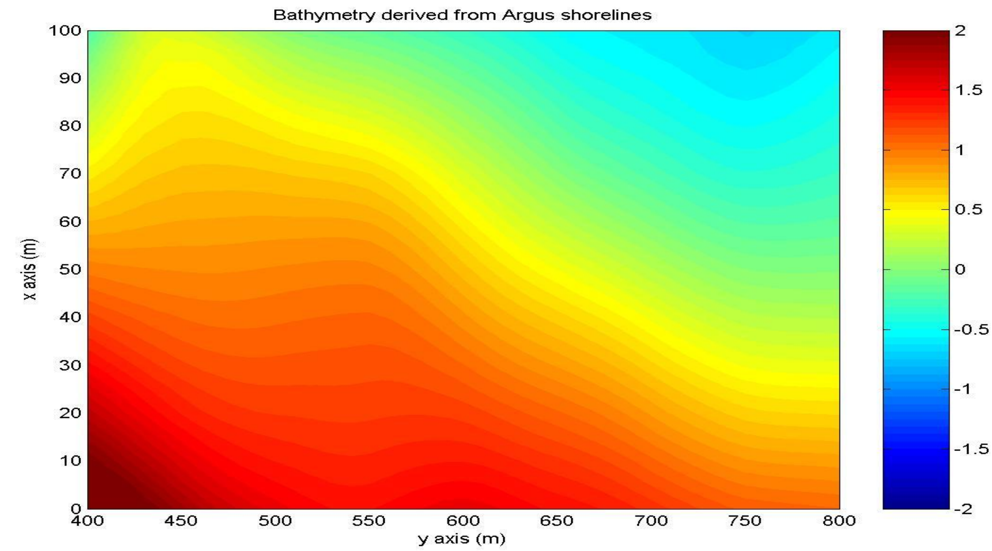

Figure 8: Surveyed bathymetry.

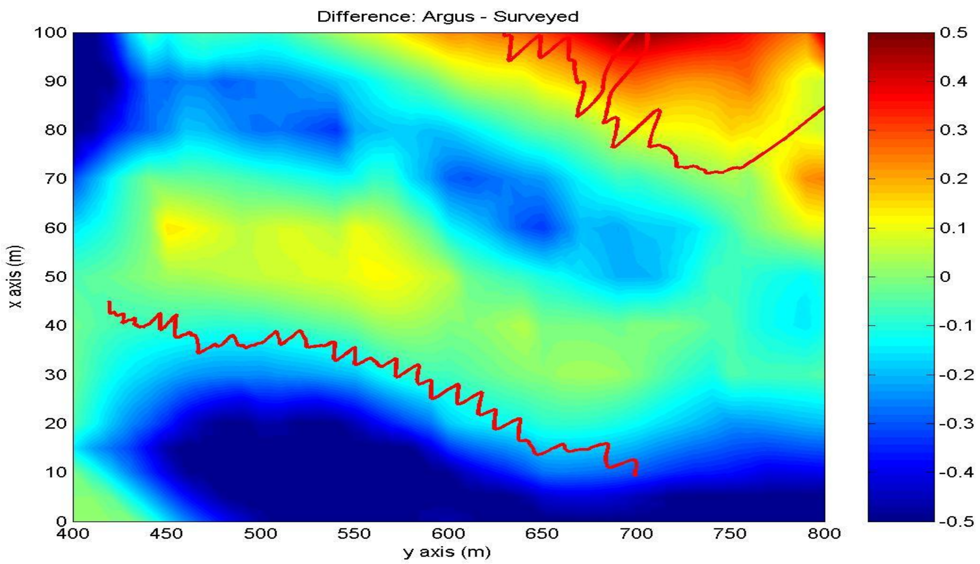

Figure 9: Difference between Argus and surveyed bathymetries for Case 4.

Looking at the Figure 9, the offsets obtained are not much smaller than the ones obtained in the Case 2. As a conclusion, we can say that the program is valid for finding shorelines and also in making accurate bathymetries to real data. For this case, the rms error is 24.91 cm.

<u>WEAK POINTS OF THE PROGRAM FOR JVSPEIJK AND TOUGH PARAMETERS TO SET</u>

- One of the biggest problems for the Jvspeijk case is that images are not good for shorelines-picking very often. Either weather conditions and the own quality of the image (bright, contrast, etc.) are not usually as good as they are in Narrabeen´s case. As a significant piece of information, good shorelines are picked around 30% - 60% of the cases. This is less than we could get in Narrabeen. But since we can get the half of the possible shorelines each day and it enables to make a good bathymetry finally, it is not bad at all.

- The method used to define the region of interest where we look for the shoreline (ROI), can be improved, since the results achieved are sometimes not good.

- The command lines (in the 'findshore_command' routine) to detect either more than a shoreline or not enough shoreline points found in the ROI, are not as accurate as they could be. They must be calibrated for each site and camera.

- ‘Shoreline_Data.Zdif’ is a tough parameter to set in Jvspeijk´s case. It is the range in which shoreline points are accepted or rejected and must be calibrated for each site. The problem is the following: for the same value of ‘Shoreline_Data.Zdif’ good points are rejected for some images and bad points are accepted for some others. After doing a calibration in Jvspeijk with 18 days of images in September 2000, the most suitable value was finally between 0.2 and 0.3 meters.

- The parameters to define the ROI (‘Shoreline_Data.Roi-tol-sea’ and ‘Shoreline_Data.Roi-tol-land’) have also to be calibrated for each site and camera. If there is high tide and the ‘Shoreline_Data.Roi-tol-land’ value is not small, the ROI sometimes can reach buildings and get their contours as part of the shoreline.

- In conclusion, the main weaknesses of the ‘findshore_command’ routine are the following: the parameters setting, the fitting of the ROI to the shoreline’s location, the influence of the quality of the images on the shorelines detection, and the impossibility of controlling that either bad shorelines are not accepted or good ones are rejected.

C Shoreline detection models

This appendix consists of three parts. In the first part the Pixel Intensity Clustering model, applied in this research, is extensively explained. The second part provides further background on other detection models that have been developed over the last few years. The last part gives an overview of the differences and similarities between the detection models.

C.1 Pixel Intensity Clustering model

The Pixel Intensity Clustering model (PIC) was developed by Aarninkhof (2003) to derive a shoreline feature from color video images. Color images show a visual contrast between the sub-aqueous and sub-aerial beach. This contrast was also used by Turner and Kingston (Plant et al., 2007) in their shoreline detection models by means of color band convergence and an artificial neural network approach respectively (part 2 of this appendix). First generation detection models, when only grey scale images were available, used grey scale pixel intensities to detect the shoreline. The visually observed shoreline break which is present especially at reflective beaches was used by Plant and Holman (1997) as a proxy for the shoreline. However, at dissipative beaches like the Dutch ones, no clear shoreline break is available. Other models using grey scale images often suffered from the absence of a clear grey scale contrast between wet and dry pixels.

In color images, the visual contrast between the sub-aqueous and sub-aerial beach is reflected by different pixel intensity characteristics. An inspection of video images collected at various Argus sites around the world showed that the distinction between the sub-aqueous and sub-aerial beach can be observed as both a color distinction as well as a luminance distinction. The color distinction distinquishes between the blueish colors of the water and the more brownish to redish colors of the dry beach. The luminance distinction distinquishes between dark sub-aerial and bright sub-aqueous pixels as low altitudes of the sun reflect on the water and not on the beach (Aarninkhof, 2003).

To use either color or luminance information as a distinction between wet and dry pixels the Hue Saturation Value (HSV) color space is used. The HSV color space treats color (hue and saturation) separately from luminance (value), whereas the RGB (red, green, blue) color space, which is normally used to encode color video images, combines this information. In Figure C.1 the HSV color space is given. When plotted in a 2D histogram the sub-aerial and sub-aqueous pixels form two clusters, respectively the dry and wet cluster (see Figure C.2). On the axis of the histogram are either hue and saturation in case of color distinction or value on both axis in case of luminance distinction. To improve the contrast between the two clusters the HSV intensity data are first filtered to remove outliers and scaled between 0 and 1. Iterative low-pass filtering is applied to yield a smooth histogram with two peaks: P_{dry} and P_{wet}. A discrimination between the two clusters can then be used as an identification of the shoreline (see Figure C.2). This discrimination is given by line l (equation C.1):

$$l : I_y = p_1 I_x + p_2 \qquad \text{C.1}$$

where I_x and I_y represent hue and saturation in case of color distinction and both value in case of luminance distinction. Line l crosses the saddle point of the filtered histogram perpendicular to the line connecting P_{wet} and P_{dry}. Weather color or luminance distinction is used to determine the shoreline depends on the degree of contrast between wet and dry pixels. This is determined using the spread of the pixels within the clusters as regard to the distance of the cluster peak P to line l.

Using line l, a discriminating function is defined such that $\Psi(I_x,I_y) = 0$ along l (equation C.2).

$$\psi(I_{x,}I_y) = p_1 I_x + p_2 - I_y \qquad \text{C.2}$$

In this equation I_x and I_y represent the values on the axes of the histogram. For dry pixels Ψ is positive, while it is negative for wet pixels. The shoreline is located at those pixels where $\Psi=0$ (Aarninkhof et al., 2003).

Ψ is calculated for every pixel within the region of interest using the scaled intensity data. Every pixel that meets the criterium of $\Psi(I_x,I_y) = 0$ is identified as a shoreline point. The discriminating function is not predefined but is based on the pixel colors within the region of interest and is thus calculated anew for every image. The model can be used at both reflective and dissipative beaches and is able to identify more than one shoreline point at a certain alongshore location. This is important on the Dutch beach as it is characterized by a complicated morphology and emerging sand bars at low water elevations.

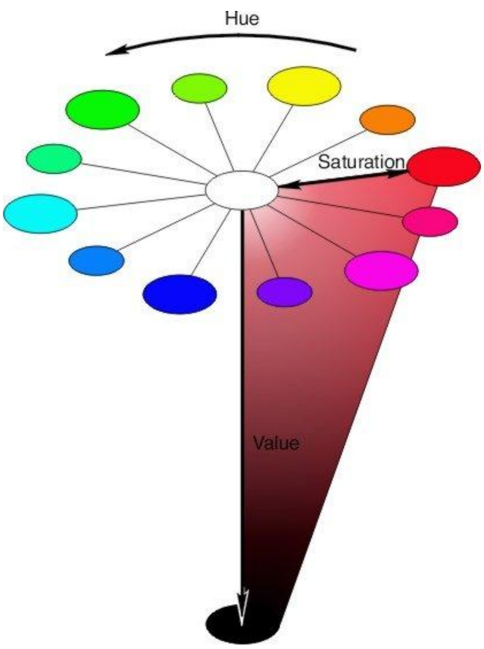

Figure C.1: Hue-Saturation-Value color space (NCSU, 2008)

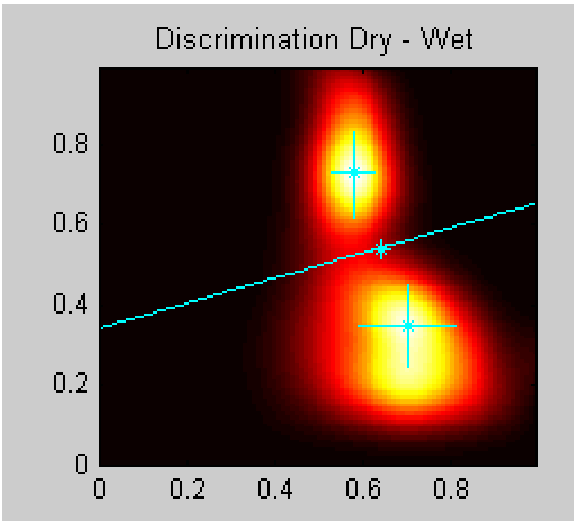

Figure C.2: Pixel clustering used for shoreline detection using hue and saturation. Figure by IBM

C.2 Other shoreline detection models

Several other waterline detection models have been developed over the last few years. This parts presents these other models

Shoreline intensity maximum model

At reflective beaches the swash motions at the shoreline generate foam that forms a bright band parallel to the shoreline. This band can clearly be seen on time exposure (timex) images. The bright band is called the shoreline intensity maximum (SLIM) by Plant and Holman (1997) and serves as a proxy for the still water level shoreline (SWLS). The SWLS is the water level in case waves are absent.

The shoreline contour is found using the intensities of the grey scale pixels. For each alongshore location the intensities of the pixels are plotted. Through these points a quadratic polynomial is fitted. The top of the curve indicates the SLIM. By doing this for all alongshore locations the contour of the shoreline is found. (Plant and Holman, 1997).

The SLIM model works best on reflective beaches, with a wave climate of waves that break just enough to be visually observed (Plant and Holman, 1997). Research by Plant et al. (2007) showed that the SLIM model can best be used in environments with an Iribarren number between 0.5 and 2. Beaches with an Iribarren number lower than 0.5 are too dissipative. On these beaches no good SLIM line can develop.
The Iribarren number is given by equation C.3.

$$\xi_0 = \frac{\tan(m)}{\sqrt{H_0 / L_0}} \tag{C.3}$$

Where m is the foreshore slope, H_0 the deep water wave height and L_0 is the deep water wave length.

Plant and Holman (1997) find an offset of 0.10 m, compared to measured field data, for the Duck (NC, USA) research site. This is a reflective beach site. The SLIM line typically lay seaward of the SWLS line (Plant and Holman, 1997).

An advantage of this model is that on relatively steep beaches with a narrow swash zone the SLIM is nearly always visible (Plant et al., 2007).

A disadvantage is that the SLIM line does not correspond exactly to the still water level. Discrepancies are dependent on the dynamic conditions at the shoreline (Plant and Holman, 1997). Another disadvantage is that the model needs an intensity maximum, caused by swash, to identify a shoreline. This leads to problems at very dissipative beaches, where the swash zone cannot be clearly identified. It also leads to problems when emerging sand bars occur. Sand bars have a shoreline on both their landward and seaward side, but at the landward side there are no waves, no swash, so no intensity maximum and no SLIM line. The SLIM model should only be applied to reflective environments (Plant et al., 2007).

Artificial Neural Network

This model also uses the colour difference between wet and dry pixels. Before the model is used the internal parameters are calibrated on tuning images, where wet and dry pixels were identified previously. The RGB values are used as input. Each pixel is identified as either land or water. The shoreline was identified at those pixels that were unlikely to be either land or water. For this an intermediate classification value was used. (Plant et al., 2007)

Comparisons with directly surveyed bathymetries show that the elevation estimates were accurate to 0.2 m.

Like the PIC model this model was developed to overcome the problems encountered by the SLIM model on dissipative beaches. This model can be used on beaches with complex geometries like emerging sand bars, sand pits and inlets. (Plant et al., 2007)

A disadvantage of this model is that it needs calibration for different beaches as the colour differences between wet and dry pixels differ per beach.

Colour Channel Divergence

This model also uses colour information from the images to distinguish the shoreline. The intensities of the colours (red, green and blue) are derived from the image for all pixels. On a white beach all colours have the same intensity. Going towards the water, the intensities first drop (wet sand) and then diverge, as the water reflects more blue. The shoreline is mapped at those pixels where the difference between the intensities of red and blue is larger than a certain threshold value. (Plant et al., 2007)

This model also performs better at dissipative beaches than the SLIM model. Like the SLIM model the Color Channal Divergence (CCD) modal cannot identify shorelines on beaches with difficult geomorpological features such as pools and emerging bars as only one shoreline point can be determined per alongshore location (Plant et al., 2007). Another disadvantage is that the threshold value needs to be calibrated for each beach. A last disadvantage is that there needs to be a clear colour difference between the beach and the water.

C.3 Differences and similarities

A comparison of the models by Plant et al. (2007) shows that shoreline positions obtained from each model differ by an offset that varies with the study site. For each of the discussed models, the table below shows on what kind of beaches the model can be used to identify the shoreline, what the definition of the shoreline is based on and what the advantages and disadvantages of the model are.

Table C.1: Comparison of the four detection models

	SLIM	PIC	ANN	CCD
Beach type	Reflective	Reflective and dissipative with difficult morphological features	Reflective and dissipative with difficult morphological features	Reflective and dissipative
Shoreline based on	Intensity maximum indicating swash zone based on grey-scale images	Histogram of intensities of wet and dry pixels in HSV colour space	RGB values of previously identified wet and dry pixels	Divergence between intensity of blue and red colour
Advantages	* Swash zone is almost always visible on reflective steep beaches	* Can identify shorelines surrounding emerging bars and runnels.	* Can identify shorelines surrounding emerging bars and runnels.	
Disadvantages	* Cannot be used well on dissipative beaches. * SLIM line does not correspond exactly to the SWLS line. * Cannot identify emerging bars	* Sensitive to factors that affect image colour (e.g. fog)	* Sensitive to factors that affect image colour (e.g. fog) * Needs to be calibrated again for each beach.	* Sensitive to factors that affect image colour (e.g. fog) * CCD is sensitive to reddishness of the environment. * Threshold value needs to be calibrated for each beach.

D Shoreline elevation model

The shoreline elevation model was developed by Aarninkhof (2003) to be used with the PIC shoreline detection model, but it can be used for the other models as well. As explained by Appendix C.1 the PIC model was developed especially for dissipative beaches. Swash motions, that play an important role on these beaches, need to be accounted for in the elevation model. As the detection model identifies the shoreline location on time exposure images, the elevation model has to account for all physical processes that play a role during the ten minutes of time exposure. These are: the offshore water level, offshore wind-induced wave set-up, breaking-induced wave set-up and swash oscillations. This Section describes the shoreline elevation model that has been developed by Aarninkhof (2003).

The basis formula to calculate the elevation of the detected shoreline (z_{sl}) is given by equation D.1.

$$z_{sl} = z_0 + \eta_{sl} + k_{osc} \cdot \frac{\eta_{osc}}{2} \qquad \text{D.1}$$

Where z_0 is the offshore tide- and wind-induced water level without contribution of wind generated waves, η_{sl} represents the breaking wave set-up and η_{osc} represents the vertical swash excursion related to shoreline oscillations at the time scale of individual waves and wave groups. K_{osc} is an empirical parameter that is related to the swash exceedence at the location of the shoreline, detected by a particular detection model.

The offshore water level (z_0) is a combination of the tidal variations (Δz_{tide}) above a reference level ($z = z_{ref}$), the storm surge elevation (z_{storm}) as a result of atmospheric pressure gradients and the local wind set-up (z_{wind}) (Aarninkhof, 2003). z_0 is preferably measured within 10 km of the coastline, so that Δz_{tide} and z_{storm} are measured directly and local wind set-up is negligible (Aarninkhof et al., 2003).

The wave set-up (η_{sl}) is calculated using the standard wave decay model of Battjes and Jansen (1978, in Aarninkhof et al., 2003), incorporating the roller concept of Svendsen (1984, in Aarninkhof et al., 2003), and using the inner surf zone bore model to extend computations to zero water depth (Aarninkhof and Roelvink, 1999 in Aarninkhof et al., 2003).

The vertical swash is given by equation D.2:

$$\eta_{osc} = \sqrt{R_{ig}^{\ 2} + R_{ss}^{\ 2}} \qquad \text{D.2}$$

Where R_{ig} is the swash height of infragrafity waves and R_{ss} is swash height of swell waves. R_{ig} is calculated using the formulation of Ruessink et al. (1998, in Aarninkhof et al., 2003) that can be used at both dissipative as well as reflective beaches (equation D.3).

$$\frac{R_{ig}}{H_0} = 0.65 \tanh(3.38\xi_0) \qquad \text{D.3}$$

Where H_0 is the deep water wave height and ξ_0 the Iribarren number, which is given in equation D.4

$$\xi_0 = \frac{\tan(m)}{\sqrt{H_0 / L_0}} \qquad \text{D.4}$$

Where m is the foreshore slope, H_0 the deep water wave height and L_0 is the deep water wave length.

R_{ss} is calculated using the formulation of Holman and Sallenger (1985, in Aarninkhof et al., 2003). For highly dissipative beaches with a small Iribarren number R_{ss}/H_0 is set to zero to avoid negative values (equation D.5). By doing so the short-wave contribution to swash oscillations is ignored at those beaches.

$$\frac{R_{ss}}{H_0} = 0.69\xi_0 - 0.19 \text{ for } \xi_0 > 0.275 \qquad \text{D.5}$$

$$\frac{R_{ss}}{H_0} = 0 \text{ for } \xi_0 < 0.275$$

As can be seen in Figure D.1 the average shoreline elevation (z_{avg}) is the sum of the offshore water level and the wave set-up. Around this average elevation the water level oscillates at the timescale of waves and wave groups: the swash zone. Somewhere in the swash zone the shoreline is detected. The parameter K_{osc} represents the part of the swash amplitude ($\eta_{osc}/2$) that corresponds to the detected shoreline.

The definition of the shoreline differs for every model. The location that is defined as the shoreline position is inherent to the detection model. To find the correct elevation of the beach, the *combination* of the detected shoreline location and the accompanying water elevation is important. The value of K_{osc} is an important parameter in this matter.

When the detected shoreline is shoreward of the average shoreline, K_{osc} is positive, when the shoreline is detected seaward of the average shoreline, K_{osc} is negative. K_{osc} needs to be calibrated for each detection model and each beach location. (Aarninkhof et al., 2003). Aarninkhof et al. (2003) concluded that K_{osc} 'accounts for uncertainties in both the location of the shoreline feature identified from time-averaged video imagery as well as the associated elevation estimated from the empirical parameterisations of the vertical swash excursion'.

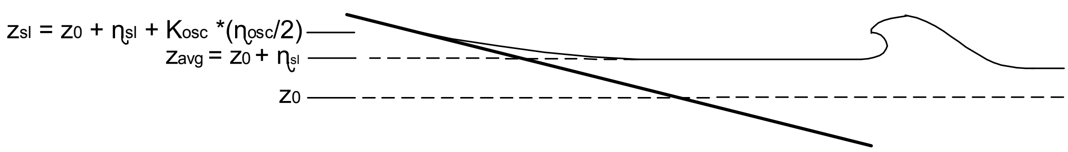

Figure D.1: Shoreline elevation model (Aarninkhof, 2003)

E Improvements to the ASM

This appendix provides an overview of the improvements made to the ASM and serves as a guidance to those who continue working with the ASM.

E.1 Technical details on the new set-up

This section describes the new set-up of the ASM and the structure that is used to pass on information from one step in ASM to another.

Set-up

The new set-up can be easily understood and provides flexibility for use and possibilities for improvement and extension. The basic idea is that, for every image, one main routine calls different second-level routines one by one to perform the various steps needed for shoreline detection. This set-up allows one second-level routine to be replaced easily by another routine that provides the same kind of output (e.g. replace the PIC detection model by another detection model).

The new set-up and the second level routines that are called in this research are visualized in Figure E.1. Output from one second-level routine is stored in a structure that is passed on to the next second-level routine by the main routine. The settings that are used by the various second-level routines are also stored in the structure. They are loaded in the first step of the main routine. The second-level routines that are called by the main routine are also listed in the settings. So, for every time step, the main routine first reads from the structure which second-level routine to call, then the second-level routine reads the settings it needs from the structure and finally the output of the second-level routine is stored in the structure. Then the next second-level routine is called. Second-level routines can be deleted or added by simply not calling for them or extending the number of second-level routines called respectively.

Structure

The structure has the following fields:

Field	What it contains
settings	initially: the settings and the second-level routines that are called (see also Section E.4). during running: the region of interest is stored in this field also (settings.roi.xy)
epochTimes	the epoch times for which the shoreline is mapped by ASM

currentIndex	the i[th] timestep (of the epoch times) of which the shoreline is mapped
image	image grid and the image color information of the i[th] timestep
bathy	this field contains the two bench-mark bathymetries: bathy.Z1 bathy.Z2 These are the output of ASM_makeBathyFromShoreline. Other output of this script is also stored in this field, but this is not (yet) used further by the ASM. Amongst these are the interpolation errors, calculated by the loess interpolation of ASM_makeBathyFromShoreline: nmse, mse and msr.
output	this fiels contains two parts: the calculated elevation (output.rectLevel); information on the detected shoreline (output.wl): the detected and stored shoreline points detected: output.wl.xyzOrig stored: output.wl.xyz information on which points are accepted/rejected on what bathymetry (output.wl.idgood/idbad)

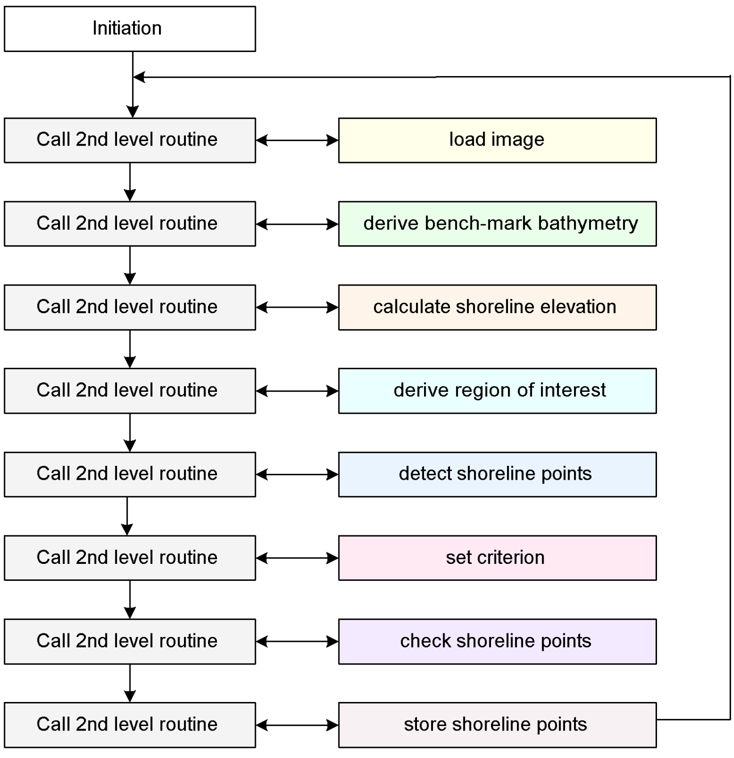

Figure E.1: New set-up with second level routines called in this research

E.2 Technical details on the improvements

This section deals with the technical details on some of the improvements presented in Chapter 3.

Extension of the region of interest

This improvement is made in the ASM_movingRoi script.

As a first step the region of interest is determined by shifting the expected shoreline location seawards and landwards. These shifted lines are the cross-shore boundaries of the region of interest (Cerezo and Harley, Appendix B). The region of interest that is determined in this way is extented to the edge of the image to make sure that the entire shoreline is included.

To extent the region of interest the outer points, in alongshore direction, of the cross-shore boundaries are determined. From these points the region of interest is exteded towards the edge of the image grid. So four new corner points are determined. The gradient of the extended part is determined by the gradient between the old corner point and a point on the boundary of the region of interest. The latter point is a certain distance away from the old corner point. This distance is a user defined percentage of the total alongshore length of the cross-shore boundary of the region of interest.

Avoid zigzagging

This improvement is made in the ASM_movingRoi script.

To avoid zigzagging of the region of interest, the most seaward and most landward points of the boundary of the region of interest are taken for each alongshore location of the expected shoreline location. However, these alongshore locations do not coincide with the grid of the bench-mark bathymetry. This is because the expected shoreline location is found on a surface that is obtained from the bench-mark bathymetry by delauney trangulation. In case both a continuous shoreline and a sand bar are found as expected shoreline locations (this initiates zigzagging), there are thus very few points on the boundaries that have similar alongshore locations. At those locations were multiple boundary points are found only the most seaward ones are accepted for the seaward boundary and the most landward for the landward boundary. Zigzagging is thus still observed, as can be seen from Figure E.2. This last bit of zigzagging is resolved by interpolating the remaining points to the grid of the image. The result can be seen in Figure 3.4 and Figure 3.5 in Chapter 3.

Although this method works rather well for the first run of Chapter 5, the zigzagging was still observed for the other two runs. It did however not block the shoreline anymore. A suggestion to better avoid all zigzagging is to subsample all locations of the expected shoreline location to the grid of the image. If the newly obtained locations are then shifted seawards and landwards really all ‘double’ points can be deleted from the boundaries.

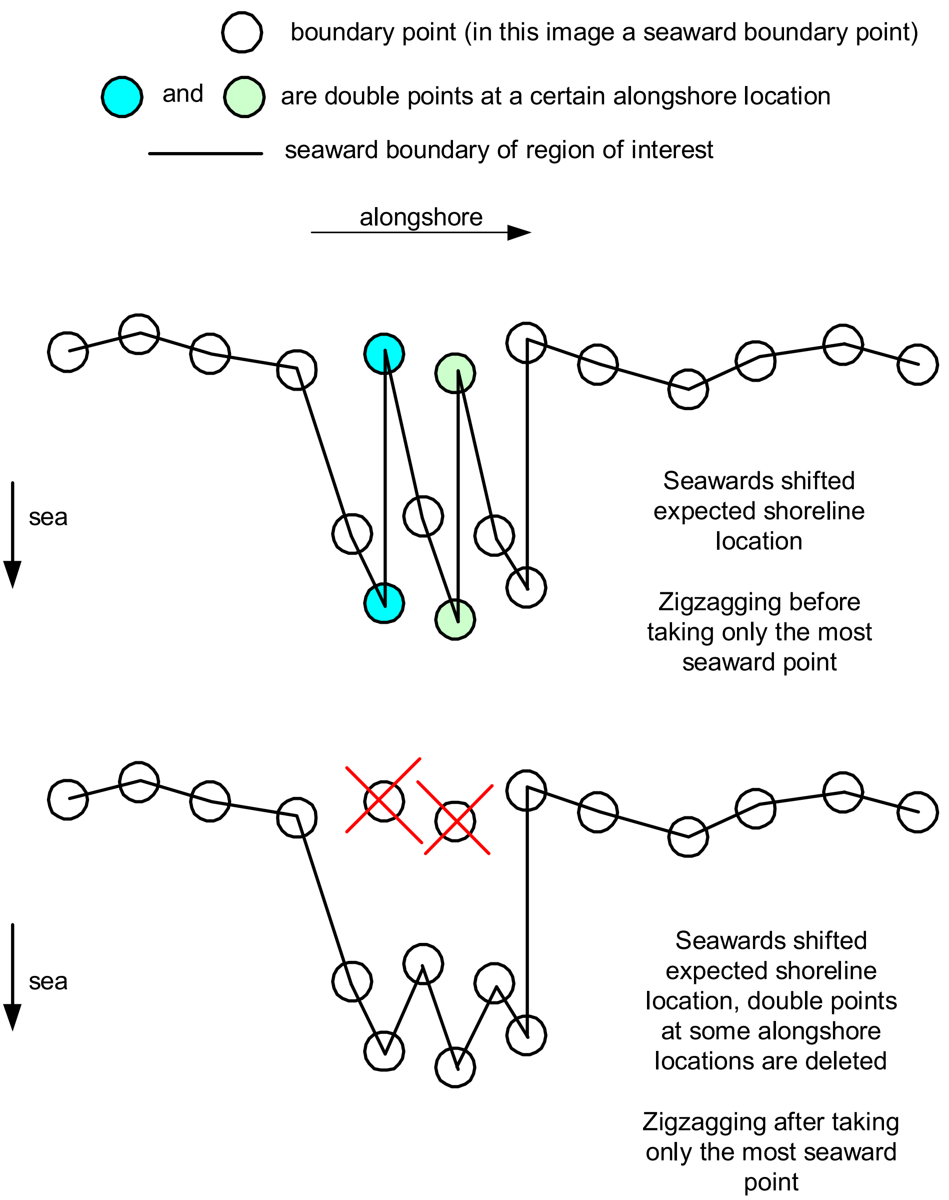

Figure E.2: Zigzagging partly resolved by taking the most seaward points of the seaward shifted expected shoreline location.

Double quality check

A double quality check was introduced. Two bench-mark bathymetries are therefore obtained from previously detected shoreline points. To this end the ASM_makeBathyFromShoreline routine calls the makeBathyFromShoreline routine twice with different loess scales and different time windows (given by the user in the settings, see table Table E.2). The makeBathyFromShoreline routine returns two calculated bathymetries: Z(1 or 2) and rawZ(1 or 2). The first Z(1 or 2) already contains gaps as part of the data has been deleted from this bathymetry based on the nmse error, calculated with the loess interpolation. The value of the nmse above which data is deleted in the makeBathyFromShoreline routines is a fixed value of 0.50. The second rawZ(1 or 2) is still complete, no data has yet been deleted from this bathymetry by the makeBathyFromShoreline routine. ASM_makeBathyFromShoreline continues with this bathymetry, from which data with a user defined nmse error is then deleted.

A suggestion is to make the value of the cut-off value of the nmse error variable in the makeBathyFromShorline routine. The ASM_makeBathyFromShoreline routine could be made more orderly in that case.

In ASM_compareWLWithBathy the detected shoreline points are first compared to the first bench-mark bathymetry. Those shoreline points that are correspond to a gap in this bench-mark bathymetry (nan-values) are then compared to the second bench-mark bathymetry. It is therefore necessary that the second bench-mark bathymetry is obtained from shoreline points of an equal or longer time window and with equal or larger smoothing scales, as these lead to less gaps in the obtained bathymetry.

E.3 Other minor improvements

Apart from the improvemetns listed in Sections E.1 and E.2 and Chapter 3 other smaller improvements have been made to the ASM. These mainly focussed on a) making the ASM more flexible by making settings variable and b) on preventing the ASM from ending its run prematurely. An example of the latter is that the ASM stopped running when no image was found. These kind of problems were solved by builing in checks on the existence of variables (e.g. Does the image exist? Was the elevation calculated? Is an expected shoreline location found?). If the checked variable is not present, the ASM now continues with the next time step.

One grave error that was found in the previous version of the ASM was that the elevation to which the oblique image was rectified (Equation (2.2)) did not correspond to the elevation that was eventually assigned to the detected shoreline points. This means that the horizontal coordinates of the detected shoreline points are not correct, as they do not correspond to the elevation that is assigned to them. Or, in other words, different shoreline locations would have been found on oblique and plan images.

E.4 Settings of ASM

The settings that are loaded in the initiation (Figure E.1) step are extracted from an initiation file (IniFile). The ASM settings can be divided in camera/station related settings and site/beach related settings. Som of the latter require knowlegde of the coastal system that is monitored and can affect the performance of the ASM. If the values for the site/beach related settings do not correspond to the beach that is monitored, the ASM may not perform at its best. Examples are the value for the seaward and landward shifts in the determination of the region of interest and the loess smoothing scales.

The tables below list the various ASM settings and their values used in this research.

Table E.1: Camera and station related settings

Setting	Explanation	Value in this research
siteID	ID of the Argus site	EGXXX
stationID	ID of the Argus station	EG00S
stationShortName	name of the Argus station	egmond
cameraNumber	The bathymetry is mapped for images of this camera	1
imageType	The images are mapped on a this kind of image: plan or oblique	plan

Table E.2: Settings related to the interpolation of the bench mark bathymetries

Setting	Explanation	Value in this research
interpolation.function	This function is called to interpolate the bench mark bathymetries	ASM_makeBathy FromShoreline
interpolation.method	This interpolation method is used by ASM_makeBathy FromShoreline to calculate the bench mark bathymetries: loess, linear or gridfit	loess
interpolation.dataFilter	SQL query to further specify what shoreline data may be extracted from the database to calculate the bench mark bathymetries	various
interpolation.grid	The grid on which the bench mark bathymetry is interpolated	[-100 300 -1500 0 5 5] [meters]

interpolation.timeWindow1	The time window used for the the first bench mark bathymetry. Previously detected shoreline points within this time window are extracted from the data base to calculate the first bench mark bathymetry. From the time of the image the time window looks 0.5 x the time window back in time and 0.5 x forward in time.	summer run (March 17th 2006 – July 14th 2006): 2*24*3600 [seconds] winter runs (November 20th 2005 to Deceber 28th 2005 and January 10th 2006 to March 16th 2006): 4*24*3600 [seconds]
interpolation.timeWindow2	The time window used for the second bench mark bathymetry. See also interpolation.timeWindow1.	summer run (March 17th 2006 – July 14th 2006): 4*24*3600 [seconds] winter runs (November 20th 2005 to Deceber 28th 2005 and January 10th 2006 to March 16th 2006): 10*24*3600 [seconds]
interpolation.settings.loessScaleX1	Cross shore smoothing scale for loess interpolation of the first bench mark bathymetry.	10 m
interpolation.settings.loessScaleY1	Alongshore smoothing scale for loess interpolation of the first bench mark bathymetry.	25 m
interpolation.settings.limitval1	Cut-off value for the normalized mean square error (nmse) of the first bench mark bathymetry. Elevation data at loctions in the bench mark bathymetry that have an nmse larger than this value are deleted, leaving gaps in the bathymetry.	0.5
interpolation.settings.loessScaleX2	Cross shore smoothing scale for loess interpolation of the second bench mark bathymetry.	25 m
interpolation.settings.loessScaleY2	Alongshore smoothing scale for loess interpolation of the second bench mark bathymetry.	100 m

interpolation.settings.limitval2	Cut-off value for the normalized mean square error (nmse) of the second bench mark bathymetry. See interpolation.settings.limitval 1 for further explanation.	0.5

Table E.3: Settings related to the calculation of the shoreline elevation

Setting	**Explanation**	**Value in this research**
elevation.function	This function is called to calculate the shoreline elevation.	ASM_elevationDissipativeBeach
elevation.settings.mb	beach slope	0.025 [m/m]
elevation.settings.kosc	Swash exceedence parameter associated with the elevation model of Aarninkhof (2003).	1.3
elevation.settings.defaultZ	elevation if tide and wave calls fail	0

Table E.4: Settings related to loading and rectifying the image

Setting	**Explanation**	**Value in this research**
image.function	This function is called to load the image and rectify it in case 'plan' is given at imageType.	ASM_findshore_load_imagedata
image.settings.mergeDir	location where rectified images are stored	local
image.settings.mergeSettings.plan.waveModelData.mb	beach slope. To rectify images the shoreline elevation is calculated again. Notice that the value of the beach slope given here is similar to the beach slope given at elevation.settings.mb.	0.025

image.settings.mergeSettings.plan.waveModelData.kosc	Swash exceedence parameter associated with the elevation model of Aarninkhof (2003). Notice that the value of the kosc given here is similar to the kosc given at elevation.settings.mb.	1.3
image.settings.mergeSettings.plan.excludeCams	These cameras are excluded from the rectification. The shoreline detection of the PIC model currently works best if it is used on only one image and not on a merge of several images. Therefore all cameras, except the one given at cameraNumber, should be excluded from the rectification process.	[2 3 4 5]
image.settings.mergeSettings.plan.imRange	Range of the rectified image. In this research the same range is used as for the bench mark bathymetries. This however is not necessary.	[-100 300 -1500 0 5 5] [meters]

Table E.5: Settings related to the definition of the region of interest

Setting	**Explanation**	**Value in this research**
roi.movingFunction	This function is called to determine a moving region of interest.	ASM_movingRoi
roi.name	Name of the fixed region of interest as stored in the database. If no moving region of interest is determined this fixed region of interest is used.	autoshoreline_EG01C
roi.settings.roi_tol_sea	Seaward shift of the expected shoreline location.	100 m
roi.settings.roi_tol_land	Landward shift of the expected shoreline location.	various [m] (40 m 300 m)
roi.settings.searight	Part of the seaward shifted shoreline that is extended in positive alongshore direction.	0.125

roi.settings.sealeft	Part of the seaward shifted shoreline that is extended in negative alongshore direction	0.125
roi.settings.landright	Part of the landward shifted shoreline that is extended in positive alongshore direction	0.125
roi.settings.landleft	Part of the landward shifted shoreline that is extended in negative alongshore dirction	0.125
roi.settings.Xbuildings	cross shore cut-off value to exclude buildings from the rectified image.	-40

Table E.6: Settings related to the detection

Setting	**Explanation**	**Value in this research**
detection.function	This function is called to detect the shoreline.	ASM_findshorePIC
detection.settings.maxDalMove	Functionality related to the PIC detection model, probably related with trough correction	0.30

Table E.7: Settings related to the quality control

Setting	**Explanation**	**Value in this research**
acceptanceCriterium.function	This function is called to determine the acceptance value.	ASM_acceptance ValueConstant
acceptanceCriterium.settings. stormwave	Hrms wave height above which the wave conditions are called storm waves.	2 m
stormDurationCrit	Time that is looked back from the time of the image to see if any storm waves occurred.	2*24*3600 [seconds]

acceptanceCriterium.Zstorm	Vertical difference that is accepted between the bench mark bathymetry and the detected shoreline point in case any storm wave occurred within the time that is looked back by stormDurationCrit.	0.8 m
acceptanceCriterium.Znorm	Vertical difference that is accecpted between the bench mark bathymetry and the detected shoreline point in case no storm wave occurred within the time that is looked back by stormDurationCrit	various [m] (0.10 m 0.25 m 0.50 m) For the longer runs, presented in Chapter 5, a value of 0.25 m for the verical acceptance criterion
compare.function	Function that is called to execute the quality control.	ASM_compareWL WithBathy

Table E.8: Settings related to storing and processing the data

Setting	**Explanation**	**Value in this research**
output.function	Function that is called to save the accepted shoreline points to the database and to further process the output.	ASM_processOutput Laura
output.plotDir	Directory to which the output is saved.	various

F CSIs from bathymetry

This appendix describes how the coastal state indicators (CSIs) are derived from the video bathymetries. The CSIs that are used in this research are the momentary intertidal coastline, elevation contours and the intertidal beach slope.

Section F.1 first gives a general introduction to the obtained bathymetries and how they are treated to obtain CSIs. Section F.2 explains how the CSIs are derived from the obtained bathymetries.

F.1 Loess interpolated video bathymetries

The loess interpolation as used in this research leads to gaps in the obtained bathymetries as elevation data is deleted at locations where the normalized mean square error (nmse, equation (3.6)) is larger than 0.5. As gaps in the bathymetry affect the CSIs that can be obtained, they are filled by linear interpolation. This is shown by Figure F.1. It may seems strange to first delete data with to high interpolation errors from the bathymetry and to fill those gaps later again with linearly interpolated data. However the loess data that was deleted was part of a plane that was added to the loess interpolation. As Figure F.2 shows it seemed that this plane was not always appropriate. Therefore the procedure of throwing away and refilling is justified.

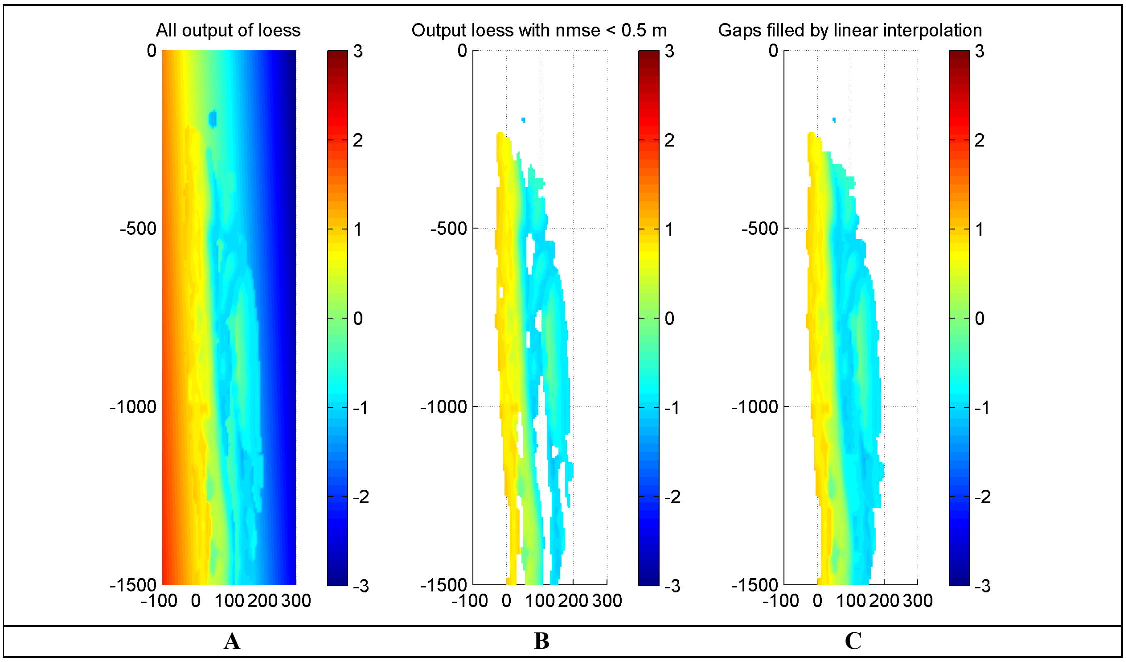

Figure F.1: Bathymetries treated to allow CSIs to be derived appropriately. Bathymetry A is the output of the loess interpolation. Bathymetry B shows those parts of bathymetry A where the nmse is smaller than 0.5. Throwing away data from bathymetry A results in gaps in bathymetry B. By using linear interpolation in the cross shore direction these gaps are filled. This results in bathymetry C.

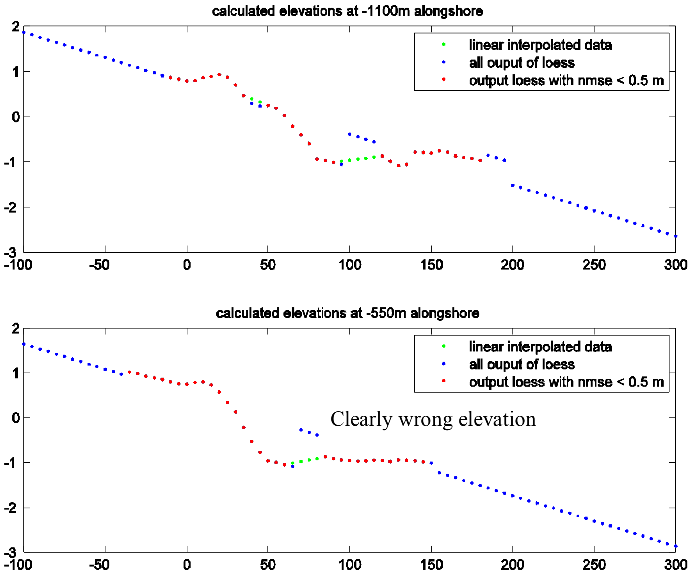

Figure F.2: Justification of throwing away data with nmse > 0.5 and filling the gaps with linear interpolation.

F.2 CSIs derived from intertidal beach bathymetries

MICL

The MICL is obtained from the interpolated bathymetry by the use of the getVolume routine available at Deltares. This routine determines a polygon following the cross shore beach variation between two user-defined elevations (0.50 m and -0.50 m NAP in this research) and two user-defined cross shore locations (optional). The volume within the polygon is then calculated. By dividing this volume by the vertical difference of the two elevations the MICL is calculated. The MICL is thus a measure of the beach volume.

Elevation contours

The elevation contours (0.50 m, 0 m and -0.50 m NAP) are determined on the obtained bathymetry. Whenever two contours are found, e.g. in case of sand bars, the longest contour is accepted and used in further data analysis. If one contour wiggles and has multiple (mostly three) cross shore locations at one alongshore location, the most seaward cross shore location is accepted as being the contour position. The use of larger smoothing scales overcomes most problems with wiggling contours.

Slope

The slope is calculated by dividing the vertical elevation difference between two contours by the cross shore distance between those contours. In this research the 0.50 m and -0.50 m contours are used. The slope is thus also a measure for the width of the intertidal beach.

G Summary statistics

This appendix lists the summary statistics of the comparison of the IBM and AMS bathymetries against DGPS data.

Table G.1 Summary statistics of the errors between DGPS measurements of March 17th and video data of March 17th. The errors of video bathymetries with time windows of three days are displayed in Table G.2.

run	summary statistic	1025	10100	25100
1_IBM	mean error (m)	0.15	0.15	0.12
	st deviation (m)	0.20	0.22	0.29
	rms error (m)	0.25	0.27	0.32
	max over estimation (m)	0.59	0.61	0.74
	max under estimation (m)	-0.31	-0.45	-0.92
	# points	169	181	215
1_largeRoi_10	mean error (m)	0.18	0.21	0.21
	st deviation (m)	0.17	0.21	0.25
	rms error (m)	0.24	0.30	0.32
	max over estimation (m)	0.47	0.91	0.90
	max under estimation (m)	-0.22	-0.35	-0.48
	# points	78	108	168
1_largeRoi_50	mean error (m)	0.12	0.14	0.08
	st deviation (m)	0.26	0.28	0.39
	rms error (m)	0.29	0.32	0.39
	max over estimation (m)	0.78	0.87	0.99
	max under estimation (m)	-0.66	-0.73	-1.08
	# points	155	176	221
1_largeRoi_25	mean error (m)	0.09	0.08	0.07
	st deviation (m)	0.28	0.30	0.37
	rms error (m)	0.29	0.31	0.37
	max over estimation (m)	0.79	0.78	0.92
	max under estimation (m)	-0.66	-0.85	-0.84
	# points	165	182	222
1_smallRoi_25	mean error (m)	0.13	0.17	0.18
	st deviation (m)	0.31	0.33	0.34
	rms error (m)	0.33	0.36	0.38
	max over estimation (m)	0.74	0.80	0.85
	max under estimation (m)	-0.57	-0.56	-0.62
	# points	129	158	199

Table G.2: Summary statistics of the errors between DGPS measurements of March 17th and video data of March 17th to 19th. The time window of the video dat is thus three days.

run	summary statistic	1025	10100	25100
1_IBM	mean error (m)	0.14	0.14	0.12
	st deviation (m)	0.21	0.23	0.29
	rms error (m)	0.25	0.27	0.31
	max over estimation (m)	0.59	0.61	0.69
	max under estimation (m)	-0.30	-0.49	-0.93
	# points	184	196	232
1_largeRoi_10	mean error (m)	0.17	0.18	0.20
	st deviation (m)	0.26	0.25	0.27
	rms error (m)	0.31	0.31	0.34
	max over estimation (m)	0.82	0.81	0.84
	max under estimation (m)	-0.51	-0.42	-0.46
	# points	138	159	186
1_largeRoi_50	mean error (m)	0.10	0.11	0.05
	st deviation (m)	0.32	0.34	0.42
	rms error (m)	0.34	0.36	0.42
	max over estimation (m)	0.86	0.86	0.94
	max under estimation (m)	-0.66	-0.84	-1.08
	# points	180	191	228
1_largeRoi_25	mean error (m)	0.70	0.60	-0.03
	st deviation (m)	0.34	0.37	0.53
	rms error (m)	0.35	0.37	0.53
	max over estimation (m)	0.84	0.84	0.96
	max under estimation (m)	-1.02	-1.06	-1.58
	# points	191	205	246
1_smallRoi_25	mean error (m)	0.04	0.06	-0.01
	st deviation (m)	0.37	0.41	0.56
	rms error (m)	0.38	0.41	0.55
	max over estimation (m)	0.76	0.81	0.89
	max under estimation (m)	-1.02	-1.06	-1.58
	# points	175	200	249